Studies on Canine Mammary Tumours with Special References to Role of Exosomes in Tumour Growth: Insights from *in vitro* Model

Thesis

Submitted to the
DEEMED UNIVERSITY
Indian Veterinary Research Institute
Izatnagar - 243 122 (U.P.), India

Dr. Manohar S
Roll No. M-6424

IN PARTIAL FULFILMENT OF THE REQUIREMENTS FOR THE DEGREE OF

Master of Veterinary Science
(Veterinary Pathology)

2025

Dedicated To...

My Beloved Family,
My Respected Guide,
Co-Guide
and
My Self

भा.कृ.अनु.प.–भारतीय पशु चिकित्सा अनुसंधान संस्थान
(सम विश्वविद्यालय)
इज्जतनगर –243122, (उ.प्र.), भारत

DIVISION OF PATHOLOGY
ICAR-INDIAN VETERINARY RESEARCH INSTITUTE
(Deemed University)
IZATNAGAR - 243 122, U.P., INDIA

Dr R.V.S. Pawaiya
M.V.Sc., Ph.D.
Principal Scientist & Head

Dated: 17/02/2025

Certificate

This is to be certified that the research work embodied in this thesis entitled **"Studies on canine mammary tumours with special references to role of exosomes in tumour growth: insights from *in vitro* model"** *submitted by* **Dr. Manohar S; Roll No. M-6424** *for the award of* **Master of Veterinary Science** *Degree in* **Veterinary Pathology** *at ICAR-Indian Veterinary Research Institute, Izatnagar, is the original work carried out by the candidate himself under my supervision and guidance.*

It is further certified that **Dr. Manohar S; Roll No. M-6424** *has worked for more than 21 months in the Institute and has put in more than 150 days attendance under me from the date of registration for the* **Master of Veterinary Science** *Degree in this Deemed University, as required under the relevant ordinance.*

(R.V.S. Pawaiya)
Chairman
Advisory Committee

Certificate

We the undersigned members of Advisory Committee of **Dr. Manohar S;** ***Roll No. M-6424,*** *a candidate for the degree of* **Master of Veterinary Science** *with the major discipline* **Veterinary Pathology**, *agree that the thesis entitled* **"Studies on canine mammary tumours with special references to role of exosomes in tumour growth: insights from *in vitro* model"** *may be submitted in partial fulfillment of the requirement for the degree.*

We have gone through the contents of the thesis and are fully satisfied with the work carried out by the candidate, which is being presented for the award of **Master of Veterinary Science** *Degree of this Institute.*

It is further certified that the candidate has completed all the prescribed requirements governing the award of **Master of Veterinary Science** *Degree of the Deemed University, Indian Veterinary Research Institute, Izatnagar.*

Signature
Name
External Examiner

Date : 25/03/25

(R.V.S. Pawaiya)
Chairman
Advisory Committee

Date : 17/02/25

MEMBERS OF STUDENT'S ADVISORY COMMITTEE

Dr Pawan Kumar, Senior Scientist
Divison of Pathology, ICAR-IVRI, Izatnagar

Dr Vidya Singh, Senior Scientist
Divison of Pathology, ICAR-IVRI, Izatnagar

Dr Ajay Kumar Yadav, Scientist
Division of Biological Products, ICAR-IVRI, Izatnagar

Dr Abhijith Pawde, Principal Scientist
Division of Surgery, ICAR-IVRI, Izatnagar

ACKNOWLEDGEMENTS

Few words of acknowledgements will hardly express the deep sense of gratitude to everyone who inspired me to move ahead, to the learned souls who put me on the ideal path, guided me and enlightened me with their knowledge and experience, I shall ever remain indebted to them.

First of all, it is my great privilege to convey my deep sense of gratitude and sincere thanks to my respected advisor **Dr R. V. S. Pawaiya**, Head of Division, Division of Pathology, ICAR-IVRI. I prevail this opportunity to express my sincere gratitude for his enlightened guidance at each step of planning and execution of research, constructive criticism and constant encouragement during my research period.

I express my heartfelt gratitude to **Dr. Pawan Kumar**, Scientist, Division of Pathology, who provided necessary facilities and for ingenious advice, constant encouragement and help in critical condition during my research. So, from the core of my heart, I want to thank my best teacher, my co-advisor for accepting me as his student and giving new dimension to my student life.

I would like to express my gratitude towards the members of my advisory committee **Dr. Vidya Singh, Dr Abhijith Pawde, Dr Ajay Kumar Yadav**for their unending guidance, valuable suggestions, constant support, providing facilities and affectionate encouragement throughout my research work.

I am especially thankful to **Dr. Karuna Irungbam**, who helped a lot in terms of guidance, advice and encouragement throughout my research.

I am thankful to all Divisional Scientists and my teachers, **Dr. Chandrakanta Jana, Dr. Asok Kumar, Dr. M. Karikalan,** Scientist, for their kind hearted support, help, introspective guidance with constructive suggestions and active persuasion.

I am also very thankful to **Dr. Vinay Kumar S. D, Dr. Neha, Dr. Hiteshwar Yadav, Dr. Sreelakshmi,** for their guidance, support, expertise, unreserved help and invaluable inspirations throughout my research work.

I am very grateful to the **Director, Joint Director (Research), Joint Director (Acad)**, and **Scientific Coordinator** for providing me the necessary facilities to carry out the research work, and a very special debt of gratitude to the ICAR for providing me financial support during this work.

I am also grateful to my colleagues, **Dr. Saran M.E, Dr. Deva, Dr. Deekshitha, Dr. Rinkal Sundriyal, Dr. Thesni** for their encouragement and enjoyable company throughout the degree course.

I am also thankful to my senior **Dr. Vinay Kumar S. D, Dr. Neha, Dr. Vidya Rani, Dr. Hiteshwar Yadav, Dr. Sreelakshmi, Dr. Avantika, Dr. Deepthi Singh, Dr. Sourabh Babu, Dr. Karthik, Dr. Faslu, Dr. Nakul P, Dr. Rahul,** for their help and encouragement and juniors **Dr. Pranati, Dr. Veena, Dr. Thilageshwaran, Dr. Ritika Jeengar, Dr. Shubham Salame, Dr. Suraj, Dr. Divya, Dr. Sangavi K. R, Dr. Alok** for their timely help and encouragement during mycourse work and research period.

I extend my sincere thanks to my juniors **Dr. Raghavesh A. N, and Dr. Nithesh H.M**, for their timely help and encouragement during my research period.

Words cannot describe the help and good association to my lovable seniors and juniors at Karnataka mess, IVRI, for their immense encouragement, helping and providing friendly environment during the present study.

The staff member of Pathology Lab deserves special mention for their assistance and cooperation during my work. I am very thankful to **Akash Bayya, Dharampal, Prakash, Chandan, Mishraji,** , and all other staff members of division of pathology, CHL facility, P.M facility and CADRAD, Izatnagar for their timely help and their cooperartion. This help throughout my research work is inexpressible in words.

(Manohar S)

Date: 17/02/2025

Place: ICAR-IVRI, Izatnagar

ABBREVIATIONS

%	:	Per cent
+ve	:	Positive
<	:	Lesser than
>	:	Greater than
°C	:	Degree Celsius
µg	:	Microgram
µL	:	Microlitre
µM	:	Micromolar
AFM	:	Atomic Force Microscopy
ASCO	:	American Society of Clinical Oncology
BC	:	Breast Cancer
BRCA	:	Breast Cancer Gene
CA IX	:	Carbonic Anhydrase IX
CAF	:	Cancer Associated Fibroblast
CC	:	Cell control
CD9/CD63	:	Cluster of Differentiation 9/63
cDNA	:	Complementary Deoxyribose Nucleic Acid
CMEC	:	Canine Mammary Epithelial Cells
CMT	:	Canine Mammary Tumor
DAB	:	3.3'-Diaminobenzidine
DLS	:	Dynamic Light Scattering
DNA	:	Deoxyribose Nucleic Acid
dNTP	:	Deoxyribonucleotide triphosphate
DW	:	Distilled Water
ECM	:	Extracellular Matrix
EGFR	:	Epidermal growth factor receptor-1
ELISA	:	Enzyme-Linked Immunosorbent Assay
EMT	:	Epithelial-Mesenchymal Transition
ER	:	Estrogen Receptor
ERs	:	Estrogen Receptors
ESCRT	:	Endosomal Sorting Complexes Required for Transport
ESE	:	Early Sorting Endosome
EV	:	Extracellular Vesicles
FACS	:	Fluorescence-Activated Cell Sorting
FBS	:	Fetal Bovine Serum

nSMase	:	Neutral Sphingomyelinase
NTA	:	Nanoparticle Tracking Analyzer
NTC	:	No Template Control
O.D.	:	Optical Density
PBS	:	Phosphate Buffer Saline
PC	:	Prostate Cancer
PCR	:	Polymerase Chain Reaction
PPIs	:	Proton Pump Inhibitors
PR	:	Progesterone Receptor
PTX	:	Paclitaxel
qPCR	:	Quantitative Polymerase Chain Reaction
RAB27A	:	Ras-Related Protein Rab-27A
RNA	:	Ribonucleic Acid
RNA-Seq	:	RNA Sequencing
RT-PCR	:	Reverse Transcription Polymerase Chain Reaction
RVP	:	Referral Veterinary Polyclinic
SASP	:	Senescence-Associated Secretory Phenotype
Sec	:	Seconds
SEC	:	Size Exclusion Chromatography
SEM	:	Standard Error of the Mean
SEM	:	Scanning Electron Microscopy
SFX	:	Sulphisoxazole
SMPD2/3	:	Sphingomyelin Phosphodiesterase 2/3
TDE	:	Tumor Derived Exosomes
TEM	:	Transmission Electron Microscopy
TIS	:	Therapeutic-Induced Senescent
TLR	:	Toll-Like Receptor
TNBC	:	Triple-Negative Breast Cancer
TSG101	:	Tumor Susceptibility Gene 101
UC	:	Ultracentrifugation
UF	:	Ultrafiltration
-ve	:	Negative
VC	:	Vehicle control
VEGF	:	Vascular Endothelial Growth Factor
WHO	:	World Health Organisation

LIST OF TABLES

LIST OF FIGURES

CONTENTS

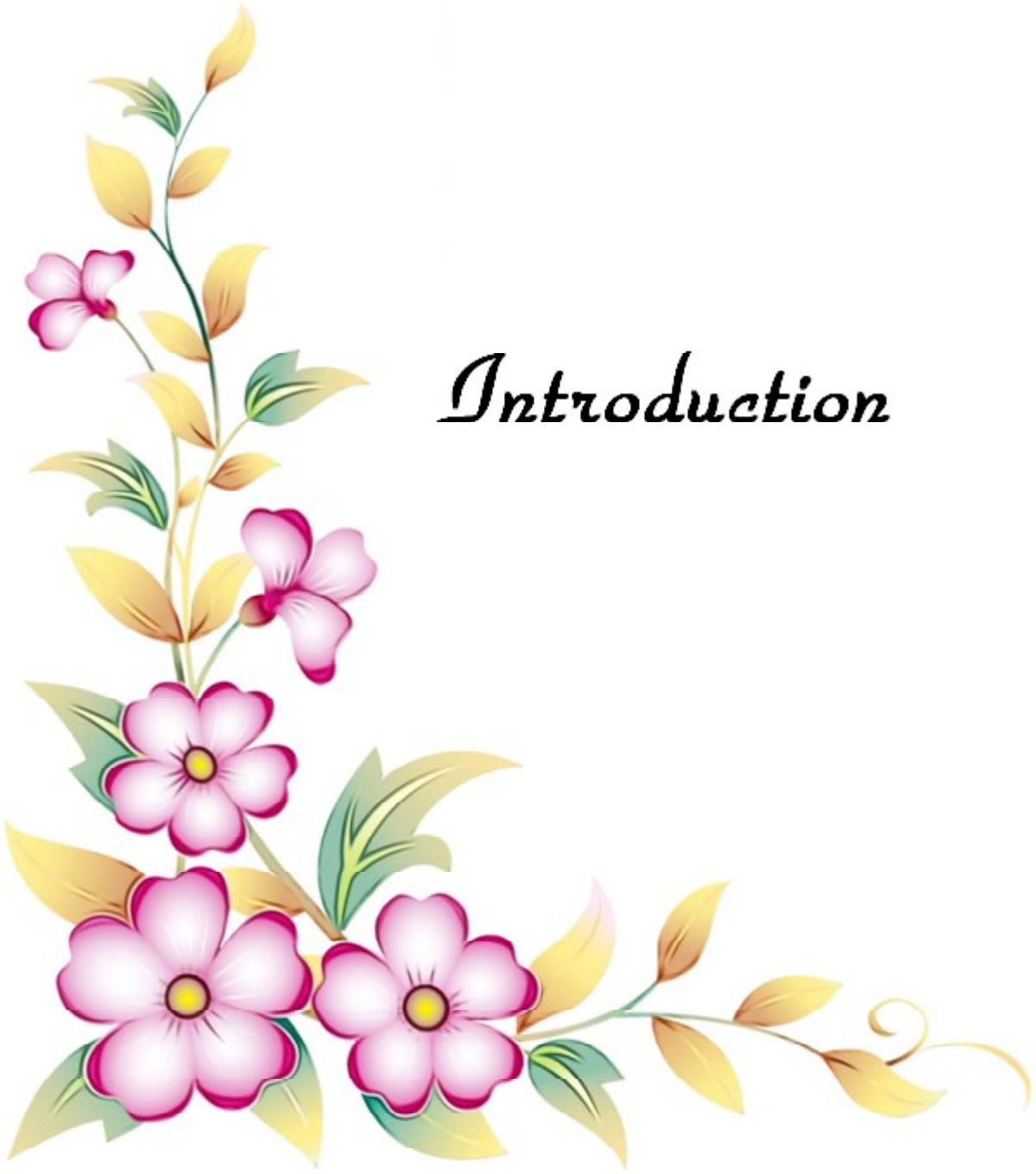

Introduction

1 INTRODUCTION

Canine mammary tumors (CMT) commonly arise in female dogs which are not spayed or in older female canines that have underwent spaying, typically occurring around 8 to 10 years of age (Salas *et al.,* 2015, Benavente *et al.,* 2016). At ages 6, 8, and 10 years, the chances of mammary tumours rose from 1% to 6% and 13%, respectively (Egenvall *et al.,* 2005). Any breed of female dog that is spayed prior first ovulation, the likelihood of developing a tumor is 0.5%; however, if the spaying occurs after or subsequently following next ovarian cycle, the possibility of CMTs elevates significantly from 8% to 26% (Beauvais *et al.,* 2012). Nearly 50% CMTs are malignant and spread to nearby lymph nodes and lungs, and eventually may affect bones (Gilbertson *et al.,* 1983). The main widely accepted treatment for these tumors is mastectomy, along with ovariohysterectomy in intact dogs. Chemotherapy using drugs like doxorubicin and docetaxel is not significantly effective in significantly extending overall survival time (Simon *et al.,* 2006). Although CMT development is known to depend on estrogen and progesterone, tamoxifen, an estrogen receptor alpha (ERα) antagonist, has not been demonstrated to be effective against CMT (Sleeckx *et al.,* 2011). The cytological criteria used in human pathology was found effective in diagnosing CMTs because they share similar cytological characteristics with human breast cancer (HBC) (Shafiee *et al.,* 2016).

Breast cancer (BC) is the leading cause of mortality and commonly diagnosed cancer type in women (Sleeckx *et al.,* 2011). The tumour development in canines is spontaneous, and they exhibit common features replicating BC in women, including histological classification, molecular marker, and biological behaviour. So CMTs are important models for researching HBC due to numerous similarities across various aspects, including histopathological features,

genetic alterations, and response to specific treatments. This similarity makes them a valuable resource for enhancing our understanding about HBC (Matos *et al.,* 2012). Hence, CMTs serve as natural replica for HBC (Abdelmegeed *et al.,* 2018). Given the difficulties in acquiring sufficient amount of HBC samples and ethical considerations regarding human research, there is critical demand for in vivo and in vitro models of HBC (Raffo Romero *et al.,* 2023). Moreover, there is minimal information available on markers that forecast antitumor responses for HBC treatment (Sawyers., 2004). Hence, CMT cell lines offer a significant opportunity for assessing antitumor responses (de Faria Lainetti *et al.,* 2020).

Extensive research in cancer biology have unveiled a distinctive mode of cellular interaction through extracellular vesicles recognized as exosomes (Sinha *et al.,* 2021). Liquid biopsies, an advanced diagnostic technique involving investigation of circulating exosomes, offer numerous advantages over conventional tissue biopsies. These benefits include significantly reduced invasiveness, simplified sample collection, and quick, cost-effective processing (Tai *et al.,* 2018). Exosomes are bilayered endosomal nanovesicles, initially identified in 1983 as 50 nm transferrin-conjugated vesicles secreted by reticulocytes (Harding *et al.,* 1983). While the exosome formation mechanism is understood to involve invagination into endosomes to develop into multivesicular bodies (MVBs), their initial perception as mere "garbage bags" facilitating the disposal of unnecessary proteins has evolved. Exosomes are now recognized, at least in part, as vesicles that are selectively secreted to aid/ help intercellular communication (Vlassov *et al.,* 2012). All exosomes are endosomal in origin and are comprised of fusion proteins (such as Annexins, GTPases, and flotillins) and membrane transport proteins, tetraspanins (including CD81, CD63, CD9, and CD82), heat shock proteins (Hsp) (like Hsp70 and Hsp90), proteins implicated in multivesicular body biogenesis (such as Alix and TSG101), phospholipases and lipid related proteins (Conde *et al.,* 2008). After their release, exosomes float within extracellular matrix (ECM), and their surface proteins aid in identifying target cells for internalization (Heusermann *et al.,* 2016). These macromolecules are involved in various pathological and physiological processes, including inflammation, angiogenesis, cell death, neurodegenerative diseases, immune response, and cancer (Diomaiuto *et al.,* 2021). Exosomes facilitate chemoresistance by bolstering drug-resistant properties within cancer cell populations

(Colombo *et al.,* 2014). As exosomes contains tumor-suppressor and oncogenic microRNAs (miRNAs), they hold immense diagnostic value because of their distinctive expression patterns in cancerous versus normal cells. This trait is particularly advantageous as it enables cancer diagnosis in early stages, underscoring importance of these miRNAs play in both medical applications and research (Salehi *et al.,* 2018). Progress in exosome isolation and characterization techniques provides valuable tools for comprehending exosomes role in cancer and other diseases. These advancements hold potential implications for diagnostics and therapeutics, leads to improved understanding and to treat various medical conditions. The cargoes carried by tumor-derived exosomes are important in cancer development. So new therapeutic approaches have been proposed to tackle this issue. These strategies encompass inhibiting exosome production, impeding their secretion, disrupting exosome-mediated cell-cell communication pathways, and eliminating specific active exosomal cargoes (Tai *et al.,* 2018). GW4869 is an example of a compound utilized as a non-competitive membrane neutral sphingomyelinase (nSMase) enzyme inhibitor. This enzyme is accountable for producing the lipid ceramide by breaking down the membrane lipid sphingomyelin, there by inhibiting the exosomes secretion (Shamseddine *et al.,* 2015).

Since there are only few studies available regarding the exosomal inhibitors in both *in vitro* and *in vivo* along with role of exosomes in tumour development. In this study we are also going to explore the exosomal inhibitor GW4869 drug (nSMase inhibitor) as a potential anti-cancer therapeutic in both *in vitro* and *in vivo* mouse model. Therefore, this study is planned with the following objectives.

1. **Histopathological diagnosis and to study the role of exosomes in the growth of canine mammary tumour.**

2. **To study the effect of exosomal inhibitor on cancer cell growth *in vitro* and *in vivo* in the mouse model study.**

Review of Literature

2 REVIEW OF LITERATURE

2.1 CMT: incidence, risk factors and etiology

Skin cancers are very common neoplasia in dogs, with mammary gland tumors (MGT) coming in second. With prevalence around 52%, they rank highest among bitches, particularly among sexually intact ones (Brodey. *et al.*, 1983). Various researchers periodically reported that around fifty percent of CMT were malignant in origin (Gilbertson *et al*., 1983). Several external factors like mechanical, chemical, nutritional, parasitic, radiological, and viral origins can cause CMT. But some endogenous factors like genetic, immunological and hormonal also come into play in developing CMT (Todorova, 2006). Dogs with CMT ranged in age from 2 to 16 years, with age group having highest incidence recorded in 10 to 12 years, followed by 8 to 10 years and 6 to 8 years (Gupta *et al*., 2012). Nadhiya *et al* in 2020 recorded, highest incidence of CMT being 9 to 13 years, followed by above 2 to 6 years and 6 to 9 years (Nadhiya *et al.,* 2020). Out of 5 pairs of mammary glands, the inguinal mammary gland commonly involved in tumour formation fallowed by the caudal abdominal and cranial abdominal mammary glands (Devarathnam *et al*., 2021). In 2015 Hemanth and his co-workers recorded that tumor involvement was observed more in inguinal pairs, followed by the caudal and cranial abdominal pairs and cranial and caudal thoracic pairs. This may be because amount of glandular and adipose tissues varies amongst glands and is more prevalent in the inguinal and abdominal glands than in the thoracic ones (Hemanth *et al*., 2015). Purebred dogs have significantly higher tendency to develop mammary tumors than mongrels (Zatloukal *et al.,* 2005). Other than mice, where some inbred strains of an oncornavirus are the source of breast tumors, the aetiology of mammary cancers in rest other animals is unknown. Although the specific mechanism

is not known, hormones are known to have significant influence in hyperplasia and neoplasia of breast tissue. Though progesterone and estrogen are needed for healthy progression of mammary glands, they are also connected to growth of tumors. Along with controlling transcription of many nuclear protooncogenes, estrogens serve as promotors of initiated cells. Both benign and malignant CMT, express Estrogen Receptors (ERs). Apart from early malignant transformation, the ER in CMT may be an appealing therapeutic target (Fesseha, 2020). Greater than 50% CMT cases express PR and ERα receptors. Apart from their capacity to anticipate the reaction to hormone treatment, the PR and ER state contributes tumour differentiation and facilitates the patient prognosis (Port Louis *et al*., 2012).

2.2 Histologic Classification, Grading and Staging of CMTs

Although research on CMTs has yielded a significant amount of information on their biology, histological evaluation is still the cornerstone used to classify and grade CMTs (Canadas *et al*., 2018). It makes it possible to examine tumor's histopathological features, including marked differentiation, pleomorphism, mitotic index, quantity of necrosis, and the invasion of tumor cells into nearby lymphatic and blood arteries, along with the tumor's margins after excised (Cassali *et al*., 2011).

2.2a Histologic Classification includes

Malignant tumors	**Benign tumors**
Noninfiltrating/in situ carcinoma	Adenoma
Complex carcinoma	Simple adenoma
Simple carcinoma	Complex adenoma
Tubulo-papillary carcinoma	Basaloid adenoma
Anaplastic carcinoma	Fibro-adenoma
Solid carcinoma	Low-cellularity fibroadenoma
Special type carcinomas	High-cellularity fibroadenoma
Squamous cell carcinoma	Benign mixed tumor
Spindle cell carcinoma	Duct papilloma
Mucinous carcinoma	

Lipid-rich carcinoma

Sarcoma

Osteosarcoma

Fibrosarcoma

Other sarcomas

Carcinosarcoma

Carcinoma or sarcoma of benign tumor.

(Misdorp., 1999)

2.2 b Tumor grading

Based on assessment of 3 histopathological features-

(1) Nuclear pleomorphism,

(2) Amount of tubular formation as a measure of glandular differentiation and

(3) Mitotic activity

Elston and Ellis scoring system used for tumour grading in which each parameter is assigned with score from 1-3 and classified into three categories (Tavasoly *et al*., 2013).

2.2 c CMT staging using TNM categorization

T- Primary tumor

T1: Maximum diameter <3 cm

T2: Maximum diameter: 3-5 cm

T3: Maximum diameter of >5 cm

N- Involvement of regional lymph nodes

N0- Absent

N1- Present

M- Distant metastasis

M0- Distant metastasis absent

M1- Distant metastasis present. (Owen and WHO 1980)

2.3 Correlation of CMT and HBC

In wealthy and developing nations, BC ranks second among women's cancer-related causes of mortality (Antuofermo *et al.,* 2007). Table 1 lists the molecular and clinical resembles between HBC and CMTs, including spontaneous tumors, hormonal aetiology, onset age, early-life obesity, and a comparable course of disease. Dogs as models for HBC is further supported by recent discoveries of strong parallels between the human and canine genomes, oncogenic factors of metastatic mammary tumors, human proteomes and gene expression profiles (Gupta *et al.,* 2012). Similar to HBC, CMT also express HER2, progesterone, and estrogen receptors (Raffo-Romero *et al.,* 2023). Therefore, dogs are being considered as natural animal model of HBC in human medicine in order to find molecular prognostic variables related to metastasis, test new medications, and determine preventive measures before conducting human clinical trials (Rezia *et al.,* 2009, Rivera and von Euler, 2011).

Table 1. Common features between CMT and HBC

Similarity features	Humans	Dogs
Onset age	Median age, 62 years	Median age, 10 years
Estrogen dependency	Long term exposure to estrogen increases	Compared to spayed dogs, non-spayed dogs are four times more likely to develop tumors.
Lymph nodes invasion	Both species identical	Both species identical
Most common histopathological type	Invasive ductal carcinoma	Carcinomas
Molecular markers: BRCA gene mutations, epidermal growth factor receptor (EGFR), Ki-67, human EGR (HER2)/ neu, p53, p63, matrix metalloproteinases	Many genes play crucial part in the carcinogenesis of breast cancers.	These genes play same role in carcinogenesis of mammary cancers in dogs.
Mammographic abnormalities	Macrocalcifications and microclacifications of mammary neoplasm in both species is similar.	Macrocalcifications and microclacifications of mammary neoplasm in both species is similar.

(Abdelmegeed *et al*., 2018)

2.4 Molecular markers expression in canine mammary tumours

2.4 1 Estrogen Receptor (ER)

The intracellular nuclear receptor family is represented by ER and PR. Both normal and malignant mammary tissues naturally express and detect these receptors, which can function as transcription factors that bind DNA. (Rutteman *et al.,* 1990). ER-alpha (ER-α) and ER-beta (ER-β) are the two ER subtypes that control the biological effects of estrogens. The nuclear receptor superfamily includes the ER-α or ER-1 and ER-β or ER-2 receptors. The many mammalian species exhibit high conservation of these receptor proteins. (Parker, 1995; Tremblay *et al.,* 1997). Mammary carcinogenesis is caused by estrogen and its metabolites through both receptor-mediated and non-receptor-mediated pathways. (Yue *et al.,* 2013). Through their epigenetic transcriptional modulation, estrogens change the expression of genes, which can lead to a decrease in apoptosis and an increase in cellular proliferation (Yager, 2015). 75% of HBC cases are ER-α positive, according to reports (Allred *et al*., 2004). A better prognosis is frequently linked to breast tumors that are ER positive, while tumors that are ERα-negative have more aggressive behavior and the capacity to spread. (Dunnwald *et al.,* 2007; Louie and Sevigny, 2017). Nearly all normal mammary tissues in dogs produce ER, and it has been noted that ER expression is rather high in benign tumors and canine mammary dysplasias but drastically lowers in canine mammary carcinomas. (Rutteman *et al.,* 1988; Nieto *et al.,* 2000). ER has shown as the most successful therapeutic target for breast cancer over the last three decades (Ariazi *et al.,* 2006). Non-steroidal chemical substances known as selective estrogen receptor modulators (SERMs) interact with the ER and have varying degrees of estrogen agonistic or antagonistic effects depending on the target tissues (Patel and Bihani, 2018).

2.4 2 Progesterone Receptor (PR)

Progesterone is essential for glandular epithelial growth and mammary alveologenesis during the development of mammary glands. In conjunction with prolactin, it promotes the ductal proliferation and differentiation of specialized structures known as mammary alveoli, which are involved in the production and secretion of milk and colostrum during lactation.

(Macias and Hinck, 2012). Two PR-isoforms, PR-A and PR-B, are primarily responsible for controlling the biological effects of progesterones. In normal tissues, two isoforms are often co-expressed; however, in different histologic types, physiological states, and disorders, their ratio of expression varies significantly. (Mylonas *et al.,* 2007). While PR-B alternates between the cytoplasm and the nucleus, PR-A is primarily found in the nucleus of the cell (Guiochon-Mantel *et al.,* 1994). Excessive local growth hormone (GH) biosynthesis in the mammary gland is one of the potential pathways causing progesterone-induced breast cancer. This promotes mammary gland stem cell growth, which aids in the onset of carcinogenesis. (Mol *et al.,* 1996; Van *et al.,* 1999). According to reports, hyperplastic, benign, and malignant mammary gland tumors in dogs show a gradual decline in PR expression. (Millanta *et al.,* 2005). Aglepristone, a competitive inhibitor of PR, is a medication used to terminate pregnancies in dogs. Research on aglepristone's impact on canine mammary tumors revealed that it significantly inhibited the growth of PR-positive CMTs. Nonetheless, a clinical correlation and more patient investigations are required (Guil-Luna *et al.,* 2011).

2.4 3 Human epidermal growth factor receptor-2 (HER-2)

Cluster of differentiation 340 (CD340), erbB-2 (erythroblastic oncogene-B), and HER2/neu (neuro/glioblastoma derived oncogene) are other names for the human epidermal growth factor receptor-2 (HER-2). HER-2, also known as the c-erbB-2 gene, is a proto-oncogene that encodes the integral membrane receptor glycoprotein with a molecular weight of 185 kDa. The canine HER-2 proto-oncogene is located on chromosome 1q11.1. (Murua *et al.,* 2001). A network of signaling pathways that control normal cell growth, cellular differentiation, adhesion, and motility in many physiologically normal cell lineages will be started by the heterodimerization of the HER-2 receptor. (Gassmann *et al.,* 1995; Lee *et al.,* 1995). It has been documented that the physiological control of HER-2 signaling pathways is impaired during breast carcinogenesis (Slamon, 1990). During breast carcinogenesis, the HER-2 gene, a crucial gene for cell survival, is amplified and the HER-2 protein is overexpressed. This causes an excess of HER-2 dimers to form even in the absence of ligands, which ultimately leads to malignant transformation. (Pierce *et al.,* 1991). According to Ahern *et al.* (1996), who examined the expression of the c-erbB-2 or HER-2 oncogene in CMTs and tumor-

derived cell lines, benign CMTs have much lower levels of HER-2 mRNA expression than malignant CMTs. HER-2 overexpression in CMTs ranges from 17.6% to 74%. (Ahern *et al.,* 1996; Rungsipipat *et al.*, 1999; De *et al.*, 2003; Kumar *et al.,* 2009; Sassi *et al.,* 2010; Ranganath *et al.,* 2011). Therapeutic approaches against breast cancer have been significantly impacted by trastuzumab, a monoclonal humanized anti-HER-2 antibody that targets the extracellular region of HER-2 (Tan and Swain, 2003). Through antibody-dependent cell-mediated cytotoxicity, trastuzumab causes neoplastic mammary gland epithelial cells to undergo apoptosis. (Agus *et al.,* 2005).

2.4 4 Epidermal growth factor receptor (EGFR)

EGFR is thought to be a promoter of cancer cell migration and invasion in cases of malignant neoplasms. (Masuda *et al.,* 2012). It has been demonstrated that EGFR expression is significantly correlated with enhanced angiogenesis, metastasis, and a poor clinical outcome. (Carvalho *et al.,* 2013). Large tumor masses, enhanced mitotic figures, necrosis, angiogenesis, and poor clinical outcomes are frequently linked to elevated EGFR expression. (Carvalho *et al.,* 2013; Guimaraes *et al.,* 2014). Other powerful angiogenic factors, such as vascular endothelial growth factor (VEGF), can also be controlled by the EGFR. In dogs, EGFR expression has been found to significantly correlate with age. (Gama *et al.,* 2009). Gefitinib is a tyrosine kinase inhibitor that targets EGFR and can block the intracellular tyrosine kinase domain's ATP binding site. (Wang and Greene, 2008).

2.5 Exosomes

Exosome research is interesting and quickly developing field in oncology. These are nanoparticles that are expelled from cells and have been detected in human, cat, and dog bodily fluids. Apart from their function as biomarkers, exosomes are connected to development of several illnesses, such as cancer (Howard *et al*., 2020). Extracellular vesicles (EV) are secreted by all cells, both prokaryotes and eukaryotes, as natural aspect of their physiology and in acquired disorders (Kalluri *et al.,* 2020). 2 classes of EVs are ectosomes and exosomes (Intraluminal vesicles (ILVs) before releasing into extracellular environment) (Cocucci, *et al.,* 2015). Ectosomes, which range from 50 nm to 1 μm in diameter, are vesicles produced by the

straight outward budding of plasma membrane. This process produces large vesicles, microparticles and microvesicles. On contrary exosomes, are endosomal in origin and range from around 40 to 160 nm in diameter (average: about 100 nm) (Kalluri, *et al.,* 2020). Exosomes are nanosized vesicles secreted by nearly all cell types, including fibroblasts, neuronal cells, epithelial cells, immunological cells, endothelial cells, and cancer cells (Tai *et al.,* 2018). Trams *et al* at first published description about exosomes in 1980s (Suchorska *et al*., 2016). Multifunctional vesicles, that have role in reticulocyte maturation, were demonstrated by Johnstone and his co-workers in 1986 (Johnstone *et al*., 1986). Exosomes are extracted from various body fluids, cell culture medium, amniotic fluid, nasal lavage fluid, ascites, breast milk, plasma, serum, urine, and saliva (Suchorska *et al*., 2016). Initially, it was believed that cells released exosomes as waste products. But the advancement of molecular tools has provided fresh perspectives on their role as essential component in tissue microenvironment control and cell-cell communication (Vlassov *et al*., 2012).

2.5.1 Exosomes biogenesis and contents

Generation of exosomes entails double fold invagination of plasma membrane and synthesis of intracellular MVBs containing ILVs (Kalluri, *et al.,* 2020). Exosome biogenesis mechanisms are closely regulated via multiple different pathways, as ESCRT-independent and ESCRT-dependent pathways (endosomal sorting complexes required for transport) (Kowal *et al*., 2014). First, there are two possible pathways by which endocytosis is mediated: clathrin-dependent or clathrin-independent. This process is often activated at the lipid raft, which contains a range of cell-specific receptors and signalling proteins (such as growth factor receptors, oncoproteins), common membrane proteins like MHC I and II, tetraspanins (eg, CD63, CD9, CD81), cadherins and integrins (Tai *et al.,* 2018). As a result, an early sorting endosome (ESE) is formed and, in certain situations, it may combine with an already-existing ESE. The golgi complex and endoplasmic reticulum may also have role in development and composition of the ESE. ESEs have the capacity to develop into multivesicular endosomes, or MVBs, after maturing to late sorting endosomes (LSEs). MVBs are created by double fold invagination of plasma membrane, or inward invagination of endosomal limiting membrane (Kalluri *et al.,* 2020). In fact, a numerous nuclear (such as transcriptional factors, longnoncoding RNAs

[lncRNAs], DNAs, etc.) and cytoplasmic (such as Hsp, ubiquitin-related proteins, mRNAs, cytoskeleton proteins, miRNAs etc.) molecules can be specifically loaded into MVB in a manner that is specific to a given cancer type or stage. Moreover, exosomes released into extracellular space when MVB merge with plasma membrane (Tai *et al.,* 2018) or the MVB combines with either autophagosomes or with lysosomes and gets degraded (Kalluri *et al.,* 2020). In contrast, lipids like sphingolipid ceramide (Trajkovic *et al*., 2008) or sphingosine 1-phosphate in ESCRT independent route (Kajimoto *et al*., 2013) control the budding or exosomes release. Exosomes are covered in lipid bilayer membrane, act as barrier to safeguard sensitive biological substances. In fact, the structure of exosomal membrane encloses and shields miRNAs or proteins from being broken down by RNases or proteinase, respectively (Tai *et al.,* 2018).

2.5.2 Tumour derived exosomes (TDE) and their functions

By transporting bioactive chemicals between cancer and other cells in nearby and distant microenvironments, exosomes contribute to cancer development and dissemination. Due to this intercellular communication, recipient cells undergo modifications in several cellular and biological activities. This exosome-mediated cell-to-cell communication has reportedly shown to affect multiple cancer hallmarks, such as immune response modulation, stromal cell reprogramming, extracellular matrix architecture remodelling, or even making cancer cells drug resistance. By selectively loading particular oncogenic molecules to exosomes made them to be potential therapeutic target and diagnostic biomarker (Tai *et al.,* 2018). Numerous studies demonstrated that the biological activity of exosomal substances genuinely alters the recipient cells' biological processes and cell signalling events (Tomasetti *et al.,* 2017). Exosome-mediated cell-to-cell communication has been demonstrated locally and distantly within tumor microenvironment, indicating that it is not just confined to cancer cells (Maia *et al*., 2018). This process is necessary for the building up premetastatic niches and the remodelling of tumor microenvironments during cancer development. Tumor microenvironments and premetastatic niches require biologically active substances from exosomes produced from cancer cells or stromal cells to offer the necessary signals for reprogramming different cells and architectures (Tai *et al.,* 2018). The dynamic and multi-step process of cancer progression involves multiple

well-studied signalling processes that work together to orchestrate cancer malignancy. Through generating autocrine/paracrine oncogenesis, reprogramming stromal cells, modifying the immune system, and stimulating angiogenesis, TDEs influences cancer progression (Maia *et al*., 2018). The transfer of oncogenic substances within oncosomes from the primary tumor to recipient cells causes morphological alteration and increases their anchorage-independent proliferation (Nedawi *et al.,* 2008). TDE triggers reprogramming of stromal cells that plays a pivotal role in the advancement of cancer. TDE transports miRNA, including miR-9, which causes fibroblasts to differentiate into cancer associated fibroblast (CAF) with increased cell motility (Baroni *et al*., 2016). Angiogenesis induced by tumors removes waste products and provides oxygen and necessary nutrients. By upregulating angiogenesis-related genes, surface tetraspanins on TDE, including Tspan8 stimulates resting endothelium cells, endothelial cell sprouting, and endothelial cell progenitor development (Nazarenko *et al.,* 2010). TDE transports enzymes that remodels extracellular matrix, including MMP2 or MMP9, causing extracellular matrix disintegration and facilitates cancer invasion and metastasis (Ge *et al.,* 2012). According to Taylor and his co-workers microvesicles from patients suffering with advanced endometrial and ovarian cancer were found to contain FasL and matrix metalloproteinases, which are involved in immune cells destruction and invasion of cancer cells, respectively but these microvesicles were not found in sera of patients with benign diseases or healthy controls (Taylor *et al.,* 2002). The remodelled microenvironment further amplifies the recruitment of macrophages derived from bone marrow, that helps to develop a premetastatic niche in the liver and creates favourable conditions for metastasis (Costa-Silva *et al*., 2015). Furthermore, the metastatic organotropism results from the function of integrin expression profiles of TDE as "ZIP codes" which direct exosomes to particular tissues/organs. Exosome integrin αvβ5 was strongly linked to liver metastasis, while exosomal integrins α6β4 and α6β1 were significantly correlated with lung metastasis (Hoshino *et al*., 2015).

2.5.3 Exosomes as biomarkers for cancer detection

The exosomal payloads is very similar to the intracellular state of original secreted cell. Finding tumor markers in liquid biopsies has several benefits over tissue biopsies, including being less invasive, simple to collect, quick, and affordable. Lipid based exosomes offers a

moreresilient and effective delivery system for sensitive biological molecules found in bloodstrem fluids like plasma, serum, saliva and urine (Tai *et al*., 2018). Under standard storage conditions, the biological components in exosomes isolated from blood plasma are highly stable (lasting more than 90 days). Furthermore, it is frequently discovered that patient with disease have significantly higher amounts of exosomes in their bodily fluids (Kalra *et al*., 2013). Because tumor-suppressor and oncogenic miRNAs express differently in normal cells than cancer cells, exosomes play a valuable tool for early diagnosis due to their differential expression. Glioblastomas, pancreatic, colorectal, liver, colon, breast, oesophageal, and ovarian cancers have linked to elevated circulating exosomal miR-21, whereas prostate and bladder cancers are associated with elevated urine-derived exosomal miR-21 (Salehi *et al*., 2018). The exosomal oncogenic microRNAs miR-155, miR-1246, and miR-17-92 cluster are associated to several forms of cancer (Li *et al*., 2018). The two examples of tumor-suppressor miRNAs associated to hematologic, pancreatic, liver, and breast cancers are miR-34a and miR-146a (Salehi *et al*., 2018). Exosomal miRNA's prognostic and diagnostic ability improved by combining various microRNAs, and exosomal miR signatures are consistently being discovered in relation to cancer diagnosis and its prognosis (Halvaei *et al*., 2018). Currently under consideration is the prospect of integrating protein, lipid, RNA, and miRNA exosomal cargos in cancer detection and its prognostic evaluation. To improve the sensitivity and specificity of an exosome-based diagnostic, a multicomponent combinatorial method that combines markers reflecting several features of disease-produced exosomes (e.g., protein content, metabolites, and RNA) may be used (Kalluri, *et al*., 2020).

2.4 CMT cell lines and primary culture

Plenty of similarities between CMTs and HBC, such as age of onset, incidence, risk factors, histological and molecular characteristics, biological behaviour, pattern of metastasis, and medication responses, make CMTs an advantageous model for studying breast cancer (Matos *et al.,* 2012). Researchers need both *in-vivo* and *in-vitro* HBC models because HBC samples are scarce and because doing such research on individuals raises ethical concerns (Abdelmegeed *et al.,* 2018). Consequently, canine tumoroids derived from dog patients experiencing spontaneous CMT may offer more ethical and representative translational model

to evaluate safety and effectiveness of drugs in pre-human research. Moreover, canine tumoroids serve as an inventive drug discovery screening tool, minimizing the need of experimental animals in *in vivo* investigations (Raffo Romero *et al.*, 2023). Several CMT cell lines have been developed in recent years, including CIPp, CTBp, CNMp and CHMp (Uyama *et al*., 2006), CMT-W1 and CMT-W2 (Krol *et al.,* 2010), DE-E and DE-F (Chang *et al.,* 2010). The initial canine inflammatory mammary cancer (CIMC) cell line to be established was IPC-366. After being injected into SCID/ Balb mice, IPC-366 generated tumors that replicated the typical neoplastic invasion of superficial dermal vessles. This suggests that IPC-366 may also find application as *in-vivo* model for CIMC. IPC-366 is described as basal epithelial cell line exhibiting mesenchymal traits, such as positive immune-expression to general epithelial cell marker pancytokeratins (AE1/AE3), basal epithelial cell marker cytokeratin 14, and general mesenchymal marker vimentin (Caceres *et al.*, 2015). A unique CMT cell line generated from primary CMT, known as B-CMT, was successfully grown for at least 50 passages over a one-year period. B-CMT single cell can multiply to create a community of cells that will serve as the basis for additional studies. A preliminary characterization of B-CMT was conducted, and sensitivity of five chemotherapeutic medicines to cells was investigated. It's interesting to note that research has shown that B-CMT has high levels of expression of the hypoxia-inducing factor HIF1 a, which plays major role in cell's resistance to doxorubicin. B-CMT cell cycle arrest was significantly impacted by imatinib and rapamycin (Li *et al.,* 2021). While there were variances in tumorigenicity, the in-vitro cultured cells showed similarities in morphology and phenotype. Two out of four cell lines that shown vasculogenic mimicry (VM) capacity in vitro also demonstrated in vivo tumorigenicity associated with aggressiveness and malignancy (de Faria Lainetti *et al.,* 2020). In another investigation, a novel CMT cell line called FR37-CMT was created. It had a fusiform or stellate shape, expressed vimentin and CD44, and demonstrated loss of E-cadherin, which is considered as crucial step in the epithelial to mesenchymal transition (EMT). The phosphorylated ERK1/2 identified, the downregulation of DICER1 and miR-200c, and the upregulation of ZEB1 are likewise consistent with the mesenchymal features of the FR37-CMT cell line. These findings back up as usage of FR37-CMT as novel CMT model, which could aid in development of new CMT-targeting therapeutics and understand the molecular pathways driving EMT (Raposo *et al.,* 2017).

2.5.4 Exosomes in tumour cell lines

According to one study, tumor exosomes from human patients with pancreatic and lung cancers might trigger myotube apoptosis via TLR7 and miR-21 signalling, simulating the cancer cachexia phenotype in an *in-vitro* system (Fish *et al.,* 2018). Canine exosomes detected in plasma, serum and in urine were immunopositive for the tetraspanin, a transmembrane protein CD9, which is known to control cancer growth, and were sporadically "cup-shaped" and unevenly rounded (Ichii *et al*., 2017). The B42 clone 16 BC cell lines produced more exosomes (measured using nanoparticle tracking analyzer (NTA) and expression of the proposed exosome markers, Alix and TSG101) [(53.2 +/- 1.6) 108 exosomes per 106 cells] in contrast to the normal mammary epithelial cells [(4.5 +/- 2.3) 108 exosomes per 106 cells] in human mammary epithelial cell line (HMEC) B42 (Riches *et al.,* 2014). Exosome production by neoplastic cells is demonstrated by double increase in exosome numbers from serum (9.9 1011 particles/ mL) and plasma (13.3 1011 particles/mL) of human prostate cancer (PC) patients compared to healthy control (4.15 1011 particles/mL) (with sizes ranging from 85–150 nm confirmed using NTA) (Kharmate *et al*., 2016). The first and, to date, only study describing *in vitro* shedding of exosome-derived miRNA by canine mammary cells was reported in 2018 by Fish *et al*. They employed particular cell-free conditioned media that contained exosome-like vesicles from five CMT cell lines that had histopathology-confirmed mammary tumor and three normal canine mammary epithelial cell lines (CMEC) from dogs without any abnormalities in mammary glands to produce several exomiRs (exosomal miRNA) that are markedly downregulated and upregulated and could be potential markers of mammary tumor. With 338 distinct exomiRs found in this detailed analysis, 145 exomiRs with differential expression (118 upregulated and 27 downregulated) between tumor and normal samples showed a difference of more than 1.5 times (Petroušková *et al.,* 2022). In another investigation, investigators discovered that some markers, like CD81, Alix, CD63, Perforin 1, HSP70, TSG101 and Granzyme B, are expressed by canine NK cell-derived exosomes (NK-exosomes), which are isolated from activated cytotoxic NK cell supernatants and investigated the anticancer effects of NK-exosomes using REM134 CMT cell line on mouse mammary tumor model. They noticed changes in control, tumor, and NK-exosome treated tumor groups with regard to tumor initiation, their size, tumour

progression, and recurrence associated markers. They observed that tumor size in group of tumors treated with NK exosomes was smaller compared to tumor group in REM134 driven mouse tumorigenic model and when NK exosomes were applied to tumor group, there was notable drop observed in expression of CD133, an important cancer stem cell marker that promotes carcinogenesis (Lee *et al* 2021). In another investigation, utilising four cell lines from canines with lymphoid tumours as model for lymphoid tumours in humans, exosomes were produced, and their protein profiles and miRNAs were thoroughly analyzed. The findings demonstrated that there were similarities between four cell lines proteins and major miRNAs obtained from exosomes. Nonetheless, each cell line's exosome had a different miRNA profile, which matched the parent cells' expression patterns. Exosomes produced by vincristine-resistant and- sensitive cell lines differed in terms of protein levels and miRNAs, specifically in relation to CD82 protein, miR-8908a-3p, miR-151, and miR-486 (Asada *et al.,* 2019).

2.5.5 Exosome isolation from mammary tumour cell lines

Exosome isolation is a topic of current study. Numerous methods have investigated, developed, and suggested, including polymer precipitation, immunoaffinity chromatography, size exclusion chromatography (SEC), ultrafiltration (UF), ultracentrifugation (UC), and methods based on microfluids. Every technique has benefits and drawbacks, and the purity and quality of exosomes produced can vary depending on how the product is pre-processed. Western blotting, dynamic light scattering (DLS) combined with zeta potential determination, electron (SEM and TEM) microscopy, atomic force microscopy (AFM), nanoparticle tracking analysis (NTA), fluorescence activated cell sorting (FACS), and enzyme-linked immunosorbent assays (ELISA) can all be used to assess the quality of the extracted exosomes (Diomaiuto *et al.,* 2021). EVs from a CMT cell line were isolated in one investigation using two distinct methods: UC and SEC. Compared to SEC, UC permitted isolation of more particles, whereas SEC EV seemed to have little stronger impact on invasion, migration, and proliferation (Moccia *et al*., 2023). Chen and his co-workers in 2023 recorded that both healthy and CMT dog plasma included a significant number of exosomes were successfully detected using NTA, TEM, and distinguishing markers. The volume and quantity of plasma exosomes in CMT dogs shown to be significantly higher than healthy dogs, possibly due to fact that they carried more

cargo to improve cell-to-cell communication. Subsequently, they employed the RNA-Seq technique to explore exosomal RNA expression profile and observed a noteworthy distinction in the RNA delivered by plasma exosomes between dogs with tumors and those without. The plasma-derived exosomes from CMT found to contain 2307 genes with variable expression, 632 genes found up-regulated and 1675 genes were down-regulated. Of the mRNAs that were differentially expressed, 4440 mRNAs were down-regulated and 1107 were up-regulated. Regarding lncRNAs, there was down-regulation of 117 lncRNAs and an up-regulation of 79 lncRNAs. How these differently expressed genes, lncRNAs, and mRNAs contribute to development of CMT needs to be further investigated (Chen *et al*., 2023).

2.5.6 Therapeutic uses of exosomes

Using exosomes to deliver miRNA or small interfering RNA (siRNA) payloads, preclinical research has concentrated on treating rodents with pancreatic, glioma, and mammary cancers, along with exploring brain targeting (Kalluri *et al.,* 2020). Additionally, ligand enrichment on modified exosomes could be utilized to direct exosomes toward particular cell types or to stimulate or inhibit signaling processes in recipient cells. For instance, RGD (arginine, glycine, and aspartic acid) αv integrin-specific-modified peptide, a modified tumor-homing peptide sequence that functions as an integrin recognition sequence, on doxorubicin-loaded exosomes generated from immature dendritic cells demonstrated a therapeutic response in mice bearing mammary tumors (Tian *et al*., 2014). miRNA let-7a was delivered to the cancer cells, and exosomes modified with GE11 synthetic peptide were used to target EGFR+ breast cancer cells, thereby inhibiting their *in-vivo* growth (Ohno *et al.,* 2013). Pancreatic cancer has been treated using clinical-grade MSC-derived exosomes carrying a KrasG12D siRNA payload (iExosomes) in number of animal models. These investigations showed that when iExosomes are used as single drug, mice's overall survival increases significantly and they can contact specific targets without showing any signs of toxicity (Mendt *et al.,* 2018). Exosomes with CD47 on them have been demonstrated to produce "don't eat me" signal that prevents phagocytosis and restricts their removal from circulation. Furthermore, the entrance of exogenously supplied iExosomes was improved by macropinocytosis linked to cancer cells (Kamerkar *et al.,* 2017). Phase I clinical trial to treat patients with pancreatic cancer linked to

KrasG12D mutations has been initiated and considered for further development of iExosome-based therapy. The modified exosomes called "dexosomes" that generated from IFN-γ-matured dendritic cells loaded with peptides known as MART1 (melanoma antigen recognized by T cells 1). Patients with stage IIIB/IV non-small-cell lung cancer showed enhanced cytolytic activity linked to natural killer cells when treated with dexosomes, despite the method not producing a significant cancer-specific T cell response (Besse *et al.,* 2015).

2.5.7 Inhibition of exosomes

Exosomes helps to remove undesirable or harmful substances from cells. They can also remove some medications that have been injected into cells and it is observed that the quantity of drug that these exosomes remove allows the cell to become resistant for treatment. Therefore, it is possible that exosomes provide an extra pathway for certain cancers to actively remove different chemotherapeutic drugs. Thus, emerging targets for treatment may be mechanisms controlling exosome secretion from tumors (Vlassov *et al.,* 2012).

2.5.7a Exosome inhibitors blocking RAB27A

The RAB27A gene encodes the protein known as RAB27A. This protein is the member of RAB family, a small GTPase superfamily. This membrane-bound protein might be involved in signal transduction mediated by small GTPases and protein transport. According to reports RAB proteins may be crucial for the synthesis or exosomes release. RAB protein (RAB27A and RAB27B) knockdown reduced exosomes release without significantly altering the normal secretory pathway's ability to secrete soluble proteins (Zhang *et al.,* 2020). Powerful farnesyl transferase inhibitor tipifarnib has ability to impede cell growth and trigger apoptosis in cells (Haluska *et al.,* 2002). Tipifarnib's underlying mechanism involves nSMase2, RAB27A, and Alix expression inhibition (Colombo *et al.,* 2014). Analyses were made on inhibitory effects of climbazole and neticonazole, which both dramatically reduced secretion of exosomes by downregulating levels of Rab27a and Alix. Neticonazole further reduced nSMase2 levels (Datta *et al.,* 2018).

2.5.7b Exosome inhibitors blocking sphingomyelinase

The hydrolase enzyme sphingomyelinase (SMase) which are responsible for converting sphingomyelin (SM) into phosphocholine and ceramide. Researchers recently found that ceramide may control the generation of exosomes, and that ceramide levels may be lowered by inhibiting nSMase. Consequently, nSMase is promising therapeutic target to prevent exosomes release (Trajkovic *et al.,* 2008). GW4869, first nSMase inhibitor to be utilized to prevent formation of exosomes. This substance has effectively been utilized to prevent MCF-7 cells, lung epithelial cells, and RAW264.7 macrophages from secreting exosomes (Luberto *et al*., 2002). Following five days of intraperitoneal injections of 100 µg GW4869 in mice, a noticeable decrease in level of exosomal marker (Alix) and EVs, along with reduction in the overall protein content found within the EVs extracted from serum of the experimental animals (Dinkins *et al.,* 2014). According to reports, DPTIP is most powerful nSMase2 inhibitor yet been discovered. Its inhibitory action is specific to nSMase2 and does not affect members of two related enzyme families, such as alkaline phosphatase or acid sphingomyelinase (Zhang *et al.,* 2020).

2.5.7c Other inhibitors of exosomes

Parolini and colleagues (2009) reported that exosome trafficking is dependent on pH of tumor cells' microenvironment. Melanoma cells generated more exosomes when the pH was low, however this low pH state had no effect on the cells' ability to survive. Moreover, cells cultivated in acidic environment showed increase in exosome uptake (Parolini *et al*., 2009). Proton transporter V-ATPases are essential for maintaining internal pH of neoplastic cells alkaline and the external pH acidic. Consequently, inhibiting V-ATPases may be a novel tactic to stop exosome release. Proton pump inhibitors (PPIs), are used for treatment of peptic illnesses due to anti-acidic effects, and are demonstrated to have potential use in cancer therapy. Additionally, their ability to inhibit V-ATPases, PPIs can also be utilized to restrict the exosomes release (Taylor *et al.,* 2015). Carbonic anhydrase IX (CA IX), an additional proton exchanger that is overexpressed in many cancer types, is also crucial for regulating tumour pH (Spugnini *et al*., 2015). Exosome release also inhibited by ketotifen (antihistamine), which is

calcium channel blocking drug that is operated like a store and utilized to stabilize mast cells. The exosomes generated by BT549, MCF7, and HeLa cells declined by 30%, 45%, and 70% respectively, after 10 mM of ketotifen (Khan *et al.,* 2018). Sulphonamide antibiotic sulphisoxazole (SFX) targets endothelin receptor A, which can prevent exosomes release (Im *et al*., 2019). Furthermore, SFX decreased the expression of RAB7, CD63, and RAB27a (Chiaverini *et al*., 2008).

2.6 GW4869 as exosomal inhibitor

GW4869 is a cell-permeable symmetrical dihydroimidazolamide compound that can be used as an effective, specific, and noncompetitive inhibitor of membrane-neutral sphingomyelinase (nSMase2), which prevents ceramide-modulated inward budding of multivesicular bodies (MVBs) and subsequent release of exosomes from MVBs (Li *et al.,* 2013) GW4869 has been reported to reduce exosome release and is often used as an exosome inhibitor to suppress the increase in exosome secretion in response to gefitinib and chemoresistance in colorectal, pancreatic, and ovarian cancer cells (Catalano and O'Driscoll, Eguchi *et al.,* 2020) GW4869 may be a helpful strategy to overcome the antagonistic effects via inhibition of exosome and miRNA secretion when EGFR-TKIs and chemotherapeutic agents are co-administered (Eguchi *et al*., 2020). In 2010, GW4869 was first utilized by Kosaka and co-workers to successfully inhibit the release of mature exosomes from multivesicular bodies (MVBs) in HEK293 cells. In 2017 Kavanagh and his co-researchers, demonstrated that chemotherapy can induce the generation of highly chemoresistant therapeutic-induced senescent (TIS) cells. In their study, TIS was induced in Cal51 TNBC cells using paclitaxel (PTX), and they observed that TIS cells released significantly more extracellular vesicles (EVs) compared to control cells. These EVs contained chemotherapy drugs and key proteins involved in cell proliferation, ATP depletion, apoptosis, and the senescence-associated secretory phenotype (SASP). TIS cells also displayed increased expression of multidrug resistance protein 1 (MDR1)/P-glycoprotein. Similarly, they explored the effect of the exosome biogenesis inhibitor GW4869 (5 μM) by treating the Cal51 TNBC cells with PTX for 7 days to induce TIS. GW4869-treated TIS cells displayed a significant reduction in cell numbers on days 9, 11, and 14 compared with TIS cells treated with control vehicle alone. Additionally,

GW4869 treatment resulted in a reduction in the number of SA-β-gal-positive cells and lowered the proliferation rate of TIS cells. In a comprehensive study investigating the impact of GW4869 on survival of Paclitaxel (PTX)-resistant prostate cancer (PCa) cells, both in controlled laboratory conditions and live mouse models, a regimen of 2.5 mg/kg GW4869 administered intraperitoneally six days a week for a duration of 21 days was utilized. Notably weight of tumor tissue exhibited significant reduction around 65% following the GW4869 treatment regimen in comparison to control group, highlighting the potent inhibitory effects of this experimental compound on growth and progression of PTX-resistant PCa cells both *in-vitro* and *in-vivo* (Kumar *et al.,* 2022). One more recent study has reported GW4869 reduced the expression of eHSP90α, which was accompanied by upregulation of E-cadherin and downregulation of vimentin. In addition, GW4869 was found to enhance the antitumor effects in combination with gefitinib *in-vivo* and demonstrated that GW4869 can inhibit Epithelial-Mesenchymal Transition (EMT) and extracellular HSP90α in gefitinib sensitive non-small-cell lung cancer (NSCLC) cells. Thus, providing a new strategies for delaying the development of acquired resistance to gefitinib, and a novel application of the exosome inhibitor GW4869 in NSCLC (Wan *et al.,* 2023).

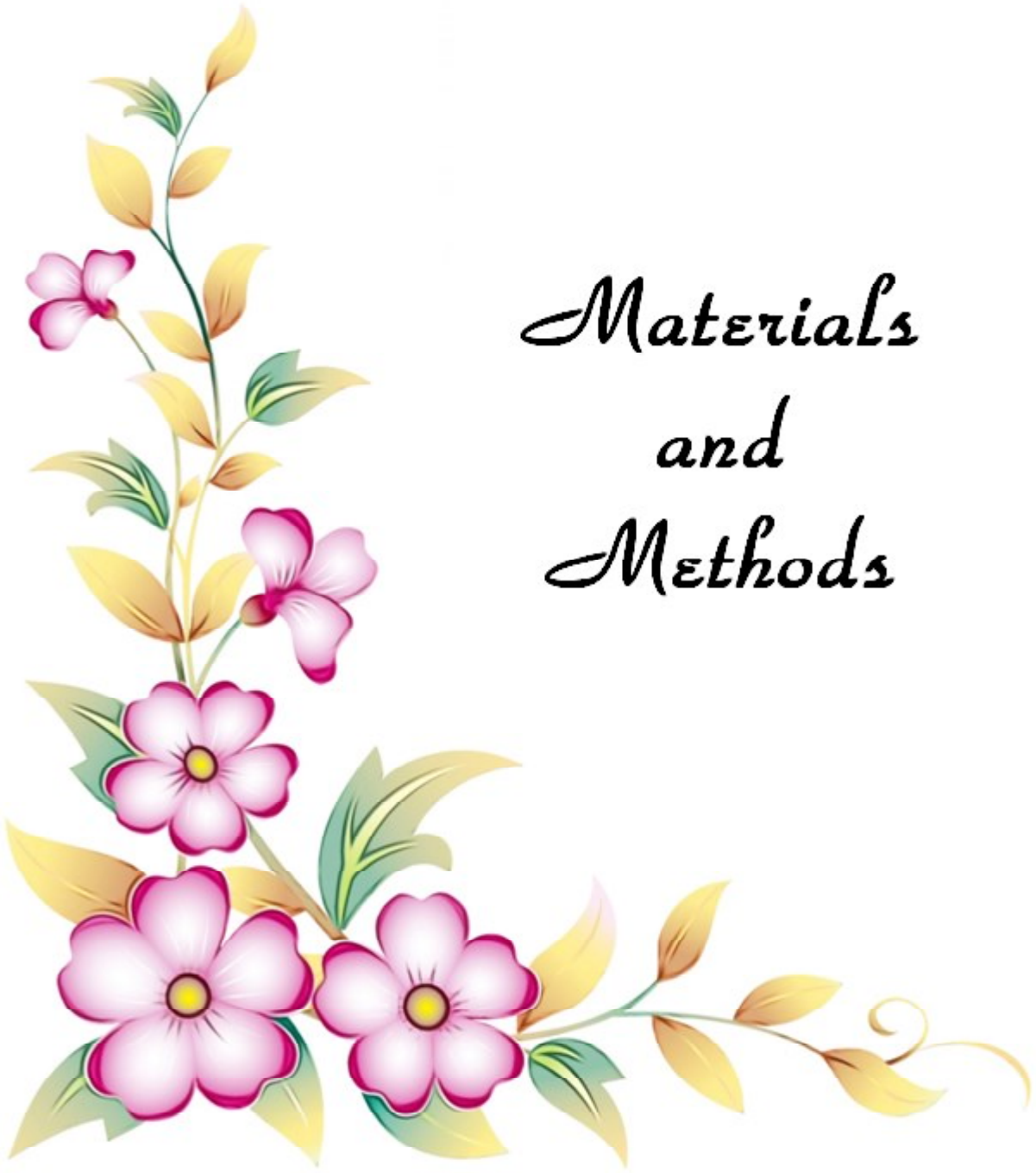

Materials and Methods

3 MATERIALS AND METHODS

The present study was carried out at Canine Disease Lab of Division of Pathology, ICAR-Indian Veterinary Research Institute (ICAR-IVRI), Izatnagar, Bareilly, Uttar Pradesh (UP).

3.1 Materials

3.1.1 Samples

Tissue samples from the suspected canine mammary tumour (CMT) cases were collected from Referral Veterinary Polyclinic (RVP) and Postmortem Facility, Division of Pathology, ICAR-IVRI, Izatnagar, Bareilly. Details of the collected samples are given in Table 2. Apparently normal mammary gland tissues were also collected during postmortem examination of female dogs to be used as control.

Table 2: Details of samples collected

S. No.	Place of sample collection	Tissues collected from suspected CMT cases	Tissues collected from normal mammary gland	Total
1	Referral Veterinary Polyclinic (RVP), ICAR-IVRI, Izatnagar	15	-	15
2	Postmortem Facility, Division of Pathology, ICAR-IVRI, Izatnagar	1	1	2

3.1.2 Chemicals, buffers and reagents

Chemicals, buffers and reagents required to perform the various techniques were purchased from different reputed firms i.e. Thermo Scientific (USA), Bio-Rad Laboratories (USA), Qiagen (USA), SRL (India), Merck (India/Germany), Novagen (EMD Biosciences), Difco (BD Company, France), Vector, Himedia (India), etc. For cell culture study, Minimum Essential Medium (MEM) with Earle's salts, L-glutamine, sodium pyruvate and sodium bicarbonate, heat inactivated US origin Sure Fetal Bovine Serum, 1X Trypsin-EDTA solution contain 0.25% trypsin and 0.02% EDTA in Hank's Balanced Salt Solution with Phenol red,antibiotic antimycotic solution 100X were procured from Himedia, HyClone and Gibco, Fetal Bovine Serum, exosome-depleted (Cat.No.A2720803, Gibco™, USA), MTT (3-(4,5-Dimethylthiazol-2-yl)-2,5-Diphenyltetrazolium Bromide) (Cat.No.M-6494 and Invitogen), Trypan Blue Stain (15250-061, Gibco, USA). CMT-U27 cell lines were procured from the Division of Animal Biochemistry, ICAR-IVRI.

The appendix and other pertinent areas provide information on the numerous reagents, solutions, media, and buffers employed in the current investigation. The appendix enlists the buffers, reagents, and media utilized in the current investigation along with information on their chemical composition and specifications. These were either made using double distilled water that was RNase or DNase free or autoclaved distilled water. The information regarding the chemicals, reagents and buffers also provided in the methods used to perform different techniques.

3.1.3 Antibodies

Primary and secondary antibodies were used for the immunohistochemistry and their details are given in Table 3.

Table 3: Details of primary and secondary antibodies used for IHC

S. No.	Particular	Catalogue number	Dilution	Manufacturer
1.	Rabbit anti estrogen receptor alpha (ER-alpha) polyclonal antibody	500-1644	1:100	AbboMax
2.	Rabbit anti-progesterone receptor	bs-0111R	1:100	Bioss
3.	Mouse monoclonal Anti-c-erbB-2 (HER-2, Neu)	E 2777	1:50	Sigma
4.	Secondary goat anti-rabbit IgG (H+L), HRP	31460	1:150	Invitrogen
5.	Secondary goat anti-mouse IgG (H+L), HRP	31340	1:150	Invitrogen

3.1.4 Kits

During the study, the different kits were used for various purposes i.e. RNeasy Mini Kit (Cat. No. 74104; Qiagen), Total Exosome Isolation Reagent (from cell culture media) (Cat. No. 4478359, Invitrogen™), complementary DNA (cDNA) synthesis High-Capacity cDNA Reverse Transcription Kit (Cat. No.4368814; Thermo Fisher Scientific), Evagreen qPCR Mastermix – ROX (Cat. No. 786-861; GBiociences, St Louis, USA), Mir-X miRNA First-Strand Synthesis Kit (Cat. No.638313; TaKaRa) was used for converting miRNAs, and other RNA molecules, into cDNA to enable specific RNAs to be quantified by real-time PCR using Mir-X™ miRNA qRT-PCR TB Green® Kit (Cat. No. 638314; TaKaRa)

3.1.5 Oligonucleotide primers for real- time PCR

The details of gene specific primers used for evaluation of expression of different receptors in the CMT are mentioned in Table 4.

Table 4: Details of oligonucleotide primer sequences used in the study

Gene name	Primer Sequence (5'-3')	Product size	References
ESR	F: AGCTCCTCCTCATCCTCTCC	100	Abbate *et al.*, 2023
	R: AGGTCGTAGAGAGGCACCAC		
PR	F: ACCTCCAGTTCTTTGCTGACGAGTC	173	Kabir. *et al.*, 2017
	R: GATCTCCATCCTAGTCCAAACACCA		
EGFR	F: ATCCGTCCTCTCCAACTATGGCTCA	153	Kabir. *et al.*, 2017
	R: TTGTCAACGATGTCCCGCCA		
HPRT	F: TGCTCGAGATGATGAAGG	191	Abbate *et al.*, 2023
	R: TCCCCTTGACTGGTCATT		
miR-19a	TCAGTTTTGCATAGATTTGCACA	-	Fish *et al.*, 2018
miR-18a	TATCTGCACTAGATGCACCTTA	-	Fish *et al.*, 2018

3.1.6 Equipment

The equipments available in the Division of Pathology, the Central Instrumentation Facility, Division of Animal Biochemistry and other laboratories of the Institute were used, whenever needed. The equipments/instruments used in the present study include Freezer (-20°C) (Vestfrost solution, India), Veriti Thermal Cycler (cat.no. 4375305; Thermo Fisher Scientific Baltics UAB), Horizontal Agarose Gel Electrophoresis Apparatus with power supply (Invitrogen), Inverted Microscope (Nikon, Japan), pH Meter (edge pH, Hanna, India), CO2 Incubator (Leec, UK), Ice Maker Machine (Blue Star, India), Gel Documentation System (Azure Biosystems, USA), Water Bath (iGeneLabServe, India), Vortex (BioSan Vortex V-1 plus, India), Autoclave (iGeneLabServe, India), Vertical Laminar Air Flow Cabinet (iGeneLabServe), Magnetic Stirrer (Tarsons, India), Refrigerator (Samsung, India), Biosafety Cabinet (ThermoScientific, U.S.A), Deep Freezer (-80°C) (Thermoscientific, USA), Centrifuge (Hermle Z326K, Germany), Electronic Balance (G&G brand scales, Asia), Hot Air Oven (Bluestar, India), and Micropipettes (Eppendorf, Germany and Thermo Scientific, USA).

3.1.7 Glasswares and plasticwares

Glasswares including beakers, bottles, flasks, measuring cylinders, test tubes etc., utilized in the laboratory were either from Borosil (India) or Schott Duran (Germany). Certified

DNAase and RNAase free (where ever necessary) plasticwares including centrifuge tubes, microfuge tubes, petriplates, pipettes, qPCR tubes, tissue culture flask etc., were from Corning (USA), Genaxy (India), Tarson (India), Thermo Fisher Scientific (USA).

3.2 Methods

3.2.1 Sample collection

The dogs with mammary growth presented at RVP, ICAR-IVRI, Izatnagar, Bareilly were examined and details of animals such as breed, age, sex, tumour location, number of mammary glands involved, consistency, etc. were recorded. Tissue samples were collected from the dogs undergone surgical removal of tumour mass. After the surgery, representative tissue samples were collected immediately without delay from the excised tumour tissue from multiple sites (minimum from 4 sites) with sterile bp blade in 10% NBF for histopathological and immunohistochemical analysis. Tissue samples were also collected in sterile vials containing RNAlater for storage at -20^{0}C for molecular studies. Small pieces of the tissues from 4 CMT cases were also collected aseptically for primary culture in 50ml centrifuge tube containing MEM media + antibiotic antimycotic solution. Normal mammary gland tissues were collected from tumour free female dogs during necropsy at Postmortem Facility, Division of Pathology, ICAR-IVRI for histopathology, IHC and molecular work.

3.2.2 Histopathological evaluation

CMT tissue samples collected in 10% NBF were allowed to fix for 2-3 days and then processed for slide preparation by following the standard protocol. Samples were submitted to Central Histopathology Laboratory, Division of Pathology for preparation of paraffin embedded tissue blocks. Briefly, CMT tissue samples were cut into small pieces with 2-4 mm thickness and were put in a cassette. The cassettes with tissue pieces were washed under running tap water for overnight. Then tissues were kept in ascending grades of ethanol for dehydration, cleared in xylene and embedded in paraffin. The tissues were cut into 4 µm thick sections in a microtome and stained with Haematoxyline and Eosin (H&E) (Luna, 1968). The stained tissue sections were examined under the brightfield microscope (Olympus, CX41) for histopathological classification and grading of CMTs.

3.2.2.1 Histopathological classification and grading

The histological classification of CMTs was done based on the modified classification of Goldschmidt *et al.,* (2011). The different CMT cases were then graded based upon nuclear pleomorphism, amount of tubular formation (as a measure of glandular differentiation) and mitotic index. Each parameter was assigned with score from 1-3 and classified into three categories (Tavasoly *et al*., 2013).

3.2.3.2 Special staining

von Kossa silver nitrate staining

The tissue sections on coated slides were deparaffinised in xylene and rehydrated in descending grades of alcohol to distilled water. The tissue sections were covered with 5% silver nitrate ($AgNO_3$) solution and incubated under ultra violet lamp for 60 minutes. Dipped the slides in 5% sodium thiosulfate for 3 minutes and washed in distilled water. After counterstaining with nuclear fast red, the slides were rinsed in distilled water, dehydrated in ascending grades of alcohol, cleared with xylene and mounted with DPX.

3.2.3 Immunohistochemistry for evaluation of expression of cancer biomarkers in CMT tissues

Immunohistochemistry (IHC) technique was used for evaluation of expression of tumour biomarkers (ER, PR, HER-2) in spontaneous CMTs. Specific primary antibodies (Table 3) were used with suitable secondary antibodies for the IHC to demonstrate the antigens in the formalin fixed paraffin embedded CMT tissue samples.

3.2.3.1 Poly L-lysine coating of slides

As IHC involves prolonged exposure of tissue sections to various solutions and heat-induced antigen/ epitope retrieval, adequate adhesion was ensured using Poly L-lysine to prevent tissue dehiscense and falling off during the process of immunostaining. For coating, slides were washed thoroughly in distilled water, dried and then immersed in 0.01% Poly L-lysine (Sigma-Aldrich, USA) for 30 min. Finally, the slides were air dried and stored in slide racks with dust proof covering for future use.

3.2.3.2 Immunostaining protocol

1. The duplicate tissue sections of 4 µm thickness were taken on the coated slides from selected tissue blocks (based on the screening of H&E-stained sections) by using microtome. Then slides with tissue sections were kept in oven at 60°C for 1 h. Then sections were deparaffinised and rehydrated using xylene and descending grades of alcohol, followed by rinsing in tap water and then taken to PBS (pH 7.4).

2. Tissue sections were processed for antigen retrieval by using microwave heating. The sections were placed in microwave resistant coplin jars and immersed in 10 mM sodium citrate buffer (pH 6) and heated for 10 min (2 cycles 5 min each) for ER-a, PR and c-erbB2.

3. Then sections were left to cool at room temperature (RT) for 20 min and then slides were washed 3 times (5 minute each) in PBS (pH 7.4).

4. Then tissue sections were incubated in freshly prepared 3% hydrogen peroxide (H_2O_2) in methanol for 45 minutes in coplin jar.

5. Then slides were washed in PBS (pH 7.4) for 3 times, 5 minutes each.

6. Then sections were covered with 5% normal goat serum and incubated at RT for 1 hour in humidifier chamber.

7. Then tissue sections were covered with appropriate dilution of primary antibodies (50-100 µL) and the negative controls were covered with 50-100 µL of PBS, and incubated overnight in a dark humidified chamber at 4°C. The dilution of 1:100 for ER and PR primary antibody was optimized for optimum immunostaining and 1:50 for HER-2 antibody was used (given in Table 3). After this, tissue sections were washed in PBS for 3 times (5 minutes each).

8. Then 50-100 µL of appropriate secondary antibody (1:150 dilution) was put on the tissue section and incubated for 1 hours at RT.

9. After washing with PBS (3 times, 5 minutes each), the tissue sections were incubated with chromogenic substrate ImmPACT™ DAB (Cat No. SK-4105, Vector

Laboratories, USA) for 10 to 30 seconds, depending on brown colour development and rinsed with distilled water for 5 minutes.

10. Then tissue sections were counter-stained with Mayer's hematoxylin for 3 minutes, rinsed in tap water and mounted with D.P.X. mountant (cat no. 23140, Molychem, Mumbai).

11. After drying, the immunostained sections were examined under brightfield microscope (Olympus, BX41) for specific immunostaining and images were captured.

3.2.3.3 Immunoscoring

The immunostained sections were scored on the basis of the staining intensity and cellular positivity percentage (%). Scoring on percent positivity for different biomarkers was done as: 0 = no immunostaining, 1 = immunostaining in <1% of cells, 2 = immunostaining in 1 to 10%, 3= immunostaining in 10 to 33%, 4 = immunostaining in 33 to 66%, and 5= immunostaining in 66 to 100%). For immunostaining intensity, the scoring done as absent = 0, weak= 1, moderate = 2 and strong = 3. The sum of both the scoring was taken as final score and it range from 0 to 8. According to recent guidelines proposed by the American Society of Clinical Oncology/College of American Pathologists (ASCO/CAP), IHC for HER2 should be scored as 0, 1+,2+, and 3+ based on the intensity and pattern of membrane labelling (Pena *et al.,* 2014)

3.2.4 Evaluation of expression ER, PR, HPRT by qPCR in CMTs

3.2.4.1 RNA extraction from tumour tissue samples

The CMT tissue samples stored in RNAlater at -20^{0}C were taken out from the Deep Freezer and total RNA were isolated using commercial RNA isolation reagent (TRIzol™ Reagent, Cat. No. 15596018, Invitrogen, USA) as per manufacturer's instructions. Briefly,

1. Prior to the RNA extraction, the CMT tissue samples preserved in deep freezer was thawed to ambient temperature.

2. Around 25-30 mg of tissue samples were taken out, cut into smaller pieces, and transferred to 2 ml eppendroff tubes containing 500 µl of TRIzol™ reagent and tissues

were homogenized using refrigerated tissue homogenizer (iGene Labserve, New Delhi). After homogenization, the clear sample suspension was transferred to a 1.5 ml of centrifuge tube and incubated at RT for 10-15 minutes.

3. Chilled chloroform (100 µl) was added to this homogenate, mixed and vortexed for 10-15 seconds and incubated at RT for 5 minutes.

4. Then tubes were centrifuged at 12,000 rpm at 4°C for 15 minutes for phase separation.

5. The upper aqueous phase containing RNA was transferred to a new 1.5 ml centrifuge tube.

6. Chilled ethanol (500 µl) was added to precipitate the RNA and kept for overnight incubation at -20°C.

7. Next day RNA isolation was carried out using RNeasy Mini Kit (Cat. No. 74104; Qiagen) by transferring up to 700 µl of the sample to RNeasy spin column placed in a 2 ml collection tube and centrifuge for 15 s at e"8000 x g (e"10,000 rpm). Discard the flow-through.

8. Add 700 µl Buffer RW1 to the RNeasy spin column and centrifuge for 15 seconds at ≥8000 x g (≥10,000 rpm) to wash spin column membrane. Discard the flow-through.

9. Add 500 µl Buffer RPE to the RNeasy spin column and centrifuge for 15 seconds at ≥8000 x g (≥10,000 rpm) to wash the spin column membrane. Discard the flow-through.

10. Add 500 µl Buffer RPE to the RNeasy spin column and centrifuge for 2 min at ≥8000 x g (≥10,000 rpm).

11. Place the RNeasy spin column in a new 1.5 ml collection tube. Add 30–50 µl RNAse-free water directly to the spin column membrane. Close the lid gently, and centrifuge for 1 min at e"8000 x g (e"10,000 rpm) to elute the RNA.

12. The extracted RNA from each tumour tissue samples were quantified by NanoDrop ND-1000 spectrophotometer (Thermos fisher scientific) to know the concentration and purity of RNA present in our sample.

3.2.4.2 Synthesis of complementary DNA (cDNA)

Equal amount of total RNA was taken for synthesis of cDNA synthesis by adjusting the concentration by dilution. The cDNA was synthesised from total RNA using commercial cDNA synthesis kit (High-Capacity cDNA Reverse Transcription Kit, Cat. No.4368814; Applied Biosystems). The reaction mixture was prepared by mixing random primers (2.0 µl), RT buffer (2.0 µl), 25mM dNTP mix (0.8µl), reverse transcriptase (1.0µl) and nuclease free water (4.2 µl) in a sterile nuclease free/ DEPC treated PCR tube (0.2 ml). After gentle mixing and brief centrifugation, 10 µl of RNA was added in the respective tubes, mixed gently and followed by incubation in a thermocycler (Veriti, Thermo Scientific, USA) as per manufacturer's instruction viz. 25°C for 10 min followed by 37°C for 120 min and 85°C for 5 min.

3.2.4.3 qPCR for gene expression analysis

The annealing temperatures for different primers were optimized by setting different annealing temperatures between 50 to 60°C in gradient thermal cycler (Applied Biosystems Veriti Thermal Cycler). The PCR products were checked by 1.5% agarose gel electrophoresis for specific amplicons. The desired yield of amplification products was obtained at an annealing temperature of 65°C for ER, and 59°C for PR as well as EGFR. The reaction mixture of qPCR was prepared (Table 5), and centrifuged briefly to settle the contents at the bottom of PCR tubes. In qPCR assay each tumour samples were tested in duplicates and a non-template control (NTC) was also used. The PCR tubes were kept in real time thermal cycler (QIAquant 96 5plex, Cat. No: 9003010) and PCR reaction was run as per the standardized thermal profile and cycling conditions (Table 6).

Table 5: Composition of qPCR mixture

Reagents	Volume for one reaction
2X SYBR® Green qPCR Mix	5 µL
Forward Primer (10µM)	0.2 µL
Reverse Primer (10µM)	0.2 µL
Nuclease-free H2O	3.6 µL
Template DNA	1 µL
Total volume	10 µL

Table 6: Thermal profile and cycling conditions for qPCR

Steps	Temperature and time	Number of cycles
Initial denaturation	95°C for 2 minutes	1
Denaturation	95°C for 10 sec	
Annealing	ER- 65°C	40
	PR-59°C for 30 seconds	
	EGFR-59°C	
Extension	72°C for 10 sec	
Melt curve analysis	60°C to 95°C with 1°C increment for every 15 seconds	1

3.2.5 Primary culture preparation for CMT tissue

The tissue samples collected in the MEM media after surgical excision of the CMT were directly brought to the lab on the ice and processed further for the cell culture. The protocol followed was as below:

1. The CMT tissue collected in 50ml centrifuge tube containing MEM media + antibiotic antimycotic solution were transferred to a petridish and rinsed with PBS for 2 times.
2. Then tumour tissues were fragmented by carefully chopping it with sterile scissor in a petridish and put in the trypsinization flask containing magnetic stirring bar. About 15 ml pre-warmed (37°C) trypsin solution (0.25%) was added to the flask and kept on a magnetic stirrer.
3. Put on the stir plate at slow speed and at a temperature of 37°C for 10 minutes.
4. The supernatant was collected and filtered through musclin cloth into 15ml centrifuge tube.
5. Then the tube was centrifuged for 10 min at 1200 rpm and supernatant was discarded without disturbing the pellet.
6. Then the cells pellet was dissolved in 5ml of 10% MEM media and cells were counted before culturing into 25cc flask.

7. The cells were seeded in the 25cc flask and incubated at 37°C in 5% CO_2 for 48 hours. The media of the plates were changed after 48 hours. The cells were incubated until there was 80-90% confluency.

8. Then cell culture was processed for subculturing. The media from the 25cc tissue culture flask of primary cultured cells was decanted and 1.0 ml of 0.25% trypsin solution (Cat.No.2062476, Gibco) was added in the flask.

9. The flask was incubated at 37°C for 3 min. to detach the cells.

10. The cells were checked for the rounding and then trypsin was decanted and the flask was tapped for detaching of cells.

11. 2 ml of MEM media was added and cells were pipetted gently. The cells were distributed equally (1 ml each) to two new 25 cc flasks containing 5 ml of media each.

12. Incubated the flasks at 37°C, 5% CO_2 until confluent monolayer was observed.

3.2.6 Isolation of exosomes from the cell culture media

The primary cultured CMT cells were seeded into 25cc flask at 1×10^5 cells/ml in 10% MEM media prepared using exosome depleted FBS (Cat. No. A2720803, Gibco™) and incubated the flasks at 37°C, 5% CO_2 until 70-80% confluent. The exosomes isolation was carried out using total exosome isolation reagent (Cat. no. 4478359, Invitrogen™), according to manufacturer's protocol. Briefly, the cell culture supernatant with exosomes depleted media was harvested and subjected for centrifugation at 2000 g for 30 min to remove precipitates. Then 3 to 4 ml supernatant was collected in fresh tube and incubated at 4°C overnight along with 1.5 to 2 ml of total exosome isolation reagent. Next day, the solution was centrifuged at 10,000 g for 1 hour at 4°C. and resuspended in 200 µL sterile cold PBS and stored at 4°C for NTA purpose and in deep freezer for miRNA analysis.

3.2.7 Evaluation of miRNA expression from exosomes by qPCR

3.2.7.1 Total RNA extraction protocol was similar to RNA extraction from CMT tissue as described previously using RNeasy Mini Kit (Qiagen), but in the initial sample here

are using 150 µL to 200 µL of exosomes samples resuspended in PBS and at final step only 15 µL total RNA was eluted.

3.2.7.2 cDNA synthesis

Mir-X miRNA First-Strand Synthesis Kit (Takara) was used to prepare the cDNA from the extracted RNA by polyadenylation and reverse transcription according to kit protocol. Briefly, the reagents mentioned in the table were taken into the RNase free 0.2ml tube, and incubated for 1hour at 37°C. Then the reaction was terminated by incubating the tubes at 85°C for 5 min to inactivate the enzymes. The cDNA prepared was stored in the -20°C for further use.

Table 7: cDNA synthesis reaction mixture

Reagents	Volume (µL)
mRQ Buffer	5
RNA sample	3.75
mRQ enzyme	1.25
Total volume	10

3.2.7.3 qPCR for miRNA expression

The reaction mixture and thermal profile was made according to TB Green Advantage qPCR Premix (Cat.No.639676; Takara Bio, USA) user manual with slight modifications (Table 8, 9 and 10). Delta-delta Ct method was used to determine the level of each miRNA relative to the level of U6 snRNA used as control. Initially qPCR amplification of U6 for each cDNA sample was performed in duplicates with no template controls (NTC) and PCR tubes were kept in real time thermal cycler (QIAquant 96 5plex, Cat. No: 9003010). The forward and reverse primer for U6 were provided along with Mir-X miRNA First-Strand Synthesis Kit.

Table 8: Composition of qPCR mixture for U6

Reagents	Volume for one reaction
Nuclease-free H2O	3.4µL
TB Green Advantage Premix (2X)	5 µL
ROX Dye (50X)	0.2 µL
U6 Forward Primer (10µM)	0.2 µL
U6 Reverse Primer (10µM)	0.2 µL
cDNA	1 µL
Total volume	10µL

Similarly, the reaction mixtures for miRNA 18a and miRNA 19a expression were prepared. The mRQ3' Primer (10 µM) was supplied along with Mir-X miRNA First-Strand Synthesis Kit and the reaction was set in duplicates. The PCR tubes were kept in real time thermal cycler (QIAquant 96 5plex, Cat. No: 9003010) and PCR reaction was run as per the standardized thermal profile and cycling conditions (Table 10).

Table 9: Constitution of qRT-PCR mixture for miRNA 18a and miRNA 19a

Reagents	Volume for one reaction
Nuclease-free H2O	3.4µL
TB Green Advantage Premix (2X)	5 µL
ROX Dye(50X)	0.2 µL
miRNA-specific primer (10µM)	0.2 µL
mRQ3' Primer (10 µM)	0.2 µL
cDNA	1 µL
Total volume	10µL

Table 10: Thermal profile and cycling conditions for qPCR

Steps	Cyclic conditions	Number of cycles
Initial denaturation	95°C for 20 seconds	1
Denaturation	95°C for 10 sec	40
Annealing	miR- 18a- 52°C	
	miR- 19a- 54°C	
Extension	72°C for 10 sec	
Melt curve analysis	60°C to 95°C with 1°C	
	increment for every 15 seconds	1

3.2.8 *In-vitro* effect of GW4869

The canine mammary gland tumour cell line CMT-U27 was obtained from Division of Animal Biochemistry, ICAR-IVRI for the *in-vitro* study. The cells were cultured in 10% MEM media and all cells were grown in 5% CO_2 humidified air at 37°C.

3.2.8.1 Preparation of GW4869 solution

The GW4869 was purchased from the commercial firm (Cat. No. HY-19363 and MedChem Express, Monmouth Junction, USA) and GW4869 stock (10mM) was prepared by dissolving 1mg of drug in 170µL DMSO. Stock solution was stored at 4°C for further use for evaluation of its effect on the cell growth by MTT assay and exosomes secretion.

3.2.8.2 GW4869 treatment to CMT-U27 cells and exosome isolation

Total $1x10^5$CMT- U27cells were seeded in each of four 25cc flasks and cells were cultures in 10% MEM media in 5% CO2 humidified air at 37°C. After 48 hours, CMT-U27 cells reached 70-80% of confluency and then media was decanted from the flasks. GW4869 compound treatment was done at 20µM, 30µM and 40 µM concentration and one flask was kept as control without any treatment and the flasks was cultured with 10% MEM media with exosome-free FBS (Cat. No. A2720803, Gibco™). After this exosomes isolation was carried out using total exosome isolation reagent (Cat. No. 4478359, Invitrogen™) by following the

manufacturer's protocol (as described in 3.2.6). Further, CMT-U27 cells in the flask were treated with 1ml of 0.25% trypsin solution and the flask was incubated at 37°C for 3 mins to detach the cells and after the cells become rounding, the flask was tapped for detaching of cells and 1 mL of media added to neutralize the trypsin and mixed properly to form a single cell suspension. Equal volume of cell suspension (20 µL) and Trypan blue (20 µL) were mixed in 0.5 ml tubes and charged onto Neubauer chamber. Cell counting was conducted using a hemocytometer. Under a10X inverted light microscope, unstained live cells were enumerated in all four corners of the hemocytometer and expressed as % of viable cells.

3.2.8.3 Nanoparticle tracking analysis (NTA) of the exosomes

Exosomes isolated in the previous section from the CMT-U27 cells and from the primary cell cultures of the CMT tissue were analysed for their size and concentration by using Nanosight NS300 (Malvern Instruments, UK) equipped with a violet laser (405/ nm) facility available at IITR, Lucknow. Before injecting into the NanoSight, samples were diluted (1:2) to achieve a working concentration. The particles in the laser beam undergo Brownian motion and videos of these particle movements were recorded. Three 60-second videos were recorded for each sample with a camera level set at 10. The temperature was maintained at 25ºC throughout the measurement process. Videos recorded for each sample were analyzed with NTA software to determine the concentration and size of measured particles with the corresponding standard error.

3.2.9 MTT assay

The 3-(4, 5-Dimethylthiazol-2-yl)-2, 5-diphenyltetrazolium bromide (MTT) (Catalogno#M6494, Invitrogen, USA) assay was employed to assess the growth inhibitory effects of GW4869 on CMT-U27 cells. The assay was conducted in triplicate to ensure reproducibility and accuracy of the results. The DMSO was utilised as a vehicle control and wells containing cells without drug or DMSO was used as cell control. In this assay total 2×104 CMT-U27 cells were seeded into pre-planned wells of 96 well plate with 10%MEM media and incubated for 24 hours to allow the cells to adhere and reach 70-80% confluence. After this, the cells were treated with various concentrations of GW4869 (10, 20, 30, 40, and

50 µM) and incubated for 24 h and 48 h. After incubation 10 µL of MTT solution (5 mg/mL in PBS) was added to pre-planned wells, and the plate was incubated in the dark at 37°C for 3 hours, allowing viable cells to metabolize MTT into purple formazan crystals. After incubation, the MTT solution was removed, and 200 µL of DMSO was added to each well to dissolve the formazan crystals. The absorbance was then measured at 590 nm using a spectrophotometer. The absorbance values were used to calculate the percentage of cell viability relative to cell control wells, with the formula:

$$\text{Cell viability (\%)} = \frac{\text{Absorbance of treated group}}{\text{Absorbance of cell control group}} \times 100.$$

3.2.12 Statistical analysis

Data were analyzed using GraphPad Prism 10 and statistical comparisons were performed using (2way ANOVA and Student's t-test), with a significance level set at $p < 0.05$.

Results

4 RESULTS

4.1 Samples details and gross lesions

In the present study, tissue samples from 16 grossly suspected cases of spontaneous CMTs were collected from Referral Veterinary Polyclinic (RVP), ICAR-Indian Veterinary Research Institute, Izatnagar, Bareilly (15) and Postmortem Facility, Division of Pathology, ICAR-IVRI, Bareilly (1). Histopathology was performed for diagnosis and classification of the CMTs and it was observed that out of total 16 cases, 15 cases were CMTs and one case was classified as lobular hyperplasia. The details of the CMTs histopathological classification are given in **Table 11**. In present investigation, it was observed that the age of all the animals with CMT were 5 years and above. The highest occurrence of CMTs was noticed in an age group of 6 - 9 years (9, 56.25%) followed by 3 - 6 years (4, 25%), and 9 - 12 years (3, 18.75%). Further, German shepherd (GSD) breed account for the highest number of CMT cases (6), followed by mongrel (5), Rottweiler (2) and one case each of Labrador, Great Dane, and Pomeranian (Plate- 1: Fig. A & B).

Grossly, CMTs observed to be present in the single or multiple mammary glands, round, elongated or irregular shaped masses with varying size and variable consistency from soft to firm to hard. Most of the CMT cases in present study were involved only single mammary gland, in 4 cases multiple mammary glands were affected. The maximum incidence of tumour was reported in inguinal pair (62.5%) of mammary glands followed by caudal abdominal pair (37.5%), cranial abdominal pair (25%), caudal thoracic pair (6.25%) (Plate- 1: Fig. C). Some tumours were severely ulcerated and exudation from the surface was noted. The diameter of tumour mass was varying from 0.5 to 20 cm, and weight varying from 3 to 3000 gm. The cut surface of tumour masses was highly diverse such as fluid filled cystic cavities, blood filled spaces (hematoma), hard bone like masses, pus, necrotic material, etc (Plate- 1 & 2: Fig. D & E & A – H).

Table 11: Details of CMT cases and their histopathological classification

S. no.	Lab ID no.	Breed	Age	Sex	Tumor Location	Place of sample collection	Gross appearance	CMT classification
1	L-821	Great Dane	7 yrs	F	R5	RVP, ICAR-IVRI	Firm to hard with pus filled cavities	Adenosquamous Carcinoma
2	L-836	Labrador	8.5 yrs	F	L5	RVP, ICAR- IVRI	Soft to firm with necrosis at centre	Intraductal papillary carcinoma
3	L-835	German Shephard	8.5 yrs	F	R3	RVP, ICAR- IVRI	Hard mass like bone	Carcinoma-mixed type
4	L-852	Mongrel	5 yrs	F	R5	RVP, ICAR- IVRI	Firm to hard with pus filled spaces	Intraductal carcinoma
5	L-853	German Shephard	6 yrs	F	R4 and R5	RVP, ICAR- IVRI	Firm with haematoma in middle and few hard areas in the tumour mass	Carcinoma-mixed type
6	L-862	German Shephard	12 yrs	F	R5 and L4	RVP, ICAR- IVRI	Firm to hard with bone like masses in the tissue	Carcinoma-mixed type
7	L-871	Rottweiler	8 yrs	F	L3	RVP, ICAR	Firm with large areas of necrosed tissue	Carcinoma-mixed type
8	L-926	Rottweiler	7 yrs	F	R5, L5 and L3	RVP, ICAR- IVRI	Soft to firm and cut surface showed cystic spaces with necrosis	Carcinoma-mixed type
9	L-927	Mongrel	12 yrs	F	L3	RVP, ICAR- IVRI	Firm with focal necrotic areas	Malignant myoepithelioma
10	M-46	German Shephard	7.5 yrs	F	L4	RVP, ICAR- IVRI	Firm to hard	Chondrosarcoma
11	M-105	Mongrel	8 yrs	F	L4 and L5	RVP, ICAR- IVRI	Firm	Lobular hyperplasia-regular
12	M-141	German Shephard	9 yrs	F	L5	RVP, ICAR- IVRI	Soft to firm	Carcinosarcoma (malignant mixed)
13	M-142	German Shephard	6 yrs	F	L2	RVP, ICAR- IVRI	Firm with nodular growth (bunch small nodules)	Intraductal papillary carcinoma
14	M-143	Pomeranian	9 yrs	F	R4	PM facility, Division of Pathology, ICAR-IVRI	Firm with necrosis of tissue	Hemangiosarcoma
15	M-264	Mongrel	12 yrs	F	R4	RVP, ICAR- IVRI	Firm to hard	Carcinoma-mixed type
16	M-265	Mongrel	6 yrs	F	L5	RVP, ICAR- IVRI	Soft to firm with cystic spaces filled with fluid.	Simple adenoma

Plate-1

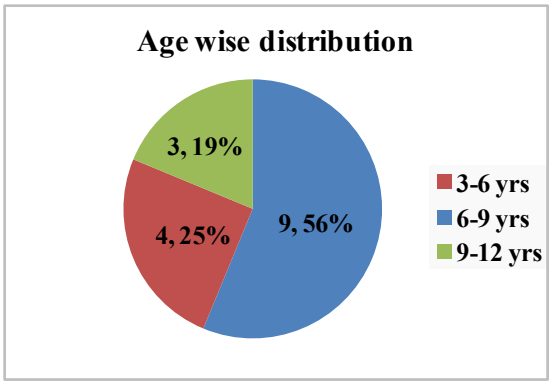

(A)

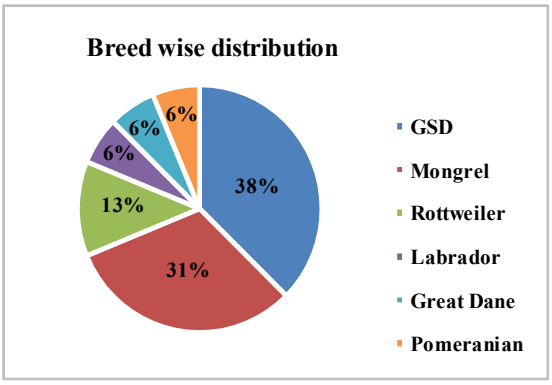

(B)

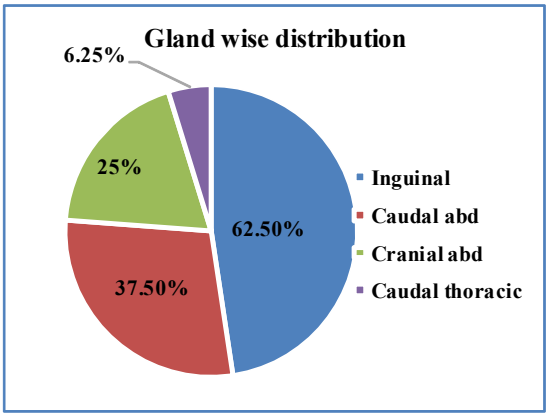

(C)

Pie charts present the distribution of CMT cases age-wise (A), breed-wise (B) and mammary gland-wise (C). Area of the pie chart reflects the proportion of the total number of cases belong to respective group.

(D)

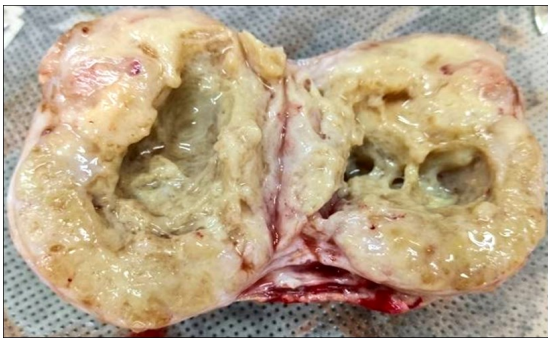

(E)

Canine mammary gland: Multiple mammary glands (L3, L5 and R5) of a female dog showing variable size swellings or growths (D). Cut section of the R5 mammary gland (D) showing greyish- yellow tissue mass with central cystic space and necrotic tissue (E).

Plate-2

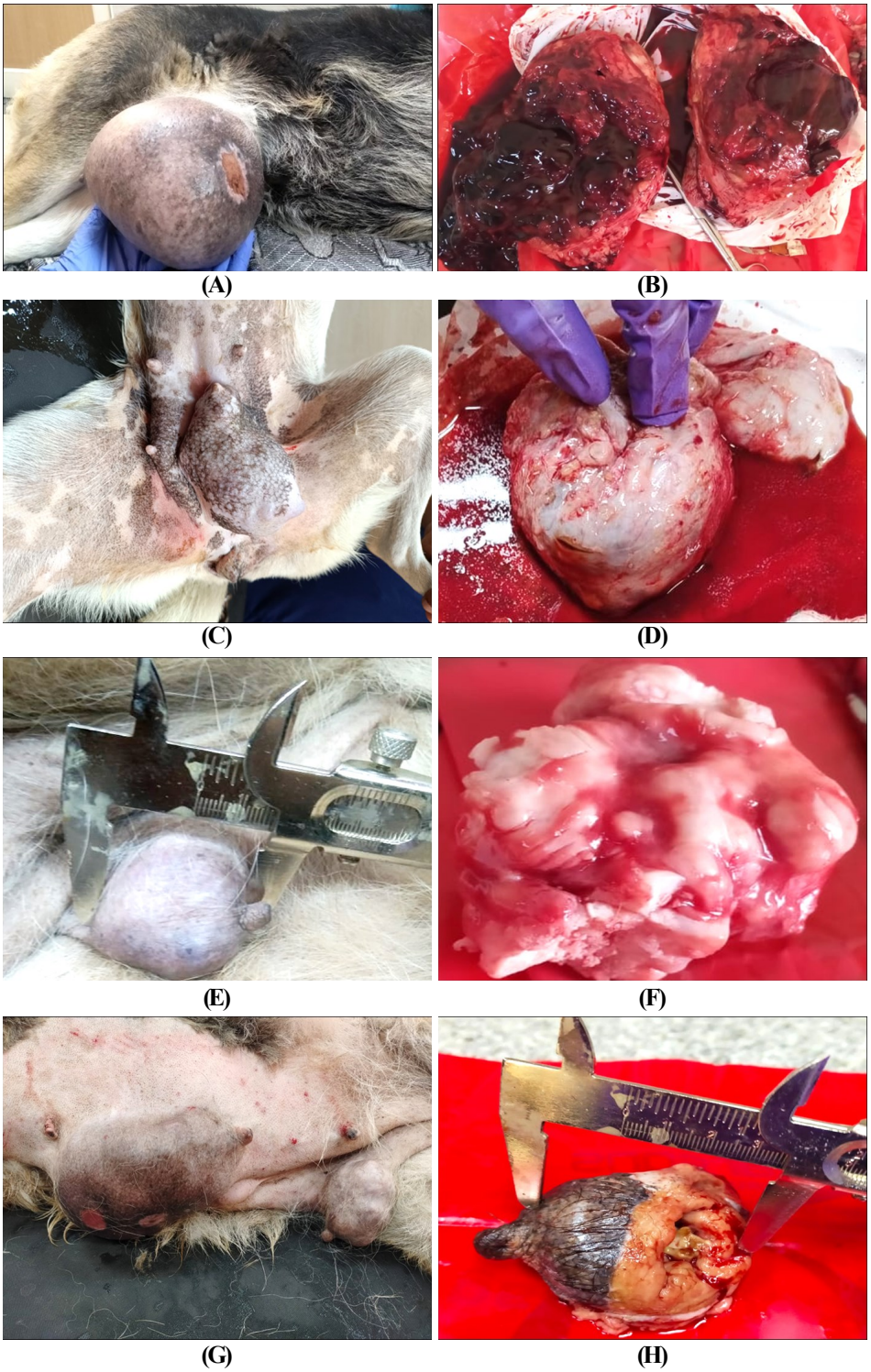

(A) **(B)**

(C) **(D)**

(E) **(F)**

(G) **(H)**

Canine mammary gland: Right caudal mammary glands (R5) of a female dog with huge spherical solid swelling or growth (A). Cut section of R5 mammary gland (Fig A) showing reddish tumour mass with central haemorrhagic area having small cystic spaces (B). Left caudal mammary glands (L5) of a female dog with large swelling or growth extending backward (C). Mammary glands (Fig. C) after excision showed tumour growth with soft consistency (D). Left caudal mammary glands (L5) of a female dog with single solitary growth (E). Cut section of the L5 mammary gland (Fig E) showing cartilaginous mass (F). Multiple mammary glands (L4 and R5) of a female dog showing variable size swellings or growths with few areas of ulcers (L4) (G). Resected tumour mass with firm consistency and central soft necrosis (H).

4.2 Histopathological classification and grading of spontaneous CMTs

4.2.1 Histological classification of spontaneous CMTs

The H & E stained tissue sections of 16 CMT cases were examined under microsope for the type of neoplastic cells involved, their cellular characteristics and distribution. Histopathological classification of CMTs was done as per modified classification of CMTs given by Goldschmidt *et al*., (2011). In the present study, 15/16 cases were confirmed as CMTs, while 1 case was classified under benign hyperplastic condition. Out of 15 CMT cases, 14 were diagnosed as malignant and one as benign. Carcinoma-mixed type (6; 40.0%) was most predominant type of CMT followed by intraductal papillary carcinoma (2; 13.3%) and one case each of ductal carcinoma (1; 6.5%), adenosquamous carcinoma (1; 6.5%), malignant myoepithelioma (1; 6.5%), carcinosarcoma (1; 6.5%), chondrosarcoma (1; 6.5%), hemangosarcoma (1; 6.5%) and simple adenoma (1; 6.5%).

4.2.1.1 Malignant epithelial neoplasms

4.2.1.1.1 Carcinoma-mixed type

Cracinoma- mixed type CMT was detected in six cases. Histopathologically, the neoplastic tissue comprised of malignant epithelial component and benign mesenchymal elements, which consisted of osteoid and cartilagenous matrix with varying degrees of calcification. The neoplasm consisted of three types of cell populations (epithelial, myoepithelial and connective tissue) with supporting fibrovascular stroma. The epithelial component showed proliferation of the glandular and tubular epithelail cells forming irregular tubules with multi-layer lining. In few cases, the epithelial cells were invasive in nature and infiltrated into the connective tissue and forming small tubular or glandular structures. Neoplastic epithelial cells showed high degree of anisocytosis, anisokaryosis and frequent mitotic figures with prominent multiple nucleoli. All cases showed elongated spindle shaped myoepithelial cells proliferation and formation of osteoid and cartilaginous tissue without any atypia. Special stain viz. von Kossa silver nitrate staining was done to demonstrate the calcium deposition and it showed black coloured calcified bone matrix in the carcinoma-mixed type CMTs (Plate – 3: Fig. A - F).

4.2.1.1.2 Intraductal papillary carcinoma

Two cases of the intraductal papillary carcinoma were diagnosed in present study. The stained canine mammary tissue sections showed presence of multi-layered pleomorphic neoplastic epithelial cells lining the ducts and forms variable projections (papillary growth) in the lumen of ducts. Neoplastic epithelial cells showed high nuclear:cytoplasmic ratio, hyperchromasia and anisokaryosis with prominent multiple nucleoli. Thin fibrovascular stroma was present in the papillary projection comprised of blood vessels and connective tissue. At few places the necrotic epithelial cells were also present between the sheets of proliferating neoplastic cells (Plate – 4: Fig. A & B).

4.2.1.1.3 Ductal carcinoma

Histologically ductal carcinoma was diagnosed in one case and it showed proliferation of the pleomorphic ductal epithelial cells aligned as cords and tubules, surrounding narrow slit like lumina. Most of the places, the ducts were lined by double layers of neoplastic epithelial cells. Moderate degree of anisocytosis and anisokaryosis was observed. Mitotic figures were frequent seen at the highly proliferating areas (Plate – 4: Fig. C & D).

4.2.1.1.4 Adenosquamous carcinoma

Single case of adenosquamous carcinoma was diagnosed out of 15 CMT cases. The tumour tissue showed presence of proliferated cuboidal to columnar neoplastic tubular epithelial cells along with multifocal areas of neoplastic cells with squamous differentiation. The poorly differentiated epithelial cells exhibited varying degrees of anisocytosis and anisokaryosis with increased nuclear:cytoplasmic ratio and nuclear hyperchromasia. Nests of squamous neoplastic cells with homogenous hyalinized keratin pearls in the centre were also seen at few areas (Plate – 4: Fig. E & F).

4.2.1.2 Malignant myoepithelial tumour

4.2.1.2.1 Malignant myoepithelioma

Out of 15 CMT cases, only one case showed histological characteristics of the malignant myoepithelioma. The tumour tissues showed presence of elongated oval to fusiform cells with

Plate-3

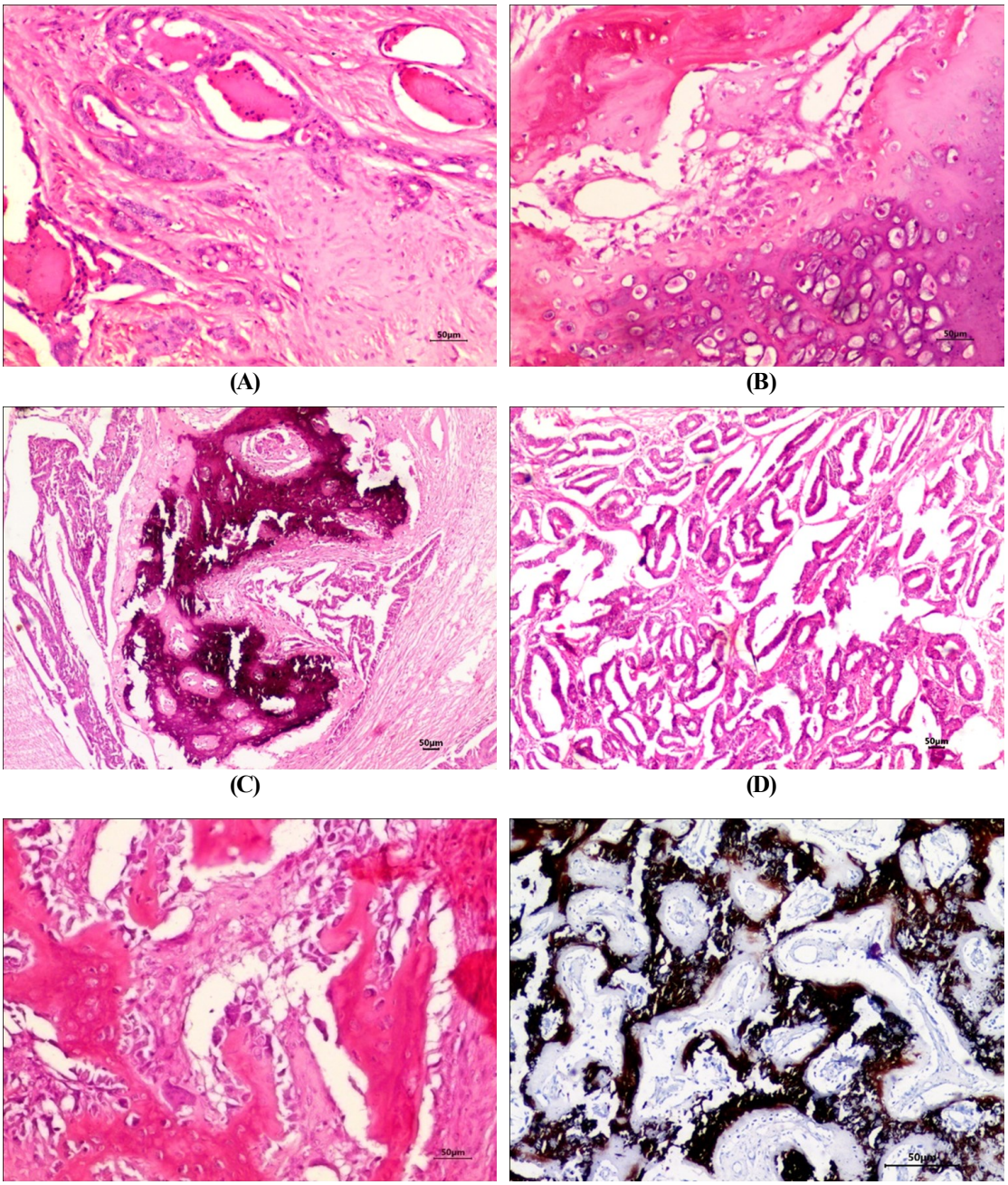

(A) (B)

(C) (D)

(E) (F)

Canine mammary gland- Carcinoma (mixed type): Proliferations of the tubular epithelial cells forming small solid structures along within connective tissues (A). H&E x100. Proliferated chondroblasts and osteoblast (B) with marked calcification (C). H&E x100. Neoplastic epithelial component forming adenoid to tubular patterns (D). H&Ex 100. Osteoid tissue in the mammary gland with hyperchromatic osteoblasts and few osteoclasts (E). H&E x 100. Calcification in the osteoid tissue of mammary gland demonstrated by black to brown colour (F). Von Kossa Silver Nitrate stain x 100.

Plate-4

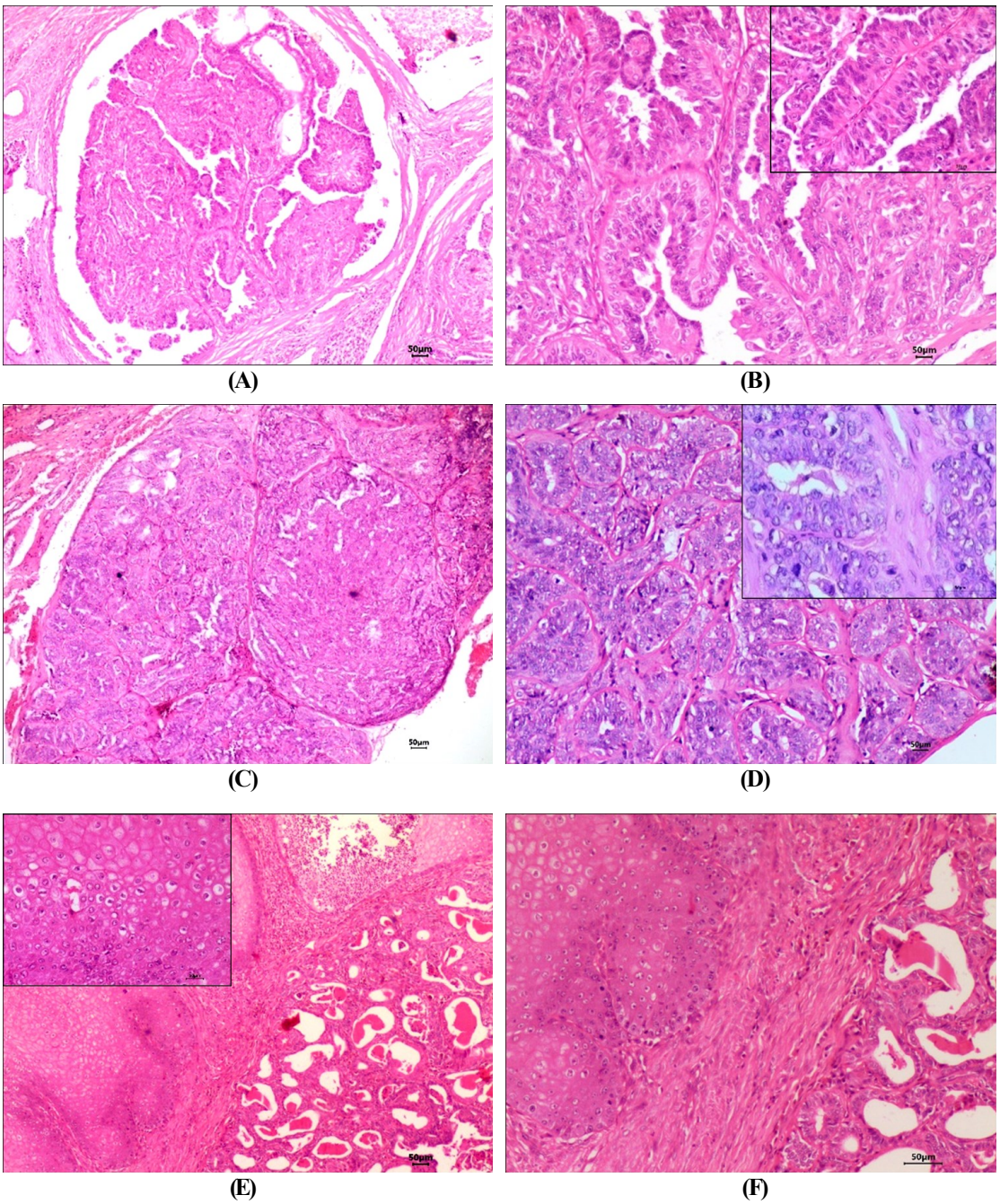

(A) **(B)**

(C) **(D)**

(E) **(F)**

Canine mammary gland- Intraductal papillary carcinoma: Papillary type growth of the neoplastic epithelial cells supported by thin fibrovascular stalk within the lumen of an ectatic duct of mammary gland (A). H&E x100. Higher magnification of Fig. A showing lining tubular epithelial cells proliferation on the thin fibrovascular connective tissue core (inset) (B). H&E x200.

Canine mammary gland- Ductal carcinoma: Neoplastic tissues with pleomorphic epithelial cells aligned as cords, small ducts and scanty stromal connective tissue (C). H&Ex100. Higher magnification of Fig. C showing proliferated tubular epithelial cells with mitotic figures and forming small ducts with minimal lumen (inset) (D). H&E x200.

Canine mammary gland- Adenosquamous carcinoma: Proliferated neolastic epithelail cells forming glandular structure on one side and another side it showed neoplastic squamous epithelial cells proliferation (inset) (E). H&E x100. Higher magnification of Fig. E showing thick connective tissue in between the both neoplastic squamous cells and glandular cells (F). H&E x200

indistinct cell borders and significant amount of slightly eosinophilic cytoplasm with few clear intracytoplasmic vacuoles. Nuclei were hyperchromatic, often central and round to oval in shape with prominant nucleoli. Area with myxoid differetntiation were frequently present in the tissue and showed moderate amount of myxoid matrix with star shaped cells. Neoplastic cells showed anisocytosis, anisokaryosis and frequent mitotic figures. Multi-focal areas of necrosis and occasional neovascularisation were also noticed (Plate – 5: Fig. A, B & C).

4.2.1.3 Malignant mixed mammary tumors

4.2.1.3.1 Carcinosarcoma

Carcinosarcoma (malignant mixed CMT) was found in one case. The tissue sections of the carcinosarcoma showed presence of neoplastic tissues composed of both malignant epithelial components and malignant mesenchymal components. Histologically, the tissue sections showed proliferation of the glandular and tubular epithelial tissue forming papillary, solid and tubular pattern at different locations. The nuclei were large hyperchromatic and showed mitotic figures frequently. The sarcomatous portion showed presence of osteomatous, chondromatous, fibromatous and myxomatous differentiations at various locations. Fibroblasts showed presence of hyperchromatic nuclei with frequent mitotic figures. The osteoid matrix of osteosarcomatous tissue showed variable degrees of calcification. Vascular invasion of neoplastic cells was also noticed in the stromal vasculature (Plate – 5: Fig. D, E & F).

4.2.1.4 Malignant mesenchymal neoplasms

4.2.1.4.1 Chondrosarcoma

One case showed histopathological characteristics of the chondrosarcoma where-in they showed extensive proliferation of chondrocytes that has replaced the normal epithelial component of mammary gland with varying degree of chondrocytes with basophilic cytoplasm (Plate – 6: Fig. A, B & C).

4.2.1.4.2 Hemangiosarcoma

One case showing histopathological characteristics of the hemangiosarcoma was also found in present study. The tumour tissue consisted of proliferated neoplastic endothelial cells

aligned as multiple and irregular vascular structures engorged with blood corpuscles and extensive haemorrhagic areas in the surroundings. Areas with numerous capillary like structures were frequently seen at various locations of the sections. Solid areas with proliferated endothelial cells without capillaries were also present. These cells showed varying degrees of anisocytosis and anisokaryosis with increased nuclear:cytoplasmic ratio and nuclear hyperchromasia. Pleomorphic nuclei with granular chromatin showed prominent nucleoli often multiple in number (Plate – 6: Fig. D, E & F).

4.2.1.5 Benign mammary tumours

4.2.1.5.1 Simple adenoma

One case of benign CMT was detected in present investigation which was diagnosed as simple adenoma. The CMT tissue sections showed glandular epithelial cells proliferation forming small acinar and tubular structures with moderate amount of fibrovascular stroma. The tubules were lined by single to multiple layers of cuboidal to columnar epithelial cells with considerable amount of eosinophilic cytoplasm. Cells showed central round nuclei with inconspicuous nucleoli. Nuclear:cytoplasmic ratio was moderate and mitotic figures were minimal. Mild to moderate degree of anisocytosis and anisokaryosis were observed in the neoplastic cells (Plate – 7: Fig. A, & B).

4.2.1.6 Hyperplasia/Dysplasia

4.2.1.6.1 Lobular hyperplasia (Adenosis)

Hyperplastic changes were noticed in one case and diagnosed as lobular hyperplasia. The foci of lesion consisted of non-neoplastic proliferation of intralobular ducts causing an increased numbers of ductules, ducts and acini per lobule. Cellular atypia of epithelium was absent. The intralobular and interlobular connective tissue stroma was abundant and relatively acellular (Plate – 7: Fig. C & D).

4.2.2 Histopathological grade of CMTs

The different CMT cases were then graded based upon nuclear pleomorphism, amount of tubular formation (as a measure of glandular differentiation) and mitotic count in H&E

Plate-5

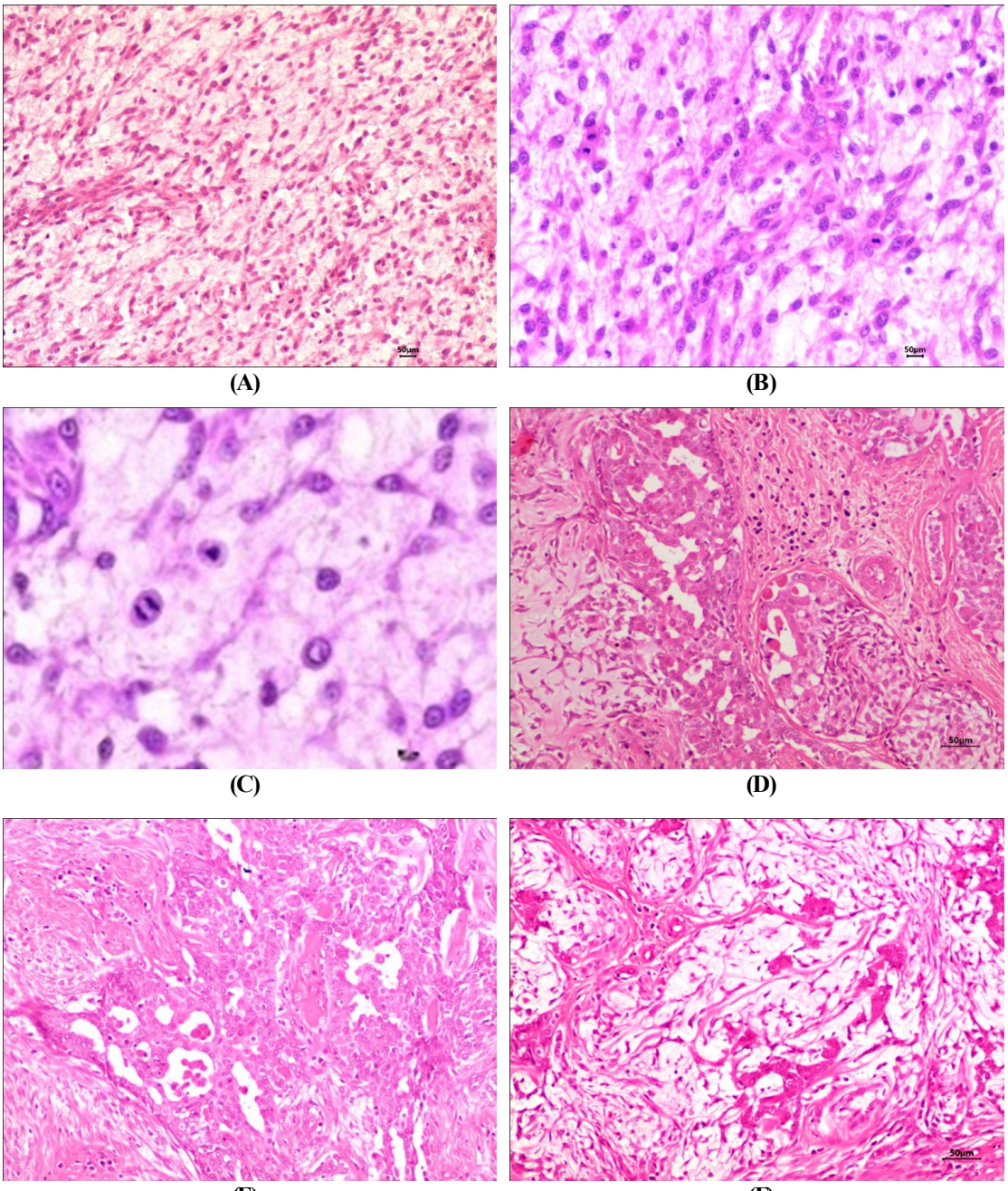

(A) (B)

(C) (D)

(E) (F)

Canine mammary gland- Malignant myoepithelioma: Proliferated myoepithelial cell with both spindle to satellite shape hyperchromatic nuclei (A&B). H&Ex 100. Proliferated myoepithelial cell with frequent mitotic figures (C). H&Ex 200.

Canine mammary gland- Carcinosarcoma: Both epithelial and myoepithelial cell proliferation along with myxomatous change and infiltration of mononuclear cells (D). H&Ex 100. Proliferated epithelial cells invaded in the adjacent stromal tissue and forming solid to papillary pattern (E). H&Ex 100. Myxomatous tissue with stellate shaped cells and myxoid stroma (F). H&Ex 100

Plate-6

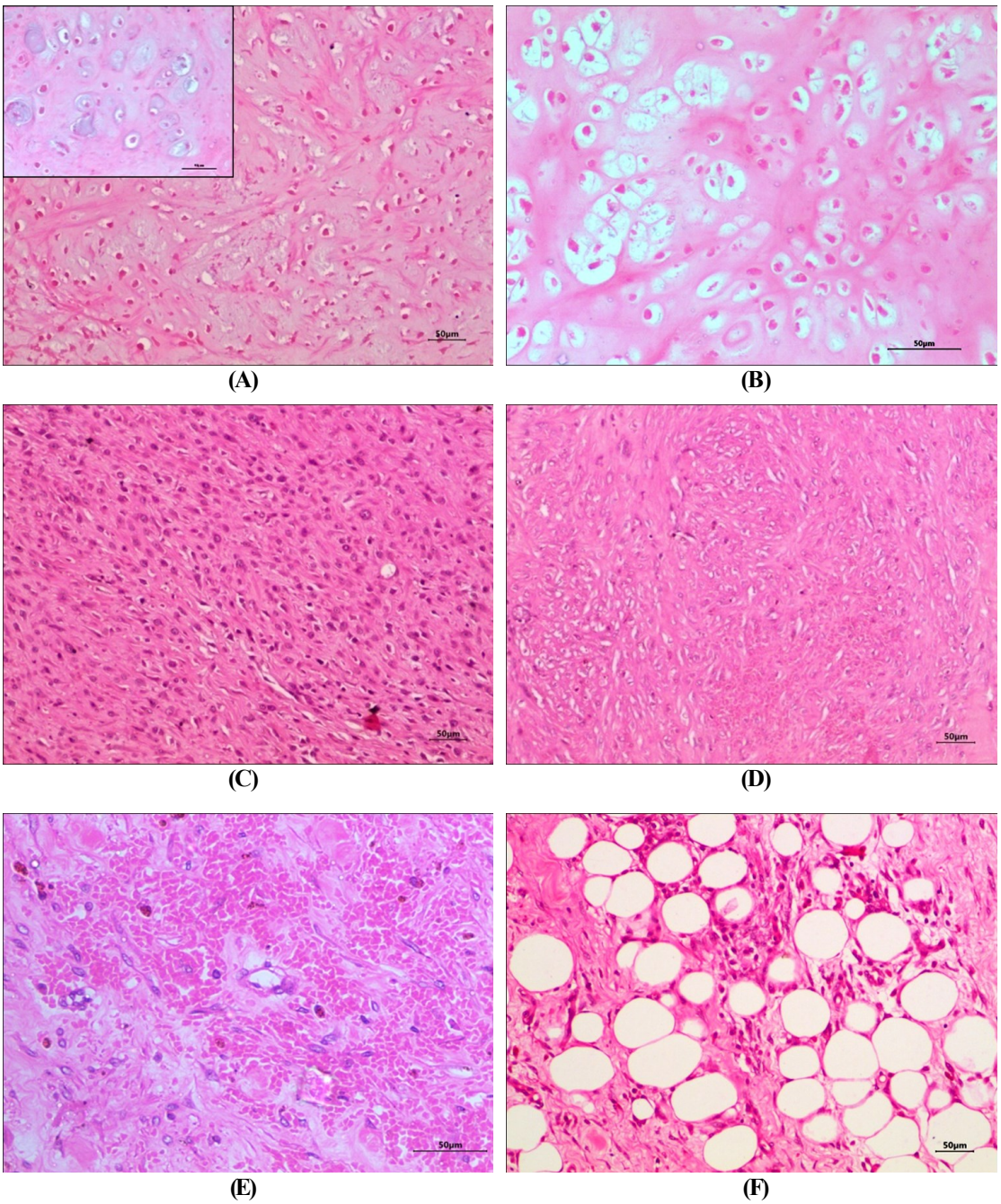

(A) (B)

(C) (D)

(E) (F)

Canine mammary gland- Chondrosarcoma: Proliferated chondroblasts with slightly basophilic cytoplasm with marked anisokaryosis (inset) (A). H&E x100. Higher magnification of Fig A showing neoplastic chondroblasts (B). H&E x100. Proliferated fibroblasts forming solid compact tissue showing hyperchromasia and marked pleomorphism in another area of the chodroblastic tissue (C). H&E x100. Canine mammary gland- Hemangiosarcoma: Proliferated endothelial cells with spindle shaped nuclei forming small blood filled spaces with marked connective tissue proliferation (D). H&E x100. Small RBCs filled capillaries lined by sparse neoplastic endothelial cells (E). H&E x200. Proliferated fibroblasts within fatty connective tissue (F). H&E x100

Plate-7

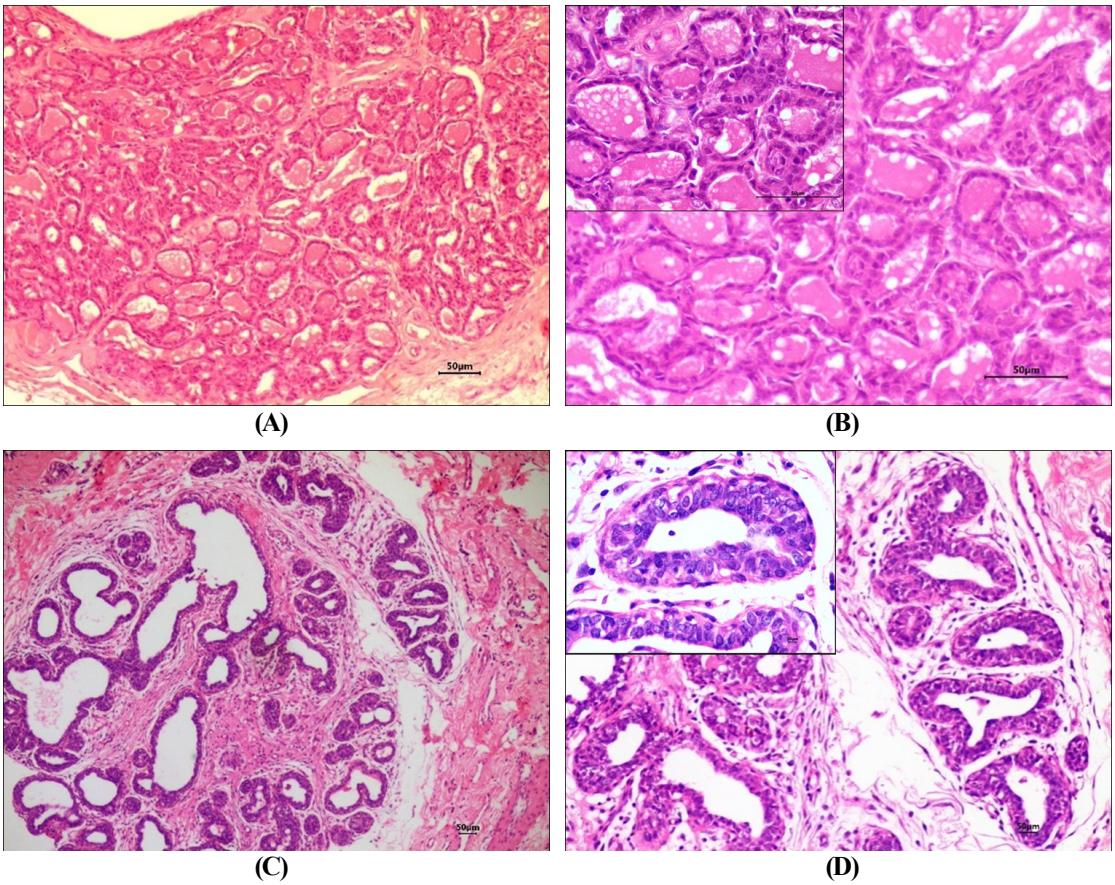

(A) (B)

(C) (D)

Canine mammary gland- Simple adenoma: Proliferated epithelial cells forming glandular pattern with thin connective tissue stroma (A). H&Ex100. Glandular epithelial cells with mild degree of pleomorphism arranged in glandular structure filled with eosinophilic contents in the lumen (inset) (B). H&Ex200. Canine mammary gland- Lobular hyperplasia: Focal areas of glands lined by single or double layered epithelial cells with supra basal type myoepithelial cells (C). H&Ex100. Lining epithelial cells of the glands with hyperchromatic nuclei and minimal pleomorphism (inset) (D). H&Ex 200

stained tumour sections. Each parameter was assigned with score from 1-3 and classified into three categories (Tavasoly *et al*., 2013). Out of 16 CMTs graded, 1 case (6.25%) were of high grade, 8 cases (50.0%) of intermediate grade and 4 cases (25%) of low grade and 2 cases were malignant sarcomas and 1 case was carcinosarcoma. (Table 12)

Table 12: Histopathological grading of CMT cases

Case number	HP classification	Amt of tubules formation	Nuclear pleomorphism	Mitotic count	Total score	HP grade
L-821	Adenosquamous Carcinoma	3	2	1	6	2
L-836	Intraductal papillary carcinoma	2	2	1	5	2
L-835	Carcinoma-mixed type	2	2	1	5	1
L-852	Intraductal carcinoma	1	2	2	5	1
L-853	Carcinoma-mixed type	2	3	1	6	2
L-862	Carcinoma-mixed type	3	3	2	8	3
L-871	Carcinoma-mixed type	2	3	1	6	2
L-926	Carcinoma-mixed type	2	2	2	6	2
L-927	Malignant myoepithelioma	2	2	3	7	2
M-105	Lobular hyperplasia- regular	1	1	1	3	1
M-142	Intraductal papillary carcinoma	1	3	2	6	2
M-264	Carcinoma-mixed type	3	2	1	2	2
M-265	Simple adenoma	1	1	1	1	1

4.3. Immunohistochemical expression of ER, PR and EGFR in spontaneous CMTs

Immunohistochemistry (IHC) technique was used for evaluation of expression of tumour biomarkers (ER, PR, HER-2) in spontaneous CMTs. Immunoscoring was done according to Pena *et al.,* 2014 and results are presented in Table 13.

4.3.1 Evaluation of ER

The immunohistochemistry for ER revealed positive strong cytoplasmic staining in the neoplastic epithelial cells of simple adenoma with immunoscore of 7 and DAB staining was also observed in the connective tissue stroma and secretions of mammary gland and negative control there was no DAB staining and 2 out of 14 malignant tumours (2 intraductal papillary

carcinoma) were positive with, one case showing moderate cytoplasmic staining in proliferated neoplastic epithelial cells along with connective tissue stroma and secretions of mammary gland showed DAB staining while the other case showed mild intracytoplasmic immunostaining with immunoscore of 6 and 4 (Plate – 8: Fig. C & E) respectively and in negative control there was no DAB staining (Plate – 8: Fig. A to F).

4.3.2 Evaluation of PR

The immunohistochemistry for PR revealed 2 out of 10 CMTs (Carcinoma- Mixed type) were positive with strong cytoplasmic staining in the proliferated neoplastic epithelial cells with immunoscore of 6 and DAB staining was also observed in the inflammatory cells and macrophages and in negative control there was no DAB staining (Plate – 9: Fig. A to F).

4.3.2 Evaluation of HER-2

HER-2 immunostaining was observed in only one out of 14 malignant (carcinosarcoma-malignant mixed) CMTs and showed moderate, heterogeneous complete membrane labeling (chicken-wire pattern) in 30% of cells along with cytoplasmic staining in proliferated neoplastic epithelial cells and was considered 2+, according to the guidelines proposed by the American Society of Clinical Oncology (ASCO) for HER-2 labelling interpretation and in negative control there was no DAB staining (Plate – 10: Fig. A to F).

Table 13: Immunohistochemistry scoring from 0-8 (based on percentage of stained cells and intensity of staining) for ER and PR

Tumour type	Receptor	Scoring for immuno positivity	Scoring for immunostaining intensity	Total Immunoscore
Simple adenoma	ER	4	3	7
Intraductal papillary carcinoma	ER	3	2	6
Intraductal papillary carcinoma	ER	3	1	4
Carcinoma- mixed type	PR	3	3	6

Plate-8

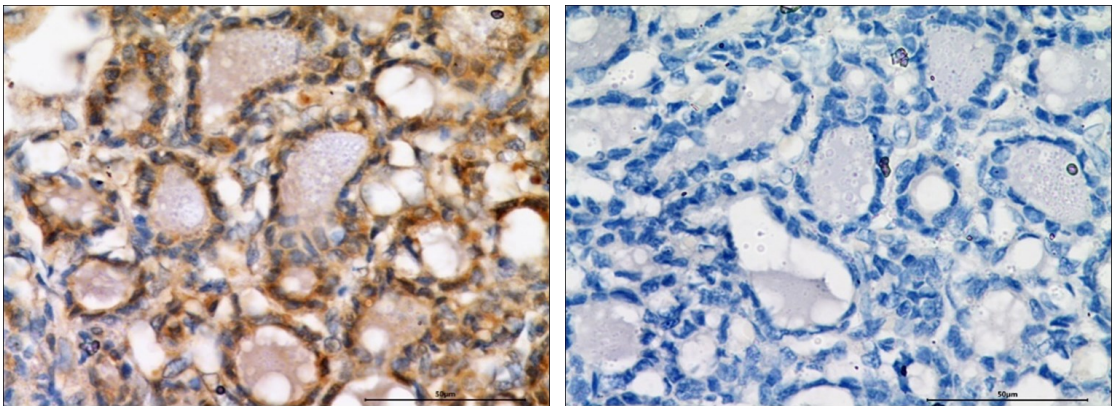

(A) (B)

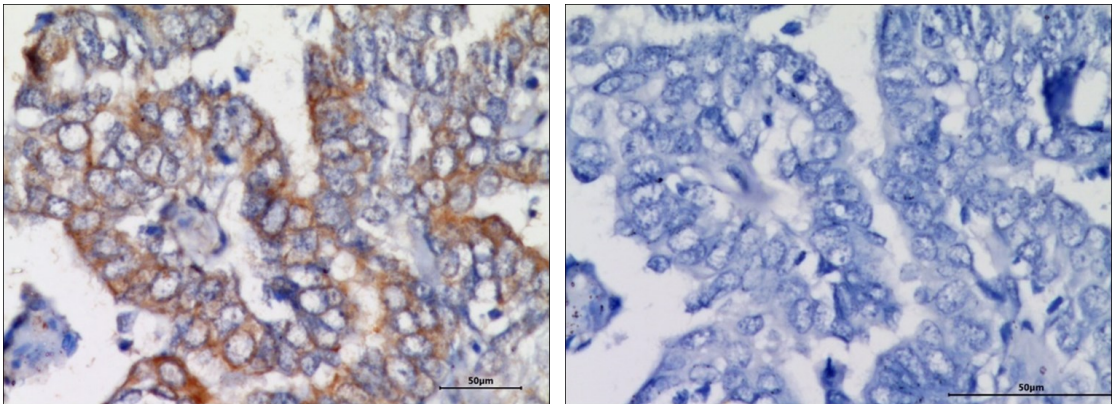

(C) (D)

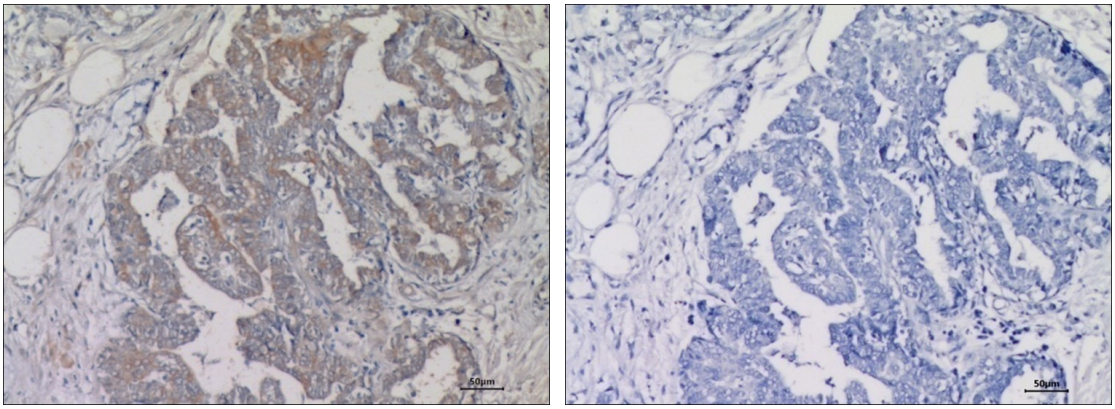

(E) (F)

Canine mammary gland: Strong immunostaining (dark brown) in the cytoplasm of proliferated epithelial cells of the mammary gland for ER in simple adenoma (A). Antibody control tissue section showed no immunostaining (B). IHCx DAB x Mayer's hematoxylin x 100. Moderate degree of cytoplasmic immunostaining (dark brown) in the proliferated epithelail cells of papillary growth in the mammary gland for ER in intraductal papillary carcinoma (C) IHCx DAB x Mayer's hematoxylin x 100. Antibody control tissue section showed no immunostaining (D). IHCx DAB x Mayer's hematoxylin x 200. Mild immunostaining (dark brown) in the proliferated epithelial cells (I/C) of duct arranged as papillary outgrowths for ER in intraductal papillary carcinoma (E). Antibody control tissue section showed no immunostaining (F). IHCx DAB x Mayer's hematoxylin x 100

Plate-9

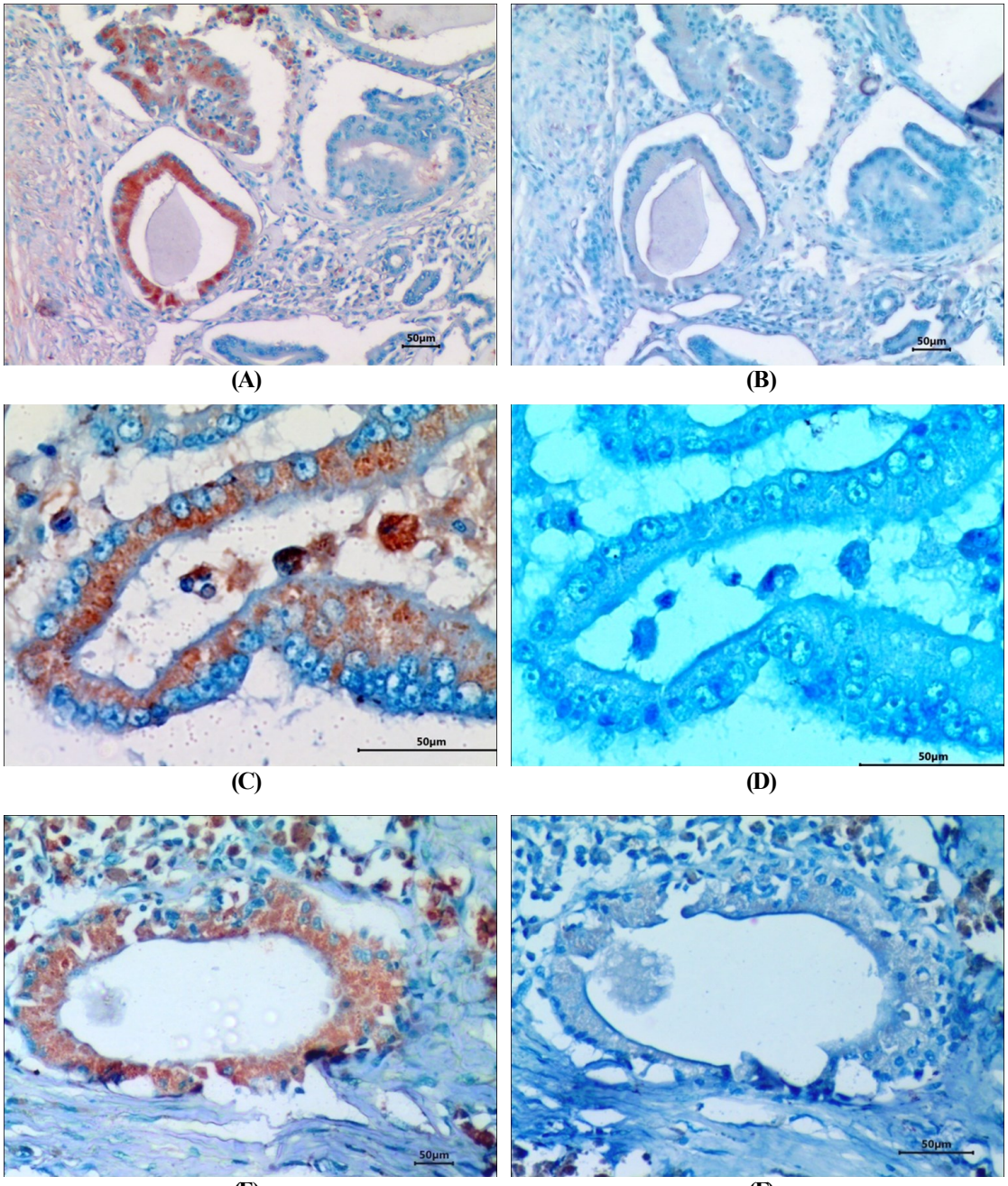

(A) (B)

(C) (D)

(E) (F)

Canine mammary gland: Strong immunostaining (dark brown) in the cytoplasm of ductal epithelial cells and few mononuclear cells of the mammary gland for PR in carcinoma mixed type (A). Antibody control tissue section showed no immunostaining (B). IHCx DAB x Mayer's hematoxylin x 100. Strong immunostaining (dark brown) in the cytoplasm of ductal epithelial of the mammary gland for PR in carcinoma mixed type (C). Antibody control tissue section showed no immunostaining (D). IHCx DAB x Mayer's hematoxylin x 400. Strong immunostaining (dark brown) in the cytoplasm of ductal epithelial cells and mononuclear cells of the mammary gland for PR in carcinoma mixed type (E). Antibody control tissue section showed no immunostaining (F). IHCx DAB x Mayer's hematoxylin x 200

Plate-10

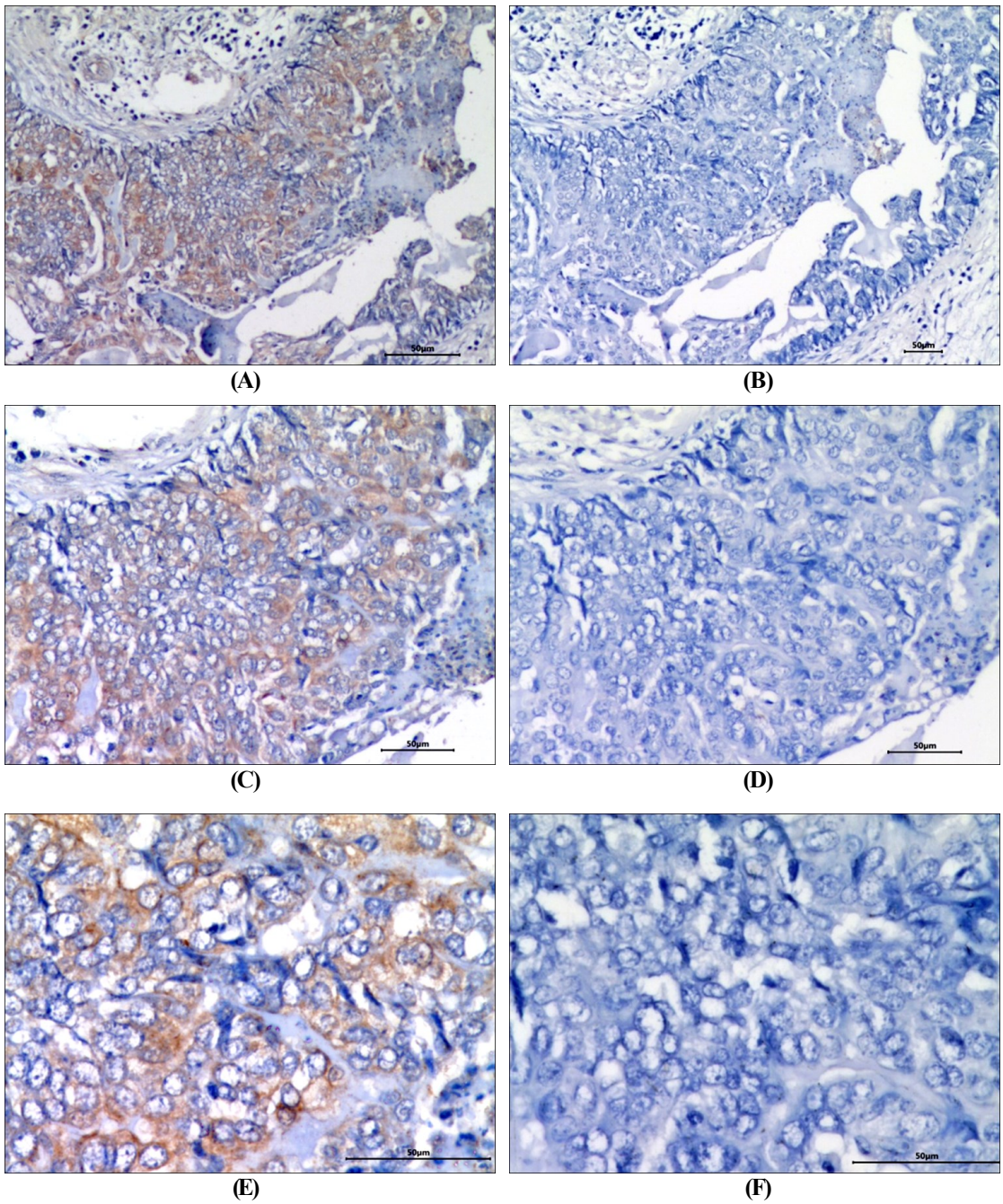

(A) (B)

(C) (D)

(E) (F)

Canine mammary gland: Moderate immunostaining (dark brown) in the membrane and cytoplasm of the epithelial cells of the mammary gland for HER-2 in carcinosarcoma (A). Antibody control tissue section showed no immunostaining (B). IHCx DAB x Mayer's hematoxylin x 100. Higher magnification of Fig A and B. (C&D) IHCx DAB x Mayer's hematoxylin x 200 and (E&F) IHCx DAB x Mayer's hematoxylin x 400.

Plate-11

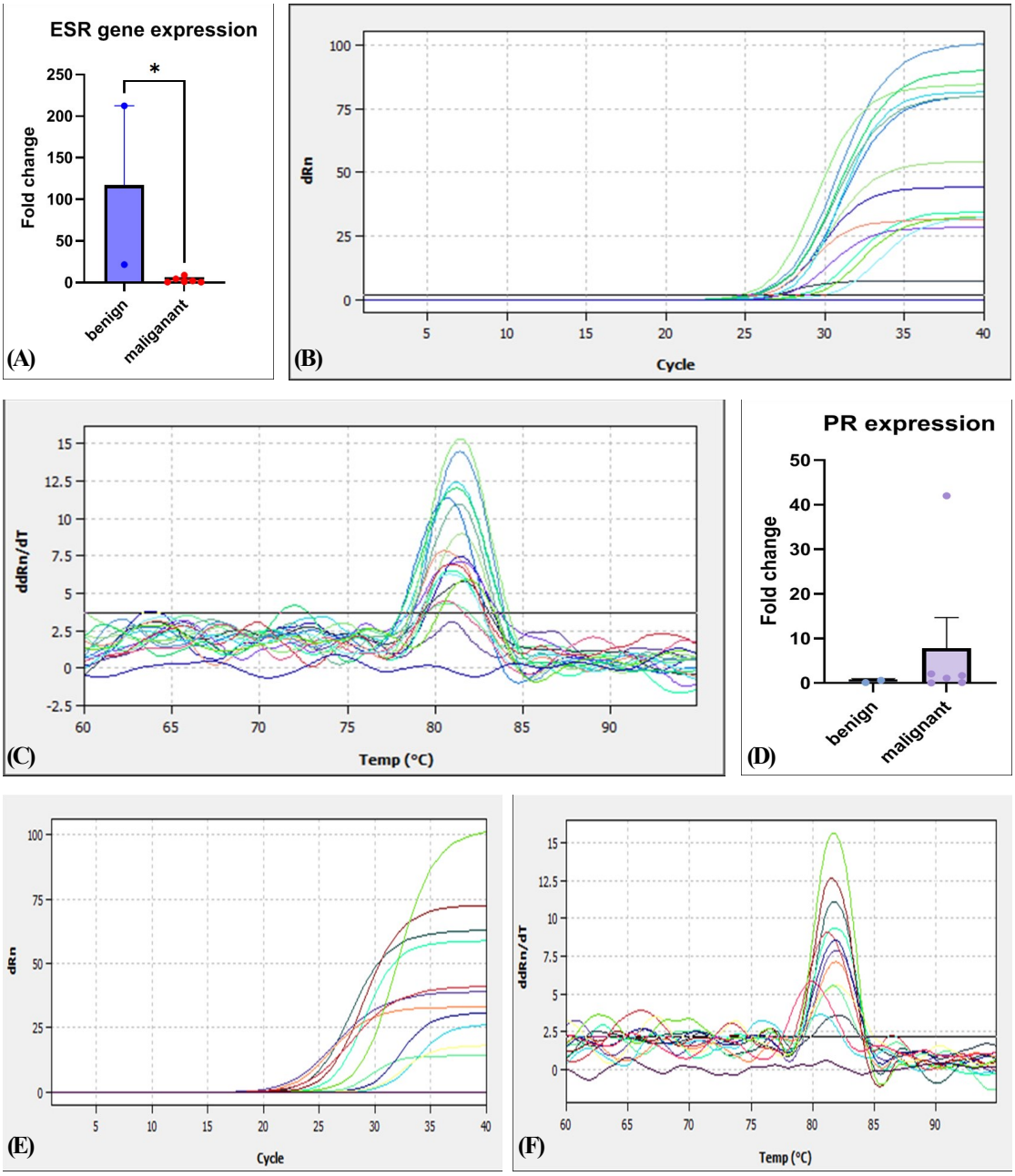

Graph showing relative expression of ESR mRNA in CMT tissues (A). Amplification (B) and melt curve (C) of real time PCR assay for ESR.

Graph showing relative expression of PR mRNA in CMT tissues (D). Amplification (E) and melt curve (F) of real time PCR assay for PR.

Plate-12

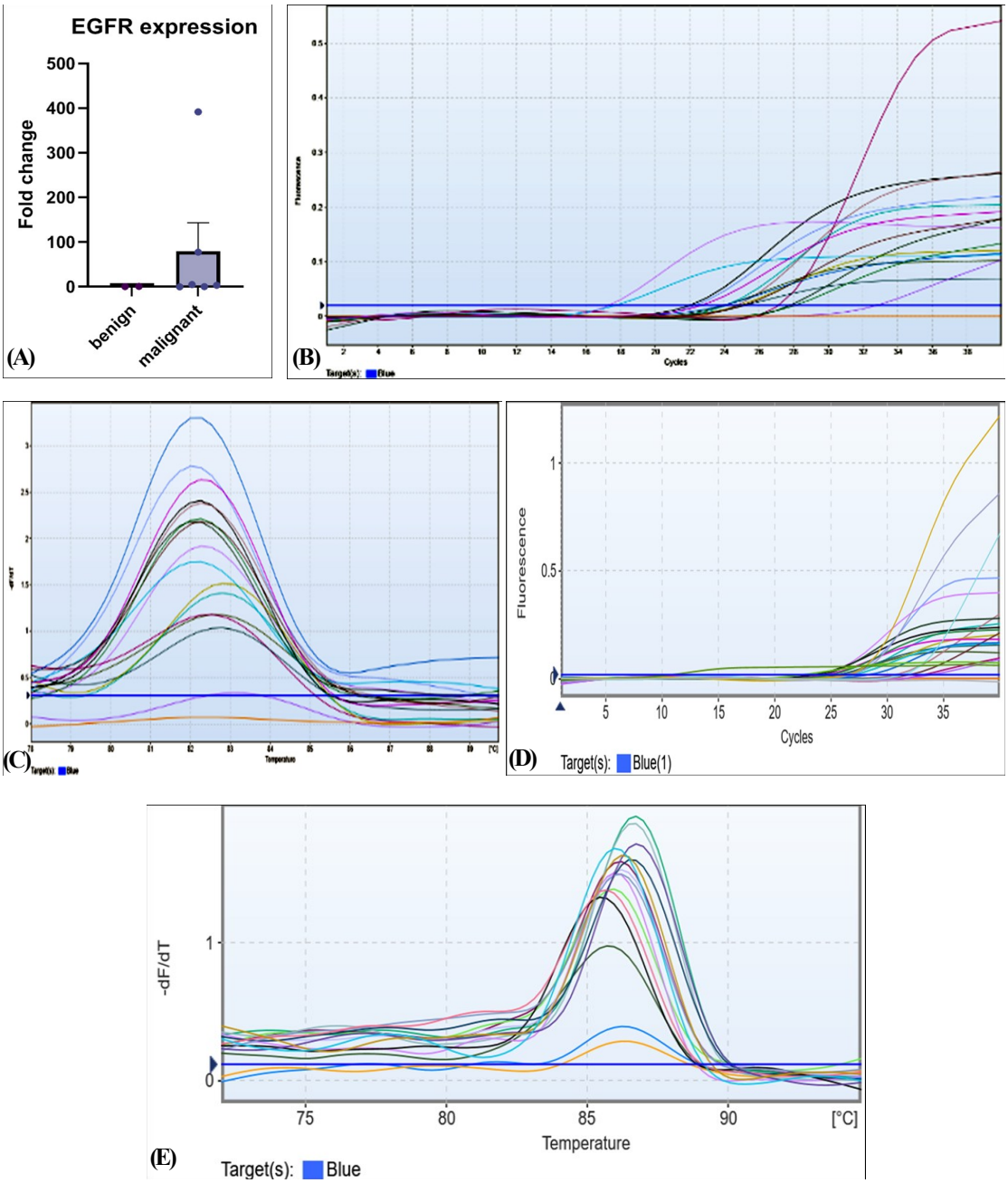

Graph showing relative expression of EGFR mRNA in CMT tissues (A). Amplification (B) and melt curve (C) of real time PCR assay for EGFR.
Amplification (D) and melt curve (E) of real time PCR assay for HPRT.

4.4 Assessment of relative expression of ESR, PR & EGFR genes in spontaneous CMTs using qPCR

In the present study, mRNA expression of ESR, PR and EGFR was evaluated to study the expression of these markers at gene level from 2 benign tumours (simple adenoma and lobular hyperplasia), 2 carcinoma- mixed type and each one from intraductal papillary carcinoma, intraductal carcinoma, malignant myoepithelioma and carcinosarcoma- malignant mixed and classified into benign and malignant group and one normal mammary gland was used as biological control for statistical analysis. SYBR green based quantitative real time PCR assay was carried out to study relative fold change in expression of these markers in spontaneous CMTs.

4.4.1 ESR expression in tumour tissues

The relative fold change in ESR expression was found in 5 out of 8 cases (55.56%) and there was a stastical difference was observed with mean relative fold change between benign tumour and malignant tumors was 114.1 +/- 45.01 and a greater fold change of 212.306 was observed in simple adenoma when compared with control sample (Plate – 11: Fig. A to bC).

4.4.2 PR expression in tumour tissues

The relative fold change in PR expression was found in 4 out of 8 cases (50%) and there was no stastical difference was observed with mean relative fold change between benign tumour and malignant tumors was 7.485 +/- 12.50 and a greater fold change of 42.008 was observed in carcinoma-mixed type when compared with control sample (Plate – 11: Fig. D to F).

4.4.2 EGFR expression in tumour tissues

The relative fold change in EGFR expression was found in 4 out of 8 cases (50%) and there was no stastical difference was observed with mean relative fold change between benign tumour and malignant tumors was 79.21 +/- 116.1 and a greater fold change of 391.91 and 77.71 was observed in carcinosarcoma and malignant myoepithelioma when compared with control sample respectively (Plate – 12: Fig. A to C).

HPRT gene was used as endogenous control for gene expression analysis (Plate – 12: Fig. D & E). Although there was positive fold change for ESR, PR and EGFR genes in some cases obtaining a stastical significance was not feasible due to less sample size.

4.5 *In vitro* culturing of primary CMT cells and evaluation of exosomal cargo

4.5.1 *In vitro* culturing of primary CMT cells

Five CMT tissue samples (4 malignant, one benign) were collected aseptically in the MEM media for processing them further for primary culture. During *in vitro* primary culture, only 2 samlpes viz. intraductal papillary carcinoma (M1) and simple adenoma (B1), were successfully cultured, other got contaiminated and did not show any cellular attachment to the flask surface and growth. Only 20-30% of M1 cells were attached to flask after 18h of seeding. M1 cells showed about greater than 50% growth after 24h. M1 cells showed fast growth and covered almost entire flask surface (95%) after 48h of incubation. The M1 cells passaged further (P1) and it was observed that M1 cells at P1 still grow very fast and formed monolayer within 24h. Further M1 (P1) cells were trypsanized and passage of (P2) further in 10% MEM media with exosome depleted FBS for exosomal study. M1 (P2) cells reached at 70 to 80% confluency after 60h, and then cell culture supernatant was collected and exosomes were isolated by using commercially available kit. After collecting supernatant, the cells were further passaged (P3) and incubated in normal 10% MEM media but the M1 cells showed minimal attachment at the surface of flask. At 72h cells were failed to form a monolayer, showed rounding and started to detach from the surface (Plate – 13: Fig. A to F).

The B1 cells were also processed similarly as M1 cells, and it was observed that <20% of B1 cells were attached to surface of the flask after 24h of seeding (Plate – 13: Fig. G). Further incubation showed 40 to 50% of confluency after 60h (Plate – 13: Fig. H) and after 72h, the cells reached around 70 to 80% confluency (Plate – 13: Fig. I). A confluency of 90% was observed after 96h showing slow growth of the B1 cells as compared to M1 cells (Plate – 13: Fig. J). B1 cells passaged further (P1) in MEM containing 10% exosome depleted FBS and cells reached 70 to 80% confluency after 72h (Plate – 13: Fig. K). At 72h the B1 cells showed prominent morphological changes such as increased size in 10% MEM media

Plate-13

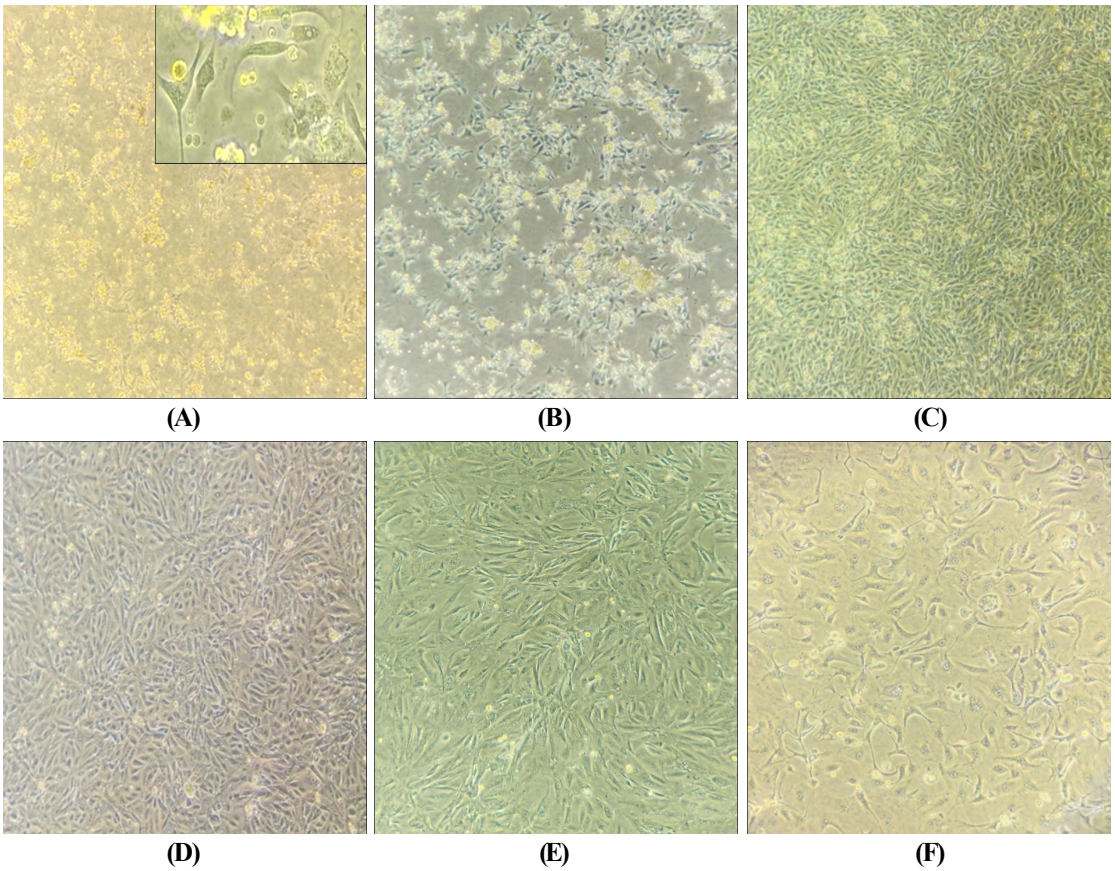

(A) (B) (C)

(D) (E) (F)

Primary cell culture- Intraductal carcinoma: Primary cell culture growth after 18 h of incubation (A); elongated attached cells at the flask base (inset); cell growth after 24 h (B); cell growth after 48 h (C); P-1 cells 80 to 90% confluency after 24 h of incubation (D); P-2 cells showing using 70 % to 80% confluency in exo depleted FBS after 60 h (E); P-3 cells showing 50-60% confluency after 72 h (F).

Conted...

Plate-13

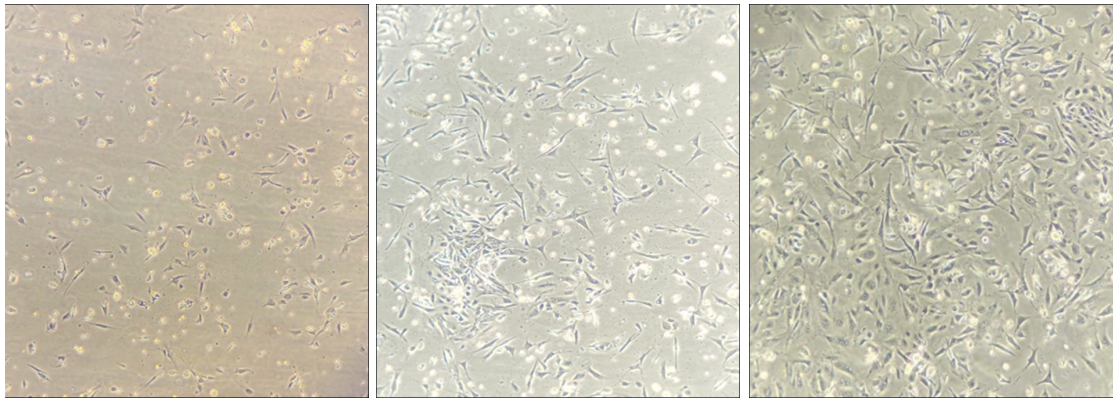

(G) (H) (I)

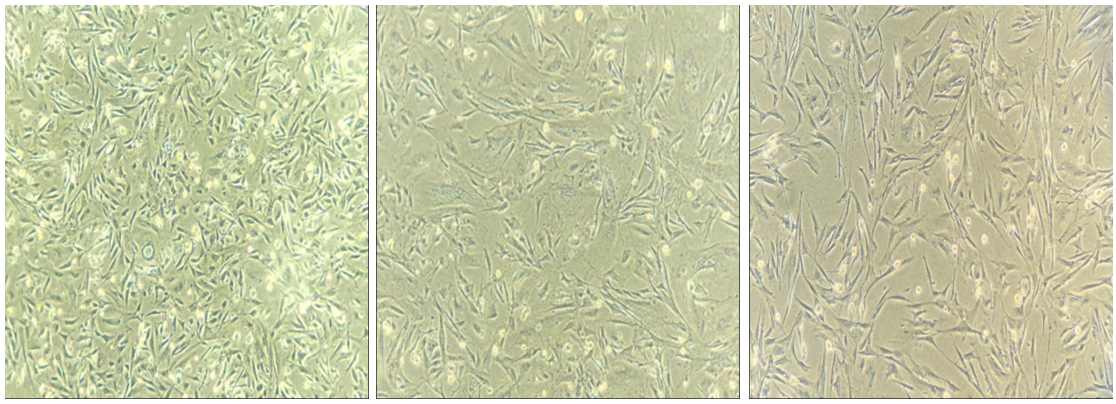

(J) (K) (L)

Primary cell culture- Simple adenoma: Primary cell culture growth after 24 h (G), 60 h (H), 72 h (I) and 96 h incubation (J); P-1 cells growth (70 % to 80% confluency) in exo depleted FBS after 72 h (K); P-2 cells growth showing elongated cells and start detaching from surface (L)

Plate-14

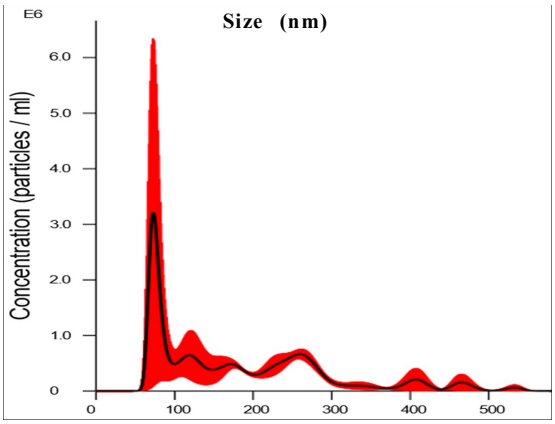

(A)

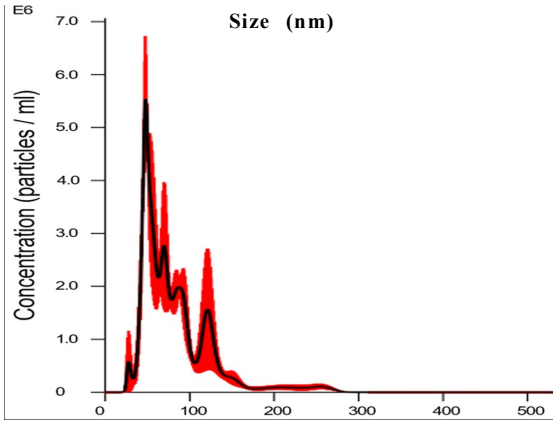

(B)

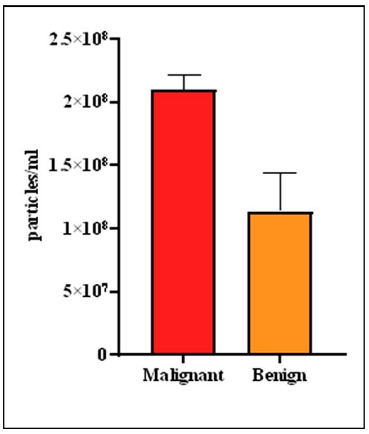

(C)

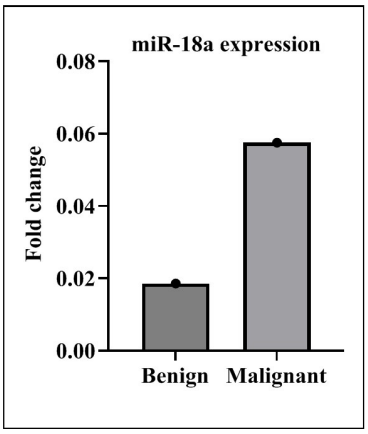

(D)

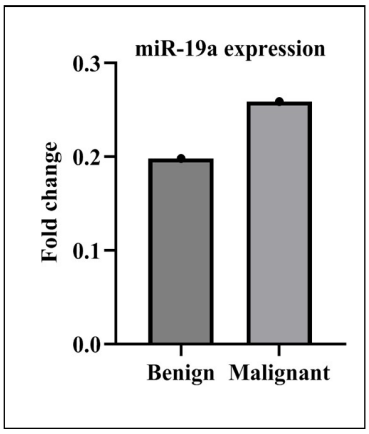

(E)

Exosomes concentration and size distribution: Exosomes concentration estimated in the cell culture supernatant of primary cell culture of intraductal papillary carcinoma (A) and simple adenoma (B) grown in media with exosome depleted FBS; graph showing comparative exosomes concentration between malignant and benign tumour cell culture supernantent (C).
Graph showing expression of miR-18a (D) and miR-19a (E) in benign and malignant tumours exosomes.

containing exosome depleted FBS. The cell culture supernatant was collected from the B1 (P1) flasks for exosomes isolation. B1 (P1) cells were further passaged of (P2) and incubated in 10% MEM media but the cells failed to attach and form a monolayer (Plate – 13: Fig. G - L).

4.5.2 Estimation of exosomes size and concentration by NTA

The exosomes isolated from the M1 and B1 primary CMT cells were analysed by NTA to know their concentration and size. Total number of exosomes released by M1 and B1 cells were 2.10e+08 +/- 1.23e+07 and 1.14e+08 +/- 2.95e+07 (mean +/- SD), respectively. The size of the exosomes vary greatly between M1 and B1. It was observed that the average size of particles was 82.3 nm in the M1 cells as compared to 180.7 nm in B1 cells, respectively and data presented in Table 14. Since there was a difference of 47.62% in the number of particles/ml released by M1 cells and B1 cells, it suggests that the production of exosomes in malignant tumours is higher than in benign tumours (Plate – 14: Fig. A to C).

Table 14 Presenting the concentration and size of particles by NTA

Primary CMT cells	Particles/ml (Mean +/- SD)	Average size of particles
M1 (Intraductal papillary carcinoma)	2.10e+08 +/- 1.23e+07	82.3 nm
B1 (Simple adenoma)	1.14e+08 +/- 2.95e+07	180.7 nm

4.5.3 Expression of miRNAs in the exosomal cargo of CMT cells by qPCR

The exosomes isolated from the primary culture of CMTs (B1 and M1) were subjected for qPCR for analysis of miR-18a and miR-19a expression. It was observed that the mean relative fold change for miR- 18a expression in B1 (simple adenoma) was 0.01858 and in M1 (intraductal papillary carcinoma) was 0.05751. Similarly, the miR- 19a expression was 0.198196 and 0.258816 fold change for B1 and M1, respectively. It was observed that the expressions of both miR-18a and miR-19a were decreased as compared to U6 in both B1 and M1. Comparison between B1 and M2 revealed that relative fold change of miR-18a in M1 was 3.09 times higher than B1. Similarly, miR-19a relative fold change was 1.3 times

higher in M1 than B1. Although the relative fold change in expression of miR -18a and miR -19a was statistically not significant between the B1 (benign CMT) and M1 (malignant CMT), yet it suggests that role of miR-18a and miR-19a expression in the exosomes for malignant transformation and progression of CMTs (Plate – 14: Fig. D &E).

4.6 Effect of GW4869 (exosomal inhibitor) on CMT-U27 cells growth and proliferation

4.6.1 Effect of GW4869 on the exosomes size and concentration secreted by CMT-U27 cells

To assess the effect of GW4869, the CMT-U27 cells were cultured in the lab which showed around 40 to 50% confluency in 18h and almost greater than 90% within 48h was treated with 3 different doses (20 µM, 30µM and 40µM) of GW4869 along with one control without any treatment. The media from the flasks collected after 24h of the treatments and exosomes were collected by using commercial kit. The exosomes were analysed by NTA for their size and concentration. Exosomes/particles size less then 200nm were considered for the statistical analysis. It was observed that the concentration of the exosomes significantly decreased in all treatment groups as compared to control group. NTA analysis revealed the mean concentration of exosomes in control, 20 µM, 30 µM and 40 µM GW4869 treatments groups as 1.23e+06 (+/- 72038), 6.38e+05 (+/- 55002), 3.58e+05 (+/- 22174) and 5.50e+05 (+/ - 55129) respectively. Among different treatment groups, the treatment of 30 µM GW4869 showed lowest exosomes concentration as compared to 20 µM and 40 µM GW4869 treatment groups (Plate – 15: Fig. A - C).

Exosome/particle size analysis revealed that exosomes/particles with size of 101.0 nm, 72.8 nm, 210 nm and 219.8nm were predominantly found in control, 20 µM, 30 µM and 40 µM GW4869 treatments groups, respectively. The concentration and mode size values of exosomes/particles at different treatment dose along with control group after 24h are listed in Table 15. Further, it was observed that the proportion of exosomes with size range 50-100 nm was significantly decreased in 30 µM and 40 µM GW4869 treatment groups, while the proportion of exosomes/particles with > 150 nm size was increased significantly with 40 µM treatment group at 24 h. These findings indicated that treatment of GW4869 significantly reduced the exosomal secretion from CMT-U27 cells in all treatment groups (Plate – 15: Fig.

Plate- 15

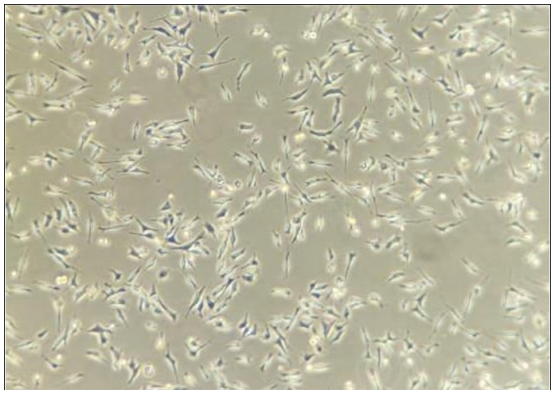

(A)

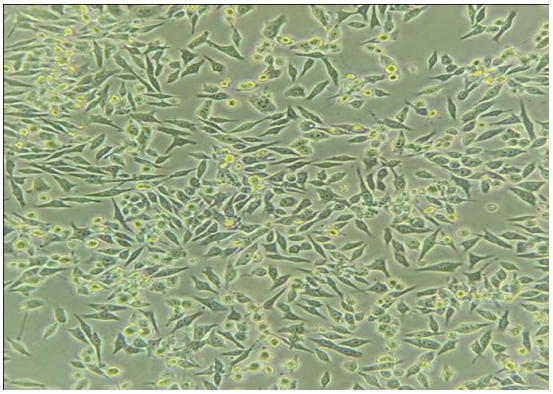

(B)

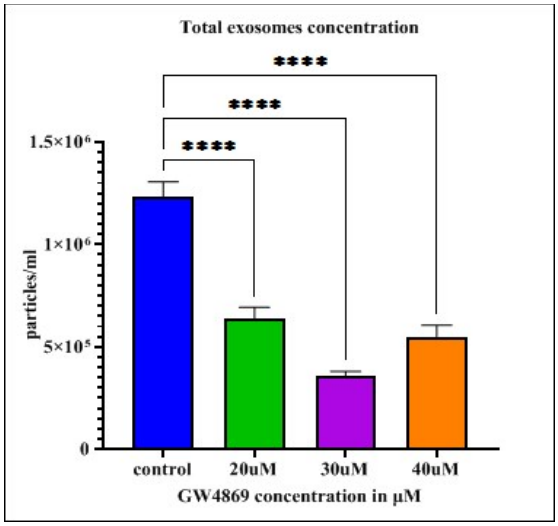

(C)

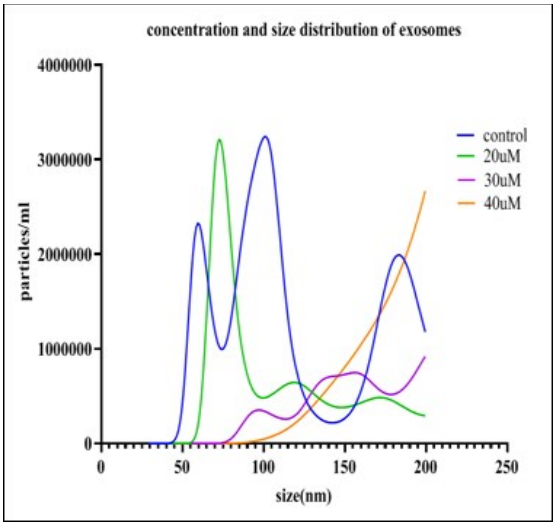

(D)

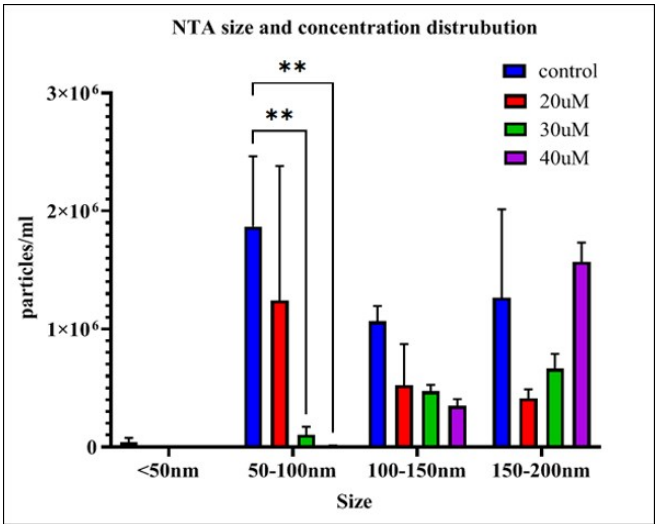

(E)

CMT-U27 cell growth after 18 h (A) and 48 h (B) incubation showing 40% and 90% confluency. Exosomes concentration and size distribution following GW4869 treatment in CMT-U27 cells: (C) Concentration and size distribution of EVs isolated from control (no drug) or GW4869 (20 µM, 30 µM and 40 µM) treated cells, respectively (n = 3). (D) Graph depicting exosomes concentration in different groups (E) Graph depicting exosomes size distribution in different groups. Each bar represents mean ± SEM (n = 3); **P < 0.005, ****P < 0.0001.

D & E).

Table 15: Concentration and size of the exosomes secreted by CMT- U27 after GW4869 treatment

GW4869 treatment groups	Particles/ml (Mean +/- SEM)	Mode size of particles (nm)
Control	1.23e+06+/-72038	101.0
20 μM	6.38e+05+/-55002	72.8
30μM	3.58e+05+/-22174	210.0
40 μM	5.50e+05+/-55129	219.8

4.6.2 Assessment of viability of CMT-U27 cells after GW4869 treatment

4.6.2.1 Trypan blue dye exclusion test

CMT-U27 cells were assessed for their viability by trypan blue dye exclusion test after GW4869 treatments (20 μM, 30 μM and 40 μM) along with control. Equal volume (10uL) of cell suspension of each flask and trypan blue dye mixed and total number of viable cells were counted. The concentration of viable cells in control group was taken as standard (100%) for the comparison with different treatment groups. It was observed that number of viable cells in control was higher compared to the GW4869 treatment groups. The results of trypan blue dye exclusion test depicted in Table 16 (Plate – 16: Fig. A & B).

Table 16: Number and percentage of viable cells of CMT-U27 after GW4869 treatment

GW4869 treatment groups	Number of viable cells/2ml	Percentage of viable cells
Control	1050000	100
20μM	872000	83.04762
30μM	620000	59.04762
40μM	320000	30.47619

4.6.2.2 MTT assay

MTT assay was performed to assess the viability and metabolic activity of the CMT-U27 cells after GW4869 treatment for 24-48 h. CMT-U27 cells were cultured in the 96-well

cell culture plate and treated with different concentration of GW4869 (10µM, 20µM, 30µM, 40µM, and 50µM). The data presenting the % cell viability at different doses of GW4869 for 24 h and 48 h are represented in the Table 17 (Plate – 16: Fig. C, D, E & F). A significant reduction in cell viability was observed compared to control in treatment with a 40 µM and 50 µM dose at both 24 and 48 h interval. Decreased cell viability was observed in 20µM and 30µM treatment groups at 48 h but treatment groups with 40µM and 50µM GW4869 showed significant decrease in cell viability. However, with a 10 µM GW4869 treatment non significant decrease in cell viability was observed at both 24 and 48h, when compared with control group (Plate – 17: Fig. A & B).

Table 17: Presenting the % cell viability of CMT- U27 cells treated with different doses of GW4869 at 24 h and 48 h by MTT Assay

GW4869 dose	24 h % cell viability	48 h % cell viability
Cell control	100	100
10 µM	87.15	85.88
20µM	79.50	75.40
30µM	75.92	69.82
40µM	68.44	60.10
50µM	60.60	50.61
Vehicle control	96.34	94.55

Plate- 16

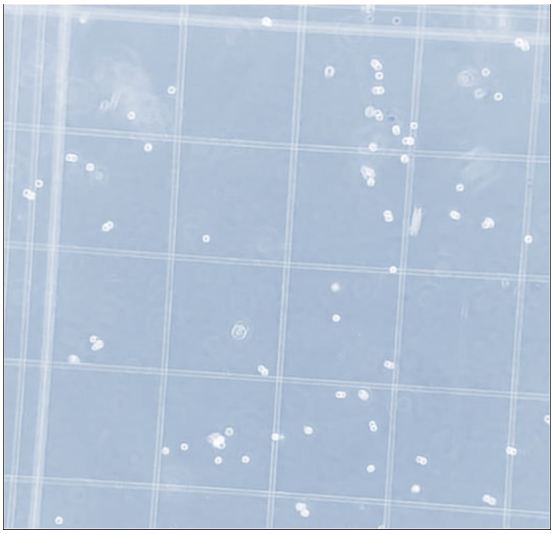

(A)

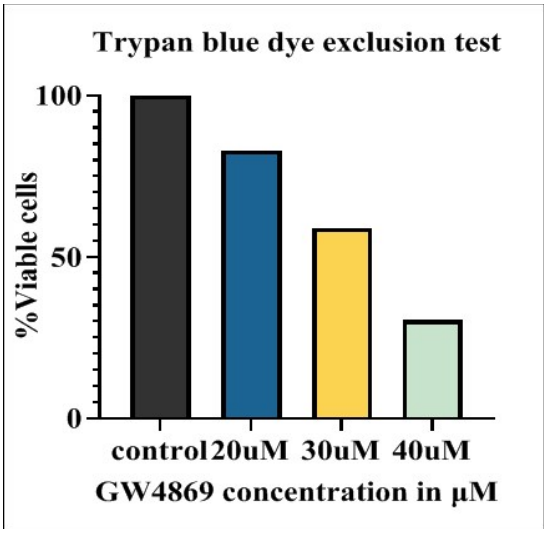

(B)

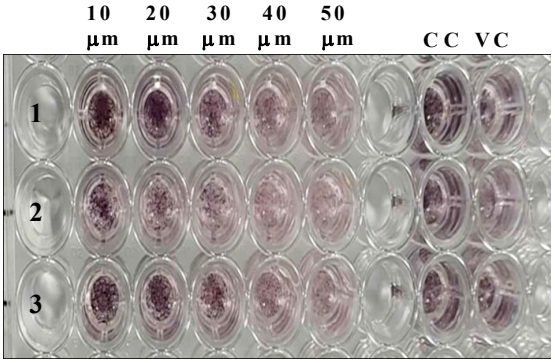

(C)

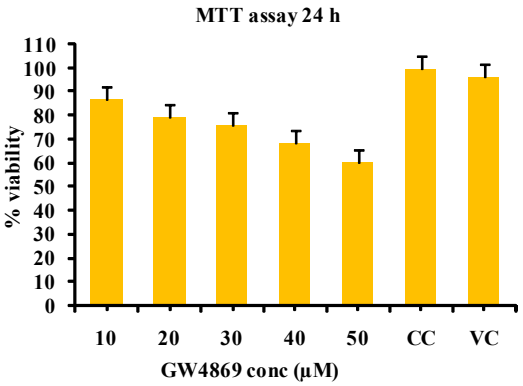

(D)

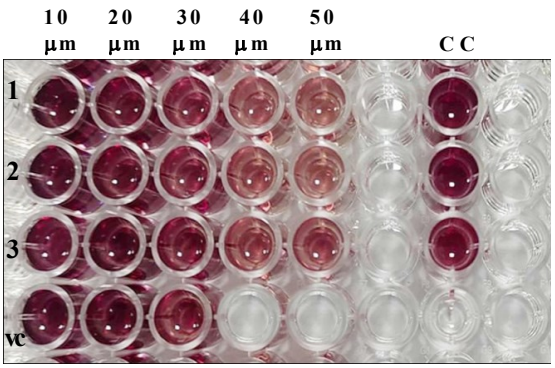

(E)

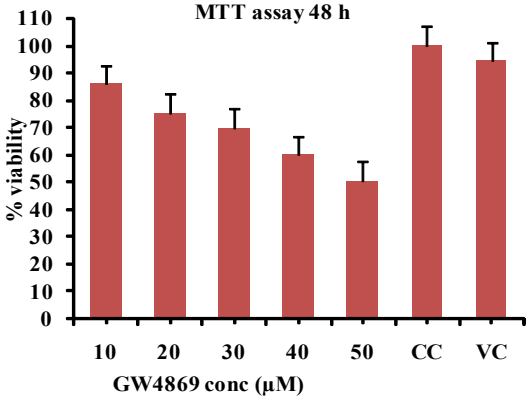

(F)

Effect of GW4869 treatment on the survival of CMT-U27 cells: Viable cells (bright and unstained) with intact membranes (A); Graph depicting the CMT-U27 cells viability (B) after treatment with GW4869 (20, 30 and 40 µM) using trypan blue dye exclusion test. Data are presented as mean % of viable cells in treated flask compared to cell control.

Effect of GW4869 treatment on the viability of CMT-U27 cells: Intensity of purple formazan product in microtiter plate (C & E); Graph depicts the CMT-U27 cells viability (D & F) after treatment with GW4869 (10, 20, 30, 40 and 50 µM) along with cell control (CC) and vehicle control (VC) using MTT assay at 24h (C & D) and 48 h (E & F).

Data are presented as mean ± SEM (n = 3 replicates per group).

Plate- 17

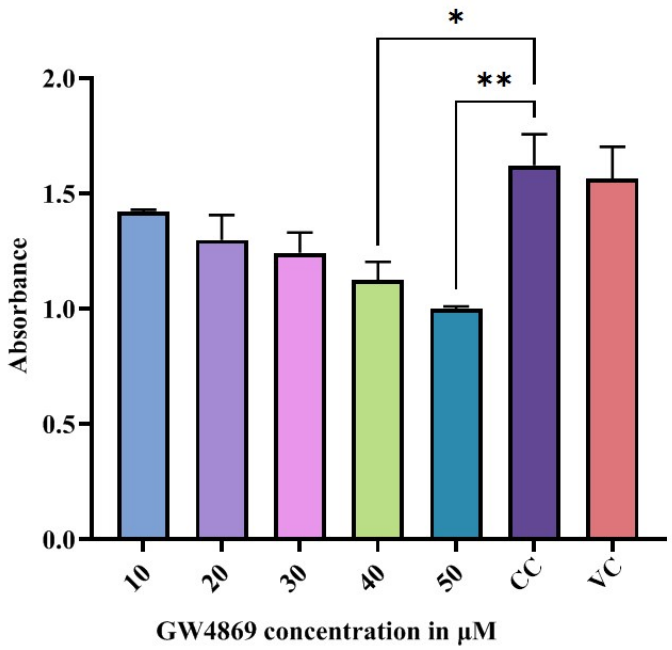

(A)

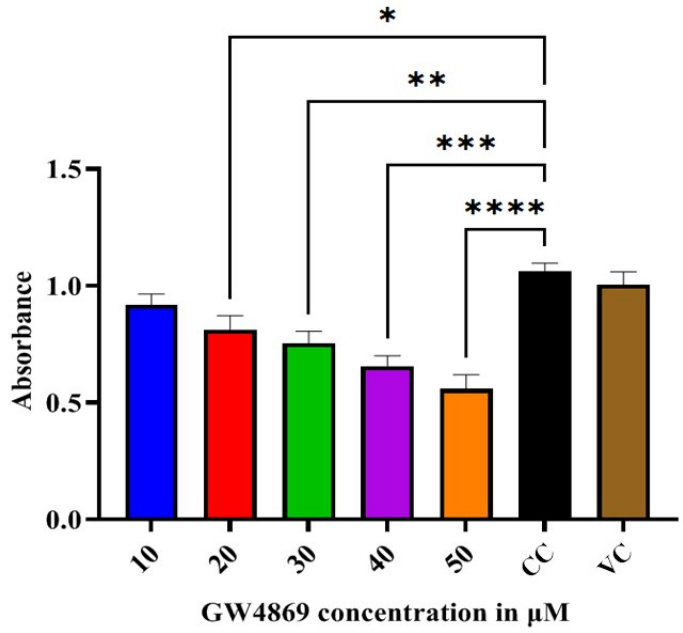

(B)

Effect of GW4869 treatment on survival and proliferation of CMT-U27 cells: Graph showing the cell viability and proliferation measured by MTT assay after 24 h (A) and 48 h (B) in different groups of the experiment, DMSO (0.5 %), GW4869 (10-50 µM) and cell control (without drug).

Data are presented as mean ± SEM (n = 3 replicates per group). *$P < 0.05$, **$P < 0.005$, ***$P < 0.0005$ and ****$P < 0.0001$

Discussion

5 DISCUSSION

Cancer is a thriving health issue in humans and animals, and its high incidence has been recorded throughout the world in pet animals especially in dogs. In dogs, mammary tumours appear as the most frequently recorded neoplasms in intact female pet dogs (Salas *et al.,* 2015). Like humans, canine mammary tumours (CMTs) have a highly heterogeneous patho-biology and diverse clinical outcomes. Early and accurate diagnosis is essential for the good prognosis and better management of the CMTs. Researchers are trying to develop new techniques along with already available techniques for diagnostic and prognostic purposes for the CMTs and also to formulate the targeted therapeutic strategies. In that direction new emerging areas in the cancer research is exosomal role in carcinogenesis. Exosomes are extracellular vesicles (EVs) with a size range of 40–160 nanometers in diameter and secreted by most eukaryotic cells including cancer cells (Ruivo *et al.,* 2017; Dai *et al.,* 2020). Exosomal contents/cargo include proteins, DNA, mRNA, microRNA, long noncoding RNA, circular RNA, etc., which can play a crucial role in tumour progression, growth, angiogenesis, metastasis and chemoresistance (Tai *et al.,* 2018; Dai *et al.,* 2020). Exploring the exosomal cargo for the identification of new biological markers for early diagnosis and prognosis of CMTs is a new approach in this direction. It is reported that exosomal cargo involved in different types of tumour progression and metastasis. Drugs or molecules having exosomes inhibition properties may inhibit the tumour progression and metastasis and thus provides pathway for certain developing cancer therapeutics.

The present investigation was aimed to characterize the CMTs on the basis of histopathology, expression of different receptors (ER, PR, EGFR) and exosomal cargo.

Histopathological classification of the CMTs was done as described by Goldschmidt *et al.* (2011). In present study, total 16 tissue samples of the mammary glands were collected from the CMT suspected cases, and out of which 14 (87.5%) were classified as malignant CMTs, one as benign CMT (6.25%) and one as lobular hyperplasia (6.25%). The higher occurrence of malignant CMTs in comparison to benign are in agreement with the previous reports(Mukhopadhayay and Som, 1997; Shekar *et al.,* 2001; Martin *et al.,* 2002; Pawaiya, 2004, Reddy, 2007; Kumar *et al.,* 2009; Baba *et al.,* 2016, Dias *et al.,* 2016). Kumar *et al.* (2009) reported 83.08% of CMTs as malignant tumours. Similarly, Martins *et al.,* (2003) observed 7.09% of mammary tumours as benign and 92.91% as malignant.Mukhopadhayay and Som(1997) reported 35.5% benign tumours in a retrospective study, which were relatively higher, but less than malignant counterparts. The higher occurrence of malignant CMTs can be a result of owner's ignorance about the CMTs, due to which they do not provide proper treatment at earliest. Usually pet owners brought them to the veterinary clinic when mammary growths starts growing fast or become ulcerated, which are mostly to be malignant CMTs (Sahabi *et al.,* 2015).Further, highest occurrence of CMTs was noticed in an age group of 6 - 9 years (56.25%), which is in accordance with earlier observations of Moulton (1990), Reddy (2007) and Kumar*et al.,* (2009).

CMTs in present study showed marked variation the their gross appearance and distribution i.e. CMTs occurred as single or multiple, round, elongated or irregular shaped masses with varying size and different consistency from soft to firm to hard. Earlier studies have been reported that synchronous multiple gland involvement is not rare in CMTs (Benjamin *et al.,* 1999, Devarathnam*et al.,* 2021). The maximum occurrence of CMTs was observed in inguinal pairs (62.5%) followed by caudal abdominal pairs (37.5%) and cranial abdominal pairs (25%), which was also reported in previous studies (Ariyarathna*et al.,* 2018, Devarathnam*et al.,* 2021). The ample amount of glandular tissue and long-term secretary activity of inguinal mammary glands in comparison with other glands is attributed to its frequent association with mammary tumours (Moulton, 1990, Sahabi *et al.,* 2015).

Histopathological classification of the CMTs revealed that out of 16 suspected CMT tissues, 14 (87.5%) were classified as malignant CMTs, one as benign CMT (6.25%) and one

as lobular hyperplasia (6.25%). The histopathological classification of CMTs was done as described by Goldschmidt (2011) and was graded as described by Travasoly*et al.,* (2013). Present study revealed that among malignant CMTs, carcinoma-mixed type tumours were most predominant and histological features were similar as described previously by Moulton (1990), Misdorp (2002) and Kumar (2008). Papillary carcinoma (intraductal) characterised by papillary growth of epithelium projection into the lumen of acini/ducts with connective tissue stalk of variable lengths and thickness within proliferating epithelial cells reported in present investigation is also in line with the features reported in earlier studies (Moulton, 1999; Misdorp *et al.,* 1999; Pawaiya, 2004; Reddy, 2007 and Kumar, 2008). The histological features of other malignant epithelial neoplasm (adenosquamous carcinoma), malignant myoepithelioma, malignant mesenchymal CMTs(chondrosarcoma, hemangiosarcoma, and carcinosarcoma) and benign tumours were in accordance with earlier reports (Moulton, 1990; Misdorp *et al.,* 1999; Reddy, 2007, Kumar, 2008; Rahman, 2022).

The expression of the different tumour markers in the CMTs tissues have been studied by various researchers to evaluate their potential for assessing tumour behaviour, metastasis, diagnosis, prognosis and identifying new cancer therapeutic targets. Evaluation of the expression of ER, PR and HER-2/ c-erbB2 by IHC helps in the prognosis of breast cancer (Clark and McGuire, 1983) and CMTs (Nieto *et al.,* 2000). It also act as a predictor of likely response of hormonal treatment to the patients (Clark and McGuire, 1983).In the present study, ER positive staining was observed in simple adenoma and intraductal carcinoma cases, with a stronger immunoscore in the benign tumor, aligning with findings from De Las Mulas *et al.,* (2005). This suggests that ER expression may play a role in early-stage tumorigenesis in CMTs and could be an important marker for identifying benign lesions, as seen in human breast cancer (Clark and McGuire, 1983).PR expression was detected in the epithelial component of carcinoma-mixed type tumors. This finding aligns with the work of Gracanin (2012), where PR isoform expression showed both nuclear and weaker cytoplasmic staining. Leeuwen *et al.,* (2000) also reported heterogeneous staining for PR in canine mammary carcinomas, including perinuclear staining in tumorous cells and cytoplasmic staining in spindle cells. PR is found in the cytoplasm, where it may interact with ER, c-Src, and is phosphorylated

by MAPK, potentially influencing tumour progression (Daniel *et al.,* 2011). However, a detailed group-wise comparison with good number of cases is required for proper statistical analysis, which may provide a conclusive interpretation.

Expression of HER-2/ c-erbB2 in the CMTs correlated with the poor prognosis in the earlier studies (Rungsipipat*et al.,* 1999; Bange *et al.,* 2001). HER-2/ c-erbB2 serves as first signal generating protein and a proto-oncogene with known normal functions.Functional abnormality of the c-erbB2 oncogene is believed to be a critical event in carcinogenesis of glandular tissues, especially of the breast, where overexpression of c-erbB2 oncoprotein has been frequently associated with the malignancy, chemo-resistance and poor prognosis of the breast cancer (Yokota *et al.,* 1986;Bange *et al.,* 2001). Low expression of HER-2/ c-erbB2 was reported in previous studies i.e.Rungsipipat *et al.,* (1999) recorded 21%, Martin *et al.,* (2003) recorded 17.6% and Mayilkumar (2009) recorded 13%. In the present study, only one CMT case showed moderate immunostaining. In contrary, Kumar *et al.,* (2009) reported higher immunopositivity of 42.59% for c-erbB2 oncoprotein expression in the malignant mammary tumours and further stated that the tumours of epithelial origin weremore predominantly showing the expression. The variation in the positivity of the different receptor in various studies may be due to the variation in the sample size, primary antibody used in study, scoring system followed and geographical area of sampling.

Real time PCR assay was performed to assess the mRNA expression of ESR, PR and Epidermal Growth Factor Receptor (EGFR) in spontaneous CMTs tissue samples. The role of these receptor markers is well established in the pathogenesis of mammary tumors, particularly in human breast cancer, and their potential utility in CMTs. In present study a significant fold difference in ESR expression (55.56%) was observed between benign and malignant tumors. The mean relative fold change for ESR in simple adenoma was high suggesting its potential role in early tumour development and progression. The variability in ESR expression have been reported in earlier studies, which vary from 12.96% to 92.3% in malignant tumour tissues and from 49% to 100% in benign tumors (Millantaa *et al.,* 2005; Mulas *et al.,* 2005; Yang *et al.,* 2006; Gama *et al.,* 2008; Morris *et al.,* 2009; Klopfleisch *et al.,* 2010; Pena *et al.,* 2014). PR mRNA expression was observed in 50% of the CMT tissues samples but no significant

statistical difference was found between benign and malignant tumours. Unlike ESR, PR expression did not significantly differentiate between natures of tumour types in our study. This finding contrasts with some previous studies, which reported consistent expression of PR in all benign CMTs and about two-thirds of malignant CMTs (Geraldes *et al.,* 2000; Guil-Luna *et al.,* 2014). Furthermore, some studies suggested higher PR expression in simple carcinomas compared to complex carcinomas (Luna *et al.,* 2014), although our findings could not replicate these differences due to the limited sample size and lack of distinction between simple and complex carcinomas. Interestingly, recent research by Galadima (2024) also did not find significant differences in PR expression between benign and malignant tumours, aligning with our observations.

Similarly, qPCR was performed to evaluate the EGFR expression in CMT tissues. Like PR mRNA expression, EGFR expression was also detected in 50% of the total tested cases (8). No significant statistical difference was found between benign and malignant tumours in present study. It is established that EGFR activation, through binding with its ligand (EGF), can induce carcinogenetic effects by enhancing gene transcription which promotes cellular proliferation and distant metastasis (Henson and Gibson, 2006). In CMTs, *in-vitro* studies have demonstrated that EGF increases cell proliferation, chemotaxis, vascular endothelial growth factor (VEGF) production, and reduces apoptosis in canine carcinomas (Kennedy *et al.,* 2011). Our findings indicated that malignant tumours showed higher expression of EGFR than benign tumour, which is similar to the earlier studies in the CMTs(Galadima, 2024). These finding suggest that EGFR could be a valuable marker for identifying malignant or more aggressive CMTs. However, the lack of statistical significance between benign and malignant tumors in EGFR expression in our study indicated the requirement of a systamatic study with appropriate numbers of both benign and malignant CMTs.

To characterize the exosomal cargo secreted by the CMT cells, the tissue samples were collected from the five CMTs cases by excisional biopsy and cultured *in-vitro* in the lab. *In-vitro* primary cell culture was established in two different types of CMTs viz. malignant intraductal papillary carcinoma (M1) and benign simple adenoma (B1). Primary culture of M1 was passaged upto P3 and for B1 upto P2. In present investigation it was observed that the

growth pattern and cellular morphology of the M1 and B1 revealed significant differences. The M1 cells showed a rapid attachment to the culture surface, followed by rapid proliferation and formation of a monolayer within 48 hours. These observations are typical of malignant tumors, which often exhibit rapid proliferation and aggressive growth patterns and the potential for metastasis(Cifone, 1982). In contrast, B1cells showed slower attachment (less than 20% of cells adhering to the flask after 24 hours) and achieved 80-90% confluency at 5th day. The slower growth of adenoma cells is consistent with the benign nature of these tumours. However, similar to the M1 cells, the B1 cells failed to maintain a stable monolayer in later passages, a phenomenon that might reflect cellular stress or altered cell behaviour after prolonged culture(Meinhovel*et al.,* 2018)

Exosomes are nano-sized vesicles released by cells and are known to play a significant role in intercellular communication, immune modulation, and tumor progression. It is reported that exosomal cargo is involved in various pathological and physiological processes, including inflammation, angiogenesis, cell death, neurodegenerative diseases, and cancer (Diomaiuto*et al.,* 2021). Exosomes facilitate chemoresistance by drug-resistant properties within cancer cell populations (Colombo *et al.,* 2014). As exosomes contains tumor-suppressor and oncogenic microRNAs (miRNAs), they hold immense diagnostic value because of their distinctive expression patterns in neoplastic cells.In present investigation, exosomes were isolated from the cell culture supernatant (M1 and B1 cells) and RNA was extracted as per the standard protocol. The isolated exosomes were analysed by NTA for their concentration and size and it was observed that M1 cells (ductal carcinoma cells) released a significantly higher number of exosomes (2.10E+08± 1.23E+07 particles/ml) compared to B1 cells (simple adenoma cells; 1.14E+08± 2.95E+07particles/ml). It indicated that malignant CMT cells (M1 cells) released 47.62% more exosomes/particles than benign CMT cells (B2). Furthermore, it was observed that exosomes secreted by malignant CMT cells (M1 cells) were smaller in size (82.3 nm) than benign CMT cells (B2) (180.7 nm).The higher concentration of exosomes released by the malignant tumours is consistent with earlier reports and it may be due to aggressive proliferation of malignant cells(Logozzi*et al.,* 2019;Chen*et al.,* 2023).Exosomes are known to carry molecules like proteins, lipids, and RNAs, which can affect distant cells

and tissues, potentially facilitating tumor progression, metastasis, and immune evasion. The smaller size of exosomes from ductal carcinoma may enhance their ability to circulate and interact with distant tissues, contributing to the malignant transformation process and metastasis(Greening*et al.,* 2015).

The RNA isolated from the exosomes was further analysed for the miRNA expression by using the commercial kits. The miR-18a and miR-19a, which are well-documented as key regulators of cancer progression, were found to be upregulated in exosomes from malignant CMT cells (M1 cells) compared to benign CMT cells (B2) in our study. It was observed that miR-18a expression was 3.09 times higher, and miR-19a expression was 1.3 times higher in malignant CMT cells (M1 cells) compared to benign CMT cells (B2). Although the difference of miR-18a and miR-19a expressions in M1 and B1 were not showed statistical significance, yet the increased expression in exosomes of M1 cells suggests their potential involvement in the proliferation, malignant transformation and progression of CMTs.These processes are characteristic of aggressive tumours, and the transfer of these miRNAs via exosomes could enhance the malignant properties of CMTs. This supports the hypothesis that exosomes serve as important vehicles for disseminating oncogenic signals between cells, contributing to tumourprogression and metastasis(Kahlert and Kalluri, 2013;Wang *et al.,* 2014).Fish *et al.,* (2018) studied the shedding of exosome-derived miRNAs by CMT cells *in-vitro* and identified 338 unique exosome-derived miRNAs, with 145 differentially expressed between tumour and normal canine mammary cells. Among them, they reported that miR-18a, miR-19a, and miR-181a were the most significantly upregulated, with fold changes of 10.34, 3.84, and 7.70, respectively. Further, they predicted that these miRNAs target the estrogen receptor (ESR1α) *in silico* and suggests their potential as non-invasive biomarkers for hormone status and phenotype in canine mammary carcinoma.

In another study, negative correlation between miR-18a, miR-18b, and the ESR1 gene has been reported in CMT tissues (Abbate *et al.,*2023).Their study revealed that miR-18a and miR-18b expressions were upregulated in malignant CMTs than normal or hyperplastic mammary glands. Further, they observed significant downregulated ESR1 mRNA expression in malignant tumours compared to benign and normal mammary tissue, which suggests a negative

correlation between miRNAs and ESR1 mRNA expression. Thus they postulated that miR-18a and miR-18b may contribute to a loss of estrogen receptor activity, potentially influencing tumour biology and the progression of CMTs. In similar lines, present study also highlights the importance of exosome-derived miRNAs as potential biomarkers and therapeutic targets in the management of CMTs.

To study the role of exosomes in the cell proliferation or progression, *in-vitro* experiments has been conducted on the CMT-U27 cells by using GW4869 compound as exosomal inhibitor. The CMT-U27 cells were treated with different concentrations of GW4869 to assess the effect on the exosomes secretion and cell proliferation and viability. GW4869 (neutral sphingomyelinase inhibitor) was first utilized in 2010 by the researchers to successfully inhibit the release of exosomes from multivesicular bodies (MVBs) of different cells (Kosaka *et al.,* 2010; Li *et al.,* 2013). It is also reported that GW4869 inhibition of exosomes secretion can sensitize the chemo-resistant cancer cells to chemotherapy (Kumar *et al.,* 2022).In present study also GW4869 significantly alters both exosome production and cell viability in a dose-dependent manner, providing important insights into the role of exosomes in CMT biology and their potential as therapeutic targets.Present investigation revealed that GW4869 treatment significantly reduced the concentration of exosomes in all tested doses (20 µM, 30 µM, and 40 µM)than control group. Further, exosome size analysis revealed notable alterations in particle size distribution.

In present study, the size of exosomes observed was 101.0 nm in the control group,however, treatment groups showed dose-dependent shift in size distribution. It was observed that in 20 µM treatment group the mode size decreased to 72.8 nm, while at higher treatment groups viz. 30 µM and 40 µM, the mode size increased to 210 nm and 219.8 nm, respectively. This shift in size distribution suggests that GW4869 may influence the biogenesis or composition of exosomes, potentially by altering lipid metabolism or membrane dynamics(Menck *et al.,* 2017). Previous studies also indicated that GW4869 treatment increases the size of exosome with higher doses (Menck *et al.,* 2017; Kumar *et al.,* 2022). Kumar *et al.,* (2022) explored the effects of GW4869 on exosome release in paclitaxel-resistant prostate cancer (PC3-R) cells and found that exosome with size range from 50-100

nm were decreased in GW4869 treated groups, while numbers of larger exosomes (>150 nm) increased with higher doses of GW4869 groups.Though they noted a non-significant reduction in the proportion of 50-100 nm exosomes at 20 μM, their findings suggest that GW4869 can modulate exosome populations by altering size distribution.

In another study by Menck *et al.,* (2017), evaluated the GW4869 effects on human SKBR3 breast cancer cells and mouse L-cells and observed that 5 μM GW4869 treatment for 16-24 hours, reduced the exosome concentrations and preferential increased the numbers of the larger vesicles (microvesicles). Moreover, their study highlighted a novel connection between ceramide generation and exosome biogenesis, showing that inhibition of neutral sphingomyelinase (SMPD2/3) by GW4869 led to reduced exosome secretion but an enhanced release of microvesicles. This indicates that GW4869 not only inhibits exosome secretion but also impacts the size and composition of exosomal subpopulations, which could alter their role in intercellular communication and tumor progression.

Experiments to evaluate the effect of GW4869 *in-vitro* in CMT-U27 cells for cell viability and proliferation were assessed by using trypan blue dye exclusion test and MTT assay. The trypan blue assay revealed a dose-dependent decrease in viable cell numbers following GW4869 treatment. It was observed in present study that cells treated with 20 μM, 30 μM, and 40 μM doses of GW4869 showed reduced viability to 83.05%, 59.05%, and 30.48%, respectively, compared to the control group. These findings suggest that higher doses of GW4869 exert a more pronounced cytotoxic effect on CMT-U27 cells, leading to a significant reduction in viable cells.MTT assay further corroborated these results, and demonstrated a marked reduction in cell proliferation, especially at 40 μM and 50 μM doses, across all time points (24-48 hours). Notably, the 40 μM and 50 μM doses caused a significant and statistically notable decrease in cell viability at 48 hours, while lower doses (10 μM and 20 μM) did not result in a significant reduction in cell proliferation at any time point. These findings indicated that GW4869 not only inhibits exosome secretion but also has a cytotoxic effect on CMT-U27 cells, with higher doses leading to a more substantial reduction in cell viability.

Similar findings were reported by Irep *et al.*, (2024) in small cell lung cancer (SCLC) cells. Irep *et al.,* (2024) evaluated the effects of GW4869 and Nexinhib20 on SCLC cells and observed that treatments of GW4869 at concentrations ranging from 0 to 50 μM to SCLC cells showed dose-dependent decrease in cell survival, with survival rates declining as the concentration of GW4869 increased from 1 to 50 μM compared to control cells. Their study also reported the IC50 values of GW4869 in these SCLC cell lines and demonstrated its ability to inhibit exosome synthesis and trafficking. They further concluded that treatment of GW4869 and Nexinhib20 to SCLC cells caused changes in exosome size and also reduced the expression of various exosomal markers i.e. TSG101, RAB27A, CD9, CD63 and nsMase2 at RNA and protein levels. Irep *et al.* (2024) demonstrated that the reduction of exosomes mediated by GW4869 and Nexinhib20 treatments leads to decreased cell proliferation and increased apoptosis.

Kavanagh *etal.,* (2017) studied the role of exosomes in chemosresistance. They demonstrated that highly chemoresistant therapeutic-induced senescent (TIS) cells can be generated in Cal51 TNBC cells using paclitaxel (PTX), and observed that TIS cells released significantly more extracellular vesicles compared to control cells. These extracellular vesicles loaded with various molecules which include drugs, proteins involved in cell proliferation, ATP depletion, apoptosis, multi-drug resistance protein 1 (MDR1)/ P-glycoprotein, etc. Similarly, they observed that treatment of GW4869 (5 μM) to Cal51 TNBC (TIS) cells displayed a significant reduction in cell numbers on days 9, 11, and 14 compared with vehicle control alone.

Exosomes play key role in metastasis, immune evasion, chemoresistance, angiogenesis, etc., and by reducing their concentration and altering their size distribution, may disrupt tumour-promoting processes and its progression. In our study, we observed significant alterations in exosome concentration and size distribution at doses as low as 20 μM, which indicated it may have profound effects on tumour biology, particularly in the context of inter cellular communication. Exosomes are known to transfer oncogenic signals between the neoplastic and normal cells through miRNAs, nucleic acids, proteins, and lipids. By inhibiting exosome secretion by GW4869 may also interfere with the transmission of these signals, thereby potentially

hindering tumour progression. Further,it was observed that GW4869 treatment causes reduction in cell viability and proliferation, particularly at higher doses of GW4869. Hence, GW4869 treatment experiments indicated that it has the potential of cancer therapeutic. However, further *in-vivo* studies are needed to fully evaluate its efficacy and safety in clinical applications.

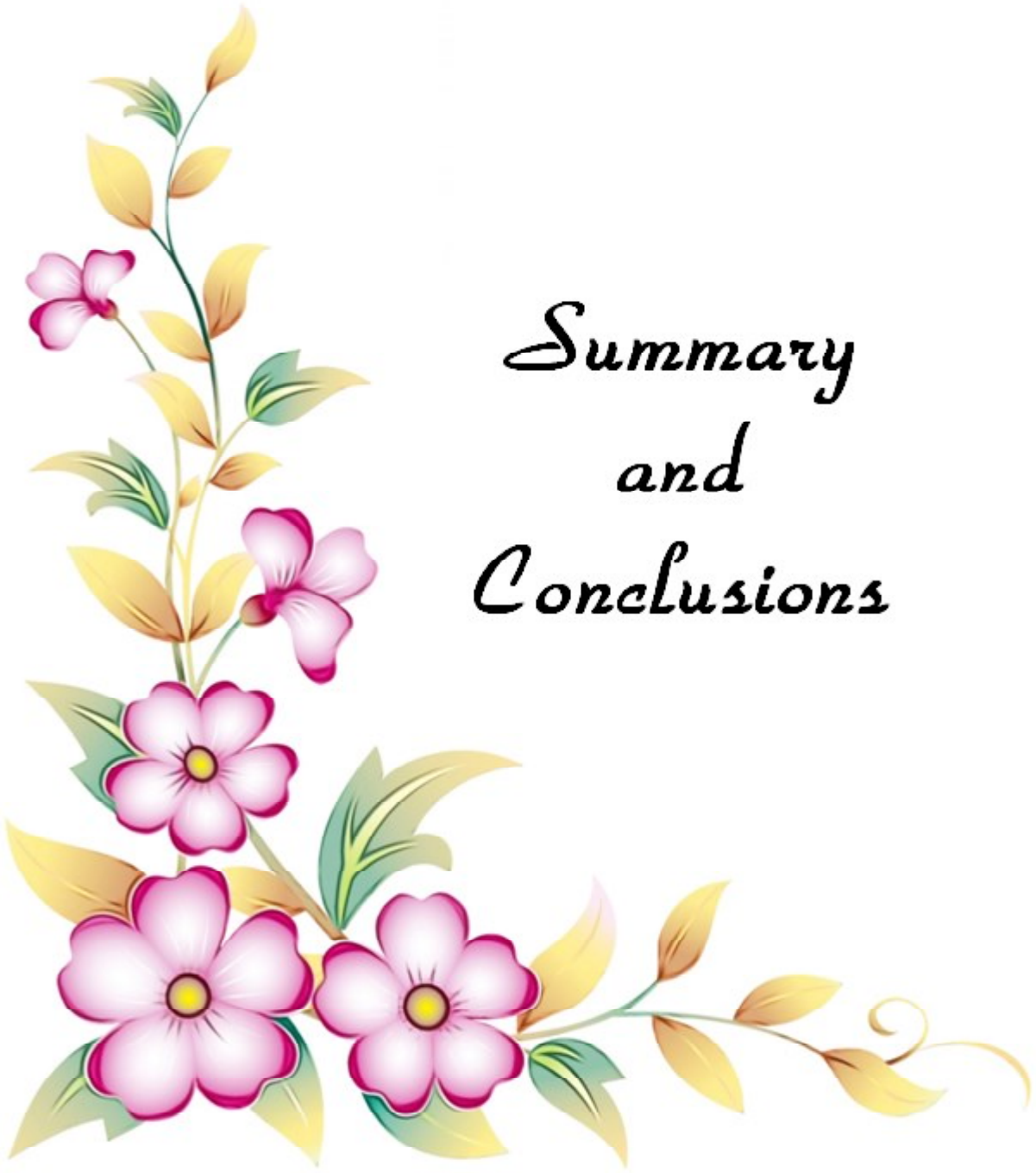

Summary and Conclusions

6 SUMMARY AND CONCLUSIONS

The present study was aimed to investigate the histological, pathobiological, and molecular characteristics of canine mammary tumors (CMT) by evaluating the expression levels of key markers such as estrogen receptor (ER), progesterone receptor (PR), and epidermal growth factor receptor (EGFR) at both the gene and protein level by using real-time PCR and IHC, respectively. These markers are crucial for assessing tumour behaviour, prognosis and identifying potential therapeutic targets. Additionally, the study was planned to analyze the exosomes secretion in benign and malignant tumours, and also to evaluate the expression of some selected exosomal miRNAs in CMT. Furthermore, *in-vitro* study was conducted by using an exosome inhibitor viz. GW4869 on exosome release in CMT-U27 cell lines.

A total of 16 mammary tumour tissue samples were collected from grossly suspected spontaneous canine mammary tumors (CMTs) cases for the histopathological classification. It was observed that 15/16 cases were CMTs and 1 diagnosed as lobular hyperplasia. Most of the CMT cases occurred in animals aged 5 years and above, with the highest occurrence in the 6-9 years age group (9, 56.25%). Among the different breeds of dogs, German Shepherd had the highest number of CMT cases in our study. Grossly, the tumours were observed in single or multiple mammary glands, with variable shapes, sizes, and consistencies. The maximum incidence of tumour was reported in inguinal pair (62.5%) of mammary glands followed by caudal abdominal pair (37.5%), cranial abdominal pair (25%), caudal thoracic pair (6.25%). Histopathological classification revealed that 14 cases were malignant and 1 was benign. Carcinoma-mixed type (6; 40.0%) was found to be the most predominant type of CMT

followed by intraductal papillary carcinoma (2; 13.3%) and one case each of ductal carcinoma (1; 6.5%), adenosquamous carcinoma (1; 6.5%), malignant myoepithelioma (1; 6.5%), carcinosarcoma (1; 6.5%), chondrosarcoma (1; 6.5%), hemangiosarcoma (1; 6.5%) and simple adenoma (1; 6.5%).

Immunohistochemical analysis was conducted to evaluate the expression of ER, PR, and HER-2 in spontaneous CMTs. ER expression was observed in simple adenoma with strong cytoplasmic staining (immunoscore 7), and two cases of intraductal papillary carcinoma. Among intraductal carcinoma, one showed moderate cytoplasmic and the other one showed mild cytoplasmic staining. PR expression was found in carcinoma-mixed type tumors, showing strong cytoplasmic staining (immunoscore 6). HER-2 expression was rare and observed in one case of carcinosarcoma-malignant mixed tumor, and was scored 2+ based on ASCO guidelines. These findings indicate differential expression of these biomarkers in various CMT types, suggesting their potential role in tumor classification and prognosis, though further studies are needed to confirm their clinical significance.

The relative expression of ESR, PR, and EGFR genes in spontaneous CMTs was evaluated by using quantitative real-time PCR assay. Tumour samples were classified into benign and malignant groups, and a normal mammary gland was used as a biological control. The RNA isolated from the tissue samples by using commercial kits were used for the assay. The study found variations in gene expression across different tumour types. ESR showed significant fold changes in 55.56% of cases, with a marked increase in simple adenoma. PR expression was observed in 50% of cases but did not show significant statistical differences between benign and malignant tumors. EGFR expression was also found in 50% of cases, with a notable increase in carcinosarcoma and malignant myoepithelioma, but no significant statistical differences were observed across tumor types.

The tissue samples (5) collected aseptically in the MEM cell culture media were processed further for primary cell culture. Primary cell culture study was primarily aimed to investigate the exosome production, their size and microRNA (miRNA) expression. Among five CMT tissue samples processed for primary cell culture, four were malignant and one

benign. Among these, only two samples viz. intraductal papillary carcinoma (M1) and simple adenoma (B1), were successfully cultured. M1 cells exhibited rapid growth, covering 95% of the flask surface within 48 hours, while B1 cells showed slower growth, reaching 80-90% confluency after five days.

Exosomes isolated from M1 and B1 cells were analyzed using Nanoparticle Tracking Analysis (NTA). M1 cells released approximately 2.10×10x exosomes per milliliter, with an average size of 82.3 nm, whereas B1 cells released about 1.14×10x exosomes per milliliter, with an average size of 180.7 nm. This indicates a higher exosome production in malignant tumors compared to benign ones.Quantitative PCR analysis of exosomal cargo revealed that miR-18a and miR-19a expressions were higher in M1 cells than in B1 cells. Specifically, miR-18a expression was 3.09 times higher, and miR-19a expression was 1.3 times higher in M1 cells compared to B1 cells. Although these differences were not statistically significant, they suggest a potential role of these miRNAs in the malignant transformation and progression of CMTs.

The *in-vitro* study was carried to investigated the effect of GW4869, an exosomal inhibitor, on the secretion and viability of CMT-U27 cells (canine mammary tumour cell line).CMT-U27 cells were treated with three different concentrations of GW4869 (20 μM, 30 μM, and 40 μM), and the exosome concentration and size distribution were analyzed after 24 hours. The results showed that GW4869 significantly reduced exosome secretion at all tested doses compared to the control group. NTA analysis revealed the mean concentration of exosomes in control, 20 μM, 30 μM and 40 μM GW4869 treatments groups as 1.23e+06 (+/- 72038), 6.38e+05 (+/- 55002), 3.58e+05 (+/- 22174) and 5.50e+05 (+/- 55129) respectively. Among different treatment groups, the treatment of 30 μM GW4869 showed lowest exosomes concentration as compared to 20 μM and 40 μM GW4869 treatment groups. Further, 30 μM and 40 μM dose groups significantly reducing exosomes in the 50-100 nm size range, while increasing larger particles (>150 nm) at higher doses.

The viability of CMT-U27 cells on treatment with GW4869 was assessed using the trypan blue dye exclusion test and MTT assay. The results indicated a dose-dependent reduction in viable cells. Trypan blue dye exclusion test showed that viability of cells treated with 20 μM,

30 µM, and 40 µM doses was 83%, 59%, and 30%, respectively, compared to the control group, which was considered as 100% for comparison. The MTT assay showed a significant reduction in cell viability with the 40 µM and 50 µM doses of GW4869 after 24-48 hours, with a strong statistically significant decrease in cell survival at 48 hours for these doses. Lower doses (10 µM and 20 µM) did not produce a significant reduction in cell viability at any time point, indicating a dose-dependent cytotoxic effect of GW4869 on CMT-U27 cells.

Conclusions:

- Carcinoma-mixed type was most predominant type of CMT.
- Expression of ER and PR vary among different types of CMTs, with ER being more prominent in benign and PR in carcinoma-mixed type tumors.
- Expression of ESR, PR, and EGFR mRNA did not show histological type of differential expression.
- Primary CMT cells from the malignant tumour (intraductal carcinoma) secrete higher number of exosomes with comparatively lower size than benign (simple adenoma).
- Expression of miRNAs viz. miR-18a and miR-19a was higher in exosomes isolated from cell culture supernatant from malignant tumours than benign one.
- GW4869 treatment (20 µM, 30 µM, and 40 µM) significantly decrease the exosomes concentration secreted by CMT-U27.
- Number of exosomes with smaller size (50-100 nm) decreases with increasing GW4869 doses.
- GW4869 treatment significantly reduces the viability of CMT-U27 cells in a dose-dependent manner particularly at higher concentrations of GW4869 (40 µM and 50 µM) caused substantial cytotoxic effects.

Future studies

- Further studies with larger sample size are needed to better understand the role of these biomarkers in CMTs and their potential clinical implications both for IHC and Real time PCR.

- Future studies should focus on further characterizing the functional roles of exosomes in CMTs and exploring their potential as diagnostic and therapeutic targets in veterinary oncology.
- Future studies should also focus on evaluating the long-term effects of GW4869 on tumor progression, including its impact on metastasis and overall survival. The potential combination of GW4869 with other therapeutic strategies, such as chemotherapy or immunotherapy, should also be explored to determine whether it can enhance the efficacy of existing treatments for CMTs
- Further studies are needed to evaluate the *in-vivo* efficacy of GW4869 and to explore its potential as part of a multi-modal approach to CMT treatment.


Mini Abstract

7 MINI ABSTRACT

The present study was designed to investigate the histological, pathobiological, and molecular characteristics of spontaneous canine mammary tumors (CMTs) and explores the role of exosomes in tumor progression. A total of 16 grossly suspected CMTs were collected, of which 15 were histologically diagnosed as CMTs and one as lobular hyperplasia. Female dogs of 6 - 9 years of age group showed highest frequency, and highest number of CMTs found in German Shepherd breed. Histopathological examination revealed that most of the CMTs were malignant (14/16), with carcinoma-mixed type being the most predominant type, followed by intraductal papillary carcinoma. Immunohistochemical analysis showed expressionof ER in simple adenoma (1 case) and intraductal carcinoma (2 cases), PR in carcinoma-mixed type (2 cases) and HER-2 in only one case of carcinosarcoma (1 case). Quantitative real-time PCR assay showed significant fold changes of ESR expression in 55.56% cases, with the highest expression found in simple adenoma. PR expression was detected in 50% of cases but did not show significant differences between benign and malignant tumors. EGFR expression was also observed in 50% of cases, with notable increases in carcinosarcoma and malignant myoepithelioma. Primary cell culture was successfully established from two cases viz. intraductal carcinoma (malignant, M1) and simple adenoma (benign, B1). Exosomes were isolated from M1 and benign B1 CMT primary cell cultures and analyzed using nanoparticle tracking analysis (NTA). M1 cells released significantly more exosomes than B1 cells, with exosome sizes averaging 82.3 nm for M1 and 180.7 nm for B1 cells. Further, it was observed that miR-18a and miR-19a expressions were higher in exomomes of M1 cells than B1. *In-vitro* experiments were performed to analyse the effect of the exosome inhibitor viz. GW4869 on exosome secretion and cell viability in CMT-U27 cells. It was observed that GW4869 treatment (20μM , 30μM , 40 μM) significantly reduced exosome secretion in a dose-dependent manner, with a marked reduction in exosome levels at 30 μM and 40 μM concentrations. Further, it was observed that the proportion of exosomes with size range 50-100 nm was significantly decreased in 30 μM and 40 μM GW4869 treatment groups, while the proportion of exosomes/particles with >150 nm size was increased significantly in 40 μM treatment group. The viability of CMT-U27 cells treated with different doses of GW4869 (10μM, 20μM, 30μM, 40μM, and 50μM) was assessed using MTT and trypan blue dye exclusion assays, which revealed a dose-dependent reduction in cell viability, particularly at the higher GW4869 concentrations. These results suggest that GW4869 may have a cytotoxic effect on CMT cells and provide further insight into the role of exosomes in CMT biology. In conclusion, the experiments with exosomes biogenesis inhibitor i.e. GW4869 indicate that GW4869 has the potential of decreasing the exosomes secretion by cancer cells, which in turn leads to inhibition of the cell proliferation. However, further *in-vivo* studies are needed to fully evaluate its efficacy and safety in clinical applications.

लघु सारांश

8 लघु सारांश

यह अध्ययन सहज रूप से होने वाले श्वान स्तन ट्यूमर के ऊतकविज्ञानिय, पैथोबायोलॉजिकल और आणविक विशेषताओं की जांच करने के लिए और ट्यूमर प्रगति में एक्सोसोम की भूमिका का पता लगाने के लिए किया गया है। कुल 16 संदिग्ध श्वान स्तन ट्यूमर नमून एकत्र किए गए, जिनमें से 15 को ऊतकविज्ञानिय रूप से श्वान स्तन ट्यूमर और एक को लोब्युलर हाइपरप्लासिया के रूप में निदानीत किया गया। यह देखा गया कि की मादा कुत्तों में इसकी सबसे अधिक आवृत्ति 6–9 वर्ष की आयु वर्ग में देखी गई, और जर्मन शेफर्ड नस्ल में श्वान स्तन ट्यूमर की संख्या सर्वाधिक पाई गई। ऊतकविज्ञानिय जांच से पता चला कि अधिकांश श्वान स्तन ट्यूमर घातक थे (14/16), जिनमें कार्सिनोमा–मिश्रित प्रकार सबसे प्रबल था। इम्यूनोहिस्टोकेमिकल विश्लेषण में एस्ट्रोजन रिसेप्टर की अभिव्यक्ति सिंपल एडेनोमा (1 मामला) और इंट्राडक्टल कार्सिनोमा (2 मामले) में देखी गई। प्रोजेस्टेरोन रिसेप्टर की अभिव्यक्ति कार्सिनोमा–मिश्रित प्रकार (2 मामले) में पाई गई, और एचइआर–2 (HER-2) की अभिव्यक्ति केवल एक मामले में (कार्सिनोसारकोमा) देखी गई। मात्रात्मक रियल–टाइम पीसीआर परीक्षण से पता चला कि 55.5% मामलों में ESR अभिव्यक्ति में महत्वपूर्ण परिवर्तन हुए, जिसमें सबसे अधिक अभिव्यक्ति सिंपल एडेनोमा में पाई गई। प्रोजेस्टेरोन रिसेप्टर अभिव्यक्ति 50% मामलों में देखी गई लेकिन सौम्य और घातक ट्यूमर के बीच कोई महत्वपूर्ण अंतर नहीं पाया गया। इजीएफआर (EGFR) अभिव्यक्ति भी 50% मामलों में देखी गई, जिसमें कार्सिनोसारकोमा और घातक मायोएपिथेलियोमा में महत्वपूर्ण वृद्धि देखी गई। प्राथमिक कोशिका संवर्धन (सेल कल्चर) को दो मामलों–इंट्राडक्टल कार्सिनोमा (घातक, एम–1) और सिंपल एडेनोमा (सोम्य, बी-1) से सफलतापूर्वक स्थापित यिका गया। एम-1 और बी-1 प्राथमिक सेल कल्चर से एक्सोसोम को पृथक किया गया और नैनोपार्टिकल ट्रैकिंग विश्लेषण (NTA) का उपयोग करके उनका विश्लेषण किया गया। एम-1 कोशिकाओं ने बी-1 की तुलना में काफी अधिक एक्सोसोम स्राव किए, जिसमें एम-1 के एक्सोसोम का औसत आकार 82.3 nm और बी-1 के लिए 180.7 nm था। इसके अलावा, यह देखा गया कि miR-18a और miR-19a की अभिव्यक्ति एम-1 कोशिकाओं के एक्सोसोम में बी-1 की तुलना में अधिक थी। कृत्रिम परिवेशीय प्रयोगों के तहत, एक्सोसोम अवरोधक GW4869 के प्रभाव का विश्लेषण किया गया। यह देखा गया कि GW4869 (20 μM, 30μm, 40μm) ने एक्सोसोम स्राव को खुराक–निर्भर तरीके से महत्वपूर्ण रूप से कम किया, विशेष रूप से 30 μM और 40 μM सांद्रता पर इसका अधिक प्रभाव देखा गया। इसके अलावा 50-100 nm आकार के एक्सोसोम का अनुपात 30 μM और 40 μM GW4869 उपचार समूहों में महत्वपूर्ण रूप से कम हो गया, जबकि >150 nm आकार के एक्सोसोम का अनुपात 40 μM उपचार समूह में बढ़ गया। CMT-U27 कोशिकाओं की जीवनक्षमता (सेल वायबिलिटी) को विभिन्न GW4869 खुराकों (10 μM, 20 μM, 30 μM, 40 μM और 50 μM) के बाद MTT और ट्रिपैन ब्लू डाई एक्सक्लूजन परीक्षणों द्वारा आंका गया। परिणामों से पता चला कि उच्च GW4869 सांद्रता पर कोशिका जीवनक्षमता खुराक–निर्भर तरीके से कम हो गई। निष्कर्षतः एक्सोसोम बायोजेनेसिस अवरोधक GW4869 पर किए गए प्रयोगों से संकेत मिलता है कि यह कैंसर कोशिकाओं द्वारा एक्सोसोम के स्राव को कम करने की क्षमता रखता है, जिससे कोशिका प्रसार (सेल प्रोलिफरेशन) में अवरोध उत्पन्न होता है। हालांकि, इसके नैदानिक अनुप्रयोगों में प्रभावशीलता और सुरक्षा का पूर्ण मूल्यांकन करने के लिए और अधिक अध्ययन की आवश्यकता है।

References

9 REFERENCES

Abbate, J.M., Arfuso, F., Riolo, K., Capparucci, F., Brunetti, B. and Lanteri, G. 2023. Epigenetics in Canine Mammary Tumors: Upregulation of miR-18a and miR-18b Oncogenes Is Associated with Decreased ERS1 Target mRNA Expression and ERα Immunoexpression in Highly Proliferating Carcinomas. Anim. **13(**6): 1086.

Abdelmegeed, S.M. and Mohammed, S. 2018. Canine mammary tumors as a model for human disease. Oncol Lett. **15**(6): 8195-8205.

Agus, D.B., Gordon, M.S., Taylor, C., Natale, R.B., Karlan, B., Mendelson, D.S., Press, M.F., Allison, D.E., Sliwkowski, M.X., Lieberman, G. and Kelsey, S.M. 2005. Phase I clinical study of pertuzumab, a novel HER dimerization inhibitor, in patients with advanced cancer. J. Clin. Oncol. **23**(11): 2534-2543.

Ahern, T.E., Bird, R.C., Bird, A.E. and Wolfe, L.G. 1996. Expression of the oncogene c erbB-2 in canine mammary cancers and tumor-derived cell lines. Am. J. Vet. Res. **57**(5): 693.

Allred, D. C., Brown, P. and Medina, D. 2004. The origins of estrogen receptor alpha positive and estrogen receptor alpha-negative human breast cancer. Breast. Cancer. Res. **6**(6): 1-6.

Al-Nedawi, K., Meehan, B., Micallef, J., Lhotak, V., May, L., Guha, A. and Rak, J. 2008. Intercellular transfer of the oncogenic receptor EGFRvIII by microvesicles derived from tumour cells. Nat. Cell Biol. **10**(5): 619-624.

Antuofermo, E., Miller, M.A., Pirino, S., Xie, J., Badve, S. and Mohammed, S.I. 2007. Spontaneous mammary intraepithelial lesions in dogs—a model of breast cancer. Cancer. Epidemiol. Biomarkers. Prev. **16**(11): 2247-2256.

Ariazi, E. A., Ariazi, J. L., Cordera, F., and Jordan, V. C. 2006. Estrogen receptors as therapeutic targets in breast cancer. Curr. Top Med. Chem. **6**(3): 181-202.

Ariyarathna, H., De Silva, N., Aberdein, D., Kodikara, D., Jayasinghe, M., Adikari, R. and Munday, J.S. 2018. Clinicopathological diversity of canine mammary gland tumors in Sri Lanka: A one-year survey on cases presented to two veterinary practices. Vet. Sci. **5**(2): 46.

Asada, H., Tomiyasu, H., Uchikai, T., Ishihara, G., Goto-Koshino, Y., Ohno, K. and Tsujimoto, H. 2019. Comprehensive analysis of miRNA and protein profiles within exosomes derived from canine lymphoid tumour cell lines. PLoS One. **14**(4): 0208567.

Baba, O.K., Sood, N.K. and Gupta, K. 2016. Classification, grading and prognostic evaluation of canine mammary tumours. Indian J. Vet. Pathol. **40**(2): 183-186

Bange, J., E. Zwick. and A. Ullrich. 2001. Molecular targets for breast cancer therapy and prevention. Nat. Med. **7**: 548-52.

Baroni, S., Romero-Cordoba, S., Plantamura, I., Dugo, M., D'ippolito, E., Cataldo, A., Cosentino, G., Angeloni, V., Rossini, A., Daidone, M.G. and Iorio, M.V. 2016. Exosome-mediated delivery of miR-9 induces cancer-associated fibroblast-like properties in human breast fibroblasts. Cell. Death Dis. **7**(7): e2312-e2312.

Beauvais, W., Cardwell, J.M. and Brodbelt, D.C. 2012. The effect of neutering on the risk of mammary tumours in dogs–a systematic review. J. Small Anim. Pract. **53**(6): 314-322.

Benavente MA, Bianchi CP, Aba MA. 2016. Canine mammary tumors: risk factors, prognosis and treatments. J. Vet. Adv. **6**:1291–300.

Benjamin, S.A., Lee, A.C. and Saunders, W.J. 1999. Classification and behavior of canine mammary epithelial neoplasms based on life-span observations in beagles. Vet. Pathol. **36**(5): 423-436.

Besse, B., Charrier, M., Lapierre, V., Dansin, E., Lantz, O., Planchard, D., Le Chevalier, T., Livartoski, A., Barlesi, F., Laplanche, A. and Ploix, S. 2016. Dendritic cell-derived exosomes as maintenance immunotherapy after first line chemotherapy in NSCLC. Oncoimmunol. **5**(4): 1071008.

Brodey, R.S., Goldschmidt, M.H. and Roszel, J.R. 1983. Canine mammary gland neoplasms. J. Am. Anim. Hosp. Assoc. **19**: 61-90.

Caceres, S., Peña, L., de Andres, P.J., Illera, M.J., Lopez, M.S., Woodward, W.A., Reuben, J.M. and Illera, J.C. 2015. Establishment and characterization of a new cell line of canine inflammatory mammary cancer: IPC-366. PLoS One. **10**(3): 0122277.

Canadas, A., França, M., Pereira, C., Vilaça, R., Vilhena, H., Tinoco, F., Silva, M.J., Ribeiro, J., Medeiros, R., Oliveira, P. and Dias-Pereira, P. 2019. Canine mammary tumors: comparison of classification and grading methods in a survival study. Vet. Pathol. **56**(2): 208-219.

Carvalho, M. I., Guimarães, M. J., Pires, I., Prada, J., Silva-Carvalho, R., Lopes, C. and Queiroga, F. L. 2013. EGFR and microvessel density in canine malignant mammary tumours. Res. Vet. Sci. **95**(3): 1094-1099.

Cassali, G.D., Lavalle, G.E., De Nardi, A.B., Ferreira, E., Bertagnolli, A.C., Estrela-Lima, A., Alessi, A.C., Daleck, C.R., Salgado, B.S., Fernandes, C.G. and Sobral, R.A. 2011. Consensus for the diagnosis, prognosis and treatment of canine mammary tumors. Braz. J. Vet. Pathol. **4**(2): 153-180.

Catalano, M. and O'Driscoll, L. 2020. Inhibiting extracellular vesicles formation and release: a review of EV inhibitors. J. Extracell. Vesicles. **9**(1): 1703244.

Chang, C.Y., Chiou, P.P., Chen, W.J., Li, Y.H., Yiu, J.C., Cheng, Y.H., Chen, S.D., Lin, C.T. and Lai, Y.S. 2010. Assessment of the tumorigenesis and drug susceptibility of three new canine mammary tumor cell lines. Res. J. Vet. Sci. **88**(2): 285-293.

Chen, Y., He, L., Zhou, H., Li, W. and Qiu, C. 2023. Transcriptional profiling of exosomes derived from plasma of canine with mammary tumor by RNA-seq analysis. Genomics. **115**(4): 110660.

Chiaverini, C., Beuret, L., Flori, E., Abbe, P., Bille, K., Bahadoran, P., Ortonne, J.P., Bertolotto, C. and Ballotti, R. 2008. Microphthalmia-associated transcription factor regulates RAB27A gene expression and controls melanosome transport. J. Biol. Chem. **283**(18): 12635-12642.

Cifone, M.A. 1982. In vitro growth characteristics associated with benign and metastatic variants of tumor cells. Cancer Metastasis Rev. **1**: 335-347.

Clark, G.M., and McGuire, W.L. 1983. Prognostic factors in primary breast cancer. Breast Cancer Res. Treat. **3**(l): 69-72.

Cocucci, E. and Meldolesi, J. 2015. Ectosomes and exosomes: shedding the confusion between extracellular vesicles. Trends Cell Biol. **25**(6): 364-372.

Colombo, M., Raposo, G. and Théry, C. 2014. Biogenesis, secretion, and intercellular interactions of exosomes and other extracellular vesicles. Annu. Rev. Cell Dev. Biol. **30**: 255-289.

Conde-Vancells, J., Rodriguez-Suarez, E., Embade, N., Gil, D., Matthiesen, R., Valle, M., Elortza, F., Lu, S.C., Mato, J.M. and Falcon-Perez, J.M. 2008. Characterization and comprehensive proteome profiling of exosomes secreted by hepatocytes. J Proteome Res. **7**(12): 5157-5166.

Costa-Silva, B., Aiello, N.M., Ocean, A.J., Singh, S., Zhang, H., Thakur, B.K., Becker, A., Hoshino, A., Mark, M.T., Molina, H. and Xiang, J. 2015. Pancreatic cancer exosomes initiate pre-metastatic niche formation in the liver. Nat. Cell Biol. **17**(6): 816-826.

Dai, J., Su, Y., Zhong, S., Cong, L., Liu, B., Yang, J., Tao, Y., He, Z., Chen, C. and Jiang, Y. 2020. Exosomes: key players in cancer and potential therapeutic strategy. Signal Transduct. Target. Ther. **5**(1): 145.

Daniel, A.R., Hagan, C.R. and Lange, C.A. 2011. Progesterone receptor action: defining a role in breast cancer. Expert Rev. Endocrinol. Metab. **6**(3): 359-369.

Datta, A., Kim, H., McGee, L., Johnson, A.E., Talwar, S., Marugan, J., Southall, N., Hu, X., Lal, M., Mondal, D. and Ferrer, M. 2018. High-throughput screening identified selective inhibitors of exosome biogenesis and secretion: A drug repurposing strategy for advanced cancer. Sci. Rep. **8**(1): 8161.

de Faria Lainetti, P., Brandi, A., Leis Filho, A.F., Prado, M.C.M., Kobayashi, P.E., Laufer-Amorim, R. and Fonseca-Alves, C.E. 2020. Establishment and characterization of canine mammary gland carcinoma cell lines with vasculogenic mimicry ability in vitro and in vivo. Front. Vet. Sci.**7**: 583874.

De las Mulas, J. M., Ordás, J., Millán, Y., Fernández-Soria, V. and y Cajal, S. R. 2003. Oncogene HER-2 in canine mammary gland carcinomas. Breast Cancer Res. Treat. **80**(3): 363-367.

De Las Mulas, J.M., Millán, Y. and Dios, R. 2005. A prospective analysis of immunohistochemically determined estrogen receptor α and progesterone receptor expression and host and tumor factors as predictors of disease-free period in mammary tumors of the dog. Vet. Pathol. **42**(2). 200-212.

Devarathnam, J., Suresh Kumar, R.V., Bharathi, S. and Anand Kumar, A. 2021. Epidemiological studies of canine mammary gland tumors. Pharm. Innov. **10**(7): 13-17.

Dias, M.L.D.M., Andrade, J.M.L., Castro, M.B.D. and Galera, P.D. 2016. Survival analysis of female dogs with mammary tumors after mastectomy: epidemiological, clinical and morphological aspects. Pes.Vet. Bra. **36**: 181-186.

Dinkins, M.B., Dasgupta, S., Wang, G., Zhu, G. and Bieberich, E. 2014. Exosome reduction in vivo is associated with lower amyloid plaque load in the 5XFAD mouse model of Alzheimer's disease. Neurobiol Aging. **35**(8): 1792-1800.

Diomaiuto, E., Principe, V., De Luca, A., Laperuta, F., Alterisio, C. and Di Loria, A. 2021. Exosomes in Dogs and Cats: an innovative approach to neoplastic and non-neoplastic diseases. Pharm. **14**(8): 766.

Dunnwald, L. K., Rossing, M. A. and Li, C. I. 2007. Hormone receptor status, tumor characteristics, and prognosis: a prospective cohort of breast cancer patients. Breast Cancer Res. **9**(1): 6.

Egenvall, A., Bonnett, B.N., Öhagen, P., Olson, P., Hedhammar, Å. and von Euler, H. 2005. Incidence of and survival after mammary tumors in a population of over 80,000 insured female dogs in Sweden from 1995 to 2002. Prev Vet Med. **69**(1-2): 109-127.

Eguchi, T., Sogawa, C., Ono, K., Matsumoto, M., Tran, M.T., Okusha, Y., Lang, B.J., Okamoto, K. and Calderwood, S.K. 2020. Cell stress induced stressome release including damaged membrane vesicles and extracellular HSP90 by prostate cancer cells. Cells. **9**(3): 755.

Eguchi, T., Taha, E.A., Calderwood, S.K. and Ono, K. 2020. A novel model of cancer drug resistance: oncosomal release of cytotoxic and antibody-based drugs. Biology. **9**(3): 47.

Fesseha, H. 2020. Mammary tumours in dogs and its treatment option-a review. Biomed J Sci & Tech Res. **30**(4): 23552-23561.

Fish, E.J., Irizarry, K.J., DeInnocentes, P., Ellis, C.J., Prasad, N., Moss, A.G. and Curt Bird, R. 2018. Malignant canine mammary epithelial cells shed exosomes containing differentially expressed microRNA that regulate oncogenic networks. BMC Cancer. **18**: 1-20.

Galadima, M. 2024., Serum and tissue biomarkers for clinical diagnosis of canine mammary tumours

Gama A, Alves A, Schmitt F. 2008. Identification of molecular phenotypes in canine mammary carcinomas with clinical implications: application of the human classification. Virchows Arch; **453**: 123–32.

Gama, A., Gartner, F., Alves, A. and Schmitt, F. 2009. Immunohistochemical expression of Epidermal Growth Factor Receptor (EGFR) in canine mammary tissues. Res. Vet. Sci. **87**(3): 432-437.

Gassmann, M., Casagranda, F., Orioli, D., Simon, H., Lai, C., Klein, R. and Lemke, G. 1995. Aberrant neural and cardiac development in mice lacking the ErbB4 neuregulin receptor. Nature. **378**(6555): 390-394.

Ge, R., Tan, E., Sharghi-Namini, S. and Asada, H.H. 2012. Exosomes in cancer microenvironment and beyond: have we overlooked these extracellular messengers? Cancer Microenviron. **5**: 323-332.

Geraldes, M., Gärtner, F. and Schmitt, F. 2000. Immunohistochemical study of hormonal receptors and cell proliferation in normal canine mammary glands and spontaneous mammary tumours. Vet. Rec. **146**(14): 403-406.

Gilbertson, S.R., Kurzman, I.D., Zachrau, R.E., Hurvitz, A.I. and Black, M.M. 1983. Canine mammary epithelial neoplasms: biologic implications of morphologic characteristics assessed in 232 dogs. Vet. Pathol. **20**(2): 127-142.

Goldschmidt, M., Peña, L., Rasotto, R. and Zappulli, V. 2011. Classification and grading of canine mammary tumors. Vet. Pathol. **48**(1): 117-131.

Gracanin, A., De Gier, J., Zegers, K., Bominaar, M., Rutteman, G.R., Schaefers Okkens, A.C., Kooistra, H.S. and Mol, J.A. 2012. Progesterone receptor isoforms in the mammary gland of cats and dogs. Reprod. Dom. Anim. **47:** 13-317.

Greening, D.W., Gopal, S.K., Mathias, R.A., Liu, L., Sheng, J., Zhu, H.J. and Simpson, R.J. 2015, April. Emerging roles of exosomes during epithelial–mesenchymal transition and cancer progression. Semin. Cell Dev. Biol. **40**: 60-71.

Guil Luna, S., Sánchez Céspedes, R., Millan, Y., De Andres, F. J., Rollon, E., Domingo, V. and Martín de Las Mulas, J. 2011. Aglepristone decreases proliferation in progesterone receptor positive canine mammary carcinomas. J. Vet. Intern.Med. **25**(3): 518-523.

Guil-Luna, S., Stenvang, J., Brünner, N., De Andrés, F.J., Rollón, E., Domingo, V., Sánchez-Céspedes, R., Millán, Y. and Martín de las Mulas, J. 2014. Progesterone receptor isoform A may regulate the effects of neoadjuvant aglepristone in canine mammary carcinoma. BMC Vet. Res. **10**: 1-8.

Guil-Luna, S., Stenvang, J., Brünner, N., Sánchez-Céspedes, R., Millán, Y., Gómez-Laguna, J. and Mulas, J.M.D.L. 2014. Progesterone receptor isoform analysis by quantitative real-time polymerase chain reaction in formalin-fixed, paraffin-embedded canine mammary dysplasias and tumors. Vet. Pathol **51**(5): 895-902.

Guimaraes, M. J., Carvalho, M. I., Pires, I., Prada, J., Gil, A. G., Lopes, C. and Queiroga, F. L. 2014. Concurrent expression of cyclo-oxygenase-2 and epidermal growth factor receptor in canine malignant mammary tumours. J. Comp. Pathol. **150**(1): 27-34.

Guiochon-Mantel, A., Delabre, K., Lescop, P. and Milgrom, E. 1994. Nuclear localization signals also mediate the outward movement of proteins from the nucleus. Proc. Natl. Acad. Sci. **91**(15): 7179–7183.

Gupta, K., Sood, N.K., Uppal, S.K., Mohindroo, J., Mahajan, S., Raghunath, M. and Singh, K. 2012. Epidemiological studies on canine mammary tumour and its relevance for breast cancer studies. IOSR J Pharm. **2**(2): 322-333.

Haluska, P., Dy, G.K. and Adjei, A.A. 2002. Farnesyl transferase inhibitors as anticancer agents. Eur. J. Cancer. **38**(13): 1685-1700.

Halvaei, S., Daryani, S., Eslami-S, Z., Samadi, T., Jafarbeik-Iravani, N., Bakhshayesh, T.O., Majidzadeh-A, K. and Esmaeili, R. 2018. Exosomes in cancer liquid biopsy: a focus on breast cancer. Mol. Ther. Nucleic Acids. **10**: 131-141.

Harding, C. and Stahl, P. 1983. Transferrin recycling in reticulocytes: pH and iron are important determinants of ligand binding and processing. Biochem Biophys Res Commun. **113**(2): 650-658.

Hemanth, I., Kumar, R., Varshney, K.C., Nair, M.G., Kumar, B.R., Sivakumar, M. and Thanislass, J. 2015. Epidemiological and clinical studies on canine mammary tumors. Indian J. Anim. Res (The). **24**(1): 11-14.

Henson, E.S. and Gibson, S.B. 2006. Surviving cell death through epidermal growth factor (EGF) signal transduction pathways: implications for cancer therapy. Cell Signal. **18**(12): 2089-2097.

Heusermann, W., Hean, J., Trojer, D., Steib, E., Von Bueren, S., Graff-Meyer, A., Genoud, C., Martin, K., Pizzato, N., Voshol, J. and Morrissey, D.V. 2016. Exosomes surf on filopodia to enter cells at endocytic hot spots, traffic within endosomes, and are targeted to the ER. J. Cell Biol. **213**(2): 173-184.

Hoshino, A., Costa-Silva, B., Shen, T.L., Rodrigues, G., Hashimoto, A., Tesic Mark, M., Molina, H., Kohsaka, S., Di Giannatale, A., Ceder, S. and Singh, S. 2015. Tumour exosome integrins determine organotropic metastasis. Nat. **527**(7578): 329-335.

Howard, J., Wyse, C., Argyle, D., Quinn, C., Kelly, P. and McCann, A. 2020. Exosomes as biomarkers of human and feline mammary tumours; a comparative medicine approach to unravelling the aggressiveness of TNBC. Biochim. Biophys. Acta, Rev. Cancer. **1874**(2): 188431.

Ichii, O., Ohta, H., Horino, T., Nakamura, T., Hosotani, M., Mizoguchi, T., Morishita, K., Nakamura, K., Hoshino, Y., Takagi, S. and Sasaki, N. 2017. Urinary exosome-derived microRNAs reflecting the changes of renal function and histopathology in dogs. Sci. Rep. **7**(1): 40340.

Im, E.J., Lee, C.H., Moon, P.G., Rangaswamy, G.G., Lee, B., Lee, J.M., Lee, J.C., Jee, J.G., Bae, J.S., Kwon, T.K. and Kang, K.W. 2019. Sulfisoxazole inhibits the secretion of small extracellular vesicles by targeting the endothelin receptor A. Nat Commun. **10**(1): 1387.

Irep, N., Inci, K., Tokgun, P.E. and Tokgun, O. 2024. Exosome inhibition improves response to first line therapy in small cell lung cancer. J. Cell. Mol. Med. **28**(4): 18138.

Johnstone, R.M., Adam, M., Hammond, J.R., Orr, L. and Turbide, C. 1987. Vesicle formation during reticulocyte maturation. Association of plasma membrane activities with released vesicles (exosomes). J. Biol. Chem. **262**(19): 9412-9420.

K. Mayilkumar. 2009. Evaluation of c-erb2 and estrogen receptor expression in chemically induced rat mammary tumours, Thesis, M.V.Sc. (Veterinary Pathology), Deemed Univeristy, I.V.R.I., Izatnagar.

Kabir, F.M.L., DeInnocentes, P., Agarwal, P., Mill, C.P., Riese 2nd, D.J. and Bird, R.C. 2017. Estrogen receptor-α, progesterone receptor, and c-erb B/HER-family receptor mRNA detection and phenotype analysis in spontaneous canine models of breast cancer. J. Vet. Sci. **18**(2): 149-158.

Kahlert, C. and Kalluri, R. 2013. Exosomes in tumor microenvironment influence cancer progression and metastasis. J. Mol. Med. **91**: 431-437.

Kajimoto, T., Okada, T., Miya, S., Zhang, L. and Nakamura, S.I. 2013. Ongoing activation of sphingosine 1-phosphate receptors mediates maturation of exosomal multivesicular endosomes. Nat. Commun. **4**(1): 2712.

Kalluri, R. and LeBleu, V.S. 2020. The biology, function, and biomedical applications of exosomes. Science. **367**(6478): 6977.

Kalra, H., Adda, C.G., Liem, M., Ang, C.S., Mechler, A., Simpson, R.J., Hulett, M.D. and Mathivanan, S. 2013. Comparative proteomics evaluation of plasma exosome isolation techniques and assessment of the stability of exosomes in normal human blood plasma. Proteomics. **13**(22): 3354-3364.

Kamerkar, S., LeBleu, V.S., Sugimoto, H., Yang, S., Ruivo, C.F., Melo, S.A., Lee, J.J. and Kalluri, R. 2017. Exosomes facilitate therapeutic targeting of oncogenic KRAS in pancreatic cancer. Nature. **546**(7659): 498-503.

Kavanagh, E.L., Lindsay, S., Halasz, M., Gubbins, L.C., Weiner-Gorzel, K., Guang, M.H.Z., McGoldrick, A., Collins, E., Henry, M., Blanco-Fernández, A. and O'Gorman, P. 2017. Protein and chemotherapy profiling of extracellular vesicles harvested from therapeutic induced senescent triple negative breast cancer cells. Oncogenesis. **6**(10): 388-e388.

Kennedy, K.C., Qurollo, B.A., Rose, B.J. and Thamm, D.H. 2011. Epidermal growth factor enhances the malignant phenotype in canine mammary carcinoma cell lines. Vet Comp Oncol. **9**(3): 196-206

Khan, F.M., Saleh, E., Alawadhi, H., Harati, R., Zimmermann, W.H. and El-Awady, R., 2018. Inhibition of exosome release by ketotifen enhances sensitivity of cancer cells to doxorubicin. Cancer biol. ther. **19**(1): 25-33.

Kharmate, G., Hosseini-Beheshti, E., Caradec, J., Chin, M.Y. and Tomlinson Guns, E.S. 2016. Epidermal growth factor receptor in prostate cancer derived exosomes. PLoS One. **11**(5): 0154967.

Klopfleisch R, Schutze M, Gruber AD. 2010. Downregulation of transforming growth factor beta (TGF beta) and latent TGF beta binding protein (LTBP)-4 expression in late stage canine mammary tumours. Vet J. **186**: 379–84

Kosaka, N., Iguchi, H., Yoshioka, Y., Takeshita, F., Matsuki, Y. and Ochiya, T. 2010. Secretory mechanisms and intercellular transfer of microRNAs in living cells. J. Biol. Chem. **285**(23): 17442-17452.

Kowal, J., Tkach, M. and Théry, C., 2014. Biogenesis and secretion of exosomes. Curr. Opin. Cell Biol. **29**: 116-125.

Król, M., Polańska, J., Pawłowski, K.M., Turowski, P., Skierski, J., Majewska, A., Ugorski, M., Morty, R.E. and Motyl, T. 2010. Transcriptomic signature of cell lines isolated from canine mammary adenocarcinoma metastases to lungs. J. Appl. Genet. **51**: 37-50.

Kumar, A., Kumar, P., Sharma, M., Kim, S., Singh, S., Kridel, S.J. and Deep, G. 2022. Role of extracellular vesicles secretion in paclitaxel resistance of prostate cancer cells. Cancer Drug Resist. **5**(3): 612.

Kumar, P. 2008. Evaluation of c-erb2 in canine mammary tumours, Thesis, M.V.Sc. (Veterinary Pathology), Deemed Univeristy, I.V.R.I., Izatnagar.

Kumar, P., Kumar, R., Pawaiya, R. V. S., Reddy, M., Maiti, G. B. and Maiti, S. K. 2009. Expression pattern of c-erbB2 oncoprotein in canine mammary tumours. Indian J. Vet. Pathol. **33**(2): 125-129.

Lantinga-van Leeuwen, I.S., van Garderen, E., Rutteman, G.R. and Mol, J.A. 2000. Cloning and cellular localization of the canine progesterone receptor: co-localization with growth hormone in the mammary gland. J. Steroid Biochem. Mol. Biol. **75**(4-5): 219-228.

Lee, J., Lee, S.A., Gu, N.Y., Jeong, S.Y., Byeon, J.S., Jeong, D.U., Ouh, I.O., Lee, Y.H. and Hyun, B.H., 2021. Canine Natural Killer Cell Derived Exosomes Exhibit Antitumor Activity in a Mouse Model of Canine Mammary Tumor. Biomed Res. Int. **1**: 6690704.

Lee, K. F., Simon, H., Chen, H., Bates, B., Hung, M. C. and Hauser, C. 1995. Requirement for neuregulin receptor erbB2 in neural and cardiac development. Nature. **378**(6555): 394-398.

Li, R., Wu, H., Sun, Y., Zhu, J., Tang, J., Kuang, Y. and Li, G. 2021. A novel canine mammary cancer cell line: Preliminary identification and utilization for drug screening studies. Front. Vet. Sci. **8**: 665906.

Li, W., Tsen, F., Sahu, D., Bhatia, A., Chen, M., Multhoff, G. and Woodley, D.T. 2013. Extracellular Hsp90 (eHsp90) as the actual target in clinical trials: intentionally or unintentionally. Int. Rev. Cell Mol. Biol. **303**: 203-235.

Li, X.J., Ren, Z.J., Tang, J.H. and Yu, Q. 2018. Exosomal MicroRNA MiR-1246 promotes cell proliferation, invasion and drug resistance by targeting CCNG2 in breast cancer. Cell. Physiol. Biochem. **44**(5): 1741-1748.

Logozzi, M., Angelini, D.F., Giuliani, A., Mizzoni, D., Di Raimo, R., Maggi, M., Gentilucci, A., Marzio, V., Salciccia, S., Borsellino, G. and Battistini, L. 2019. Increased plasmatic levels of PSA-expressing exosomes distinguish prostate cancer patients from benign prostatic hyperplasia: a prospective study. Cancers, **11**(10):1449.

Louie, M. C. and Sevigny, M. B. 2017. Steroid hormone receptors as prognostic markers in breast cancer. Am. J. Cancer Res. **7**(8): 1617.

Luberto, C., Hassler, D.F., Signorelli, P., Okamoto, Y., Sawai, H., Boros, E., Hazen-Martin, D.J., Obeid, L.M., Hannun, Y.A. and Smith, G.K. 2002. Inhibition of tumor necrosis factor-induced cell death in MCF7 by a novel inhibitor of neutral sphingomyelinase. J. Biol. Chem. **277**(43): 41128-41139.

Luna, G. 1968. Manual of Histological Staining Method of the Armed Forces Institute of Pathology, 3rd ed. New York, McGraw-Hill Book Company.

Macias, H. and Hinck, L. 2012. Mammary gland development. Wiley Interdiscip. Rev. Dev. Biol., **1**(4), 533-557.

Maia, J., Caja, S., Strano Moraes, M.C., Couto, N. and Costa-Silva, B. 2018. Exosome-based cell-cell communication in the tumor microenvironment. Front. Cell Dev. Biol. **6**: 18.

Martín de las Mulas J, Millán Y, Dios R. 2005. A prospective analysis of immunohistochemically determined estrogen receptor α and progesterone expression and host and tumor factors as predictors of disease-free period in mammary tumors of the dog. Vet Pathol. **42**(2): 200-12.

Martin, M.J., Ordas, J., Millan, Y., Fernandez-Soria, V. and Ramony, C.S. 2003. Oncogene HER-2 in canine mammary gland carcinomas: an immunohistochemical and chromogenic in situ hybridization study. Breast Cancer Res. Treat. **80**: 363-367.

Masuda, H., Zhang, D., Bartholomeusz, C., Doihara, H., Hortobagyi, G. N. and Ueno, N. T. 2012. Role of epidermal growth factor receptor in breast cancer. Breast Cancer Res. Treat. **136**(2): 331-345.

Matos, A.J.F., Baptista, C.S., Gärtner, M.F. and Rutteman, G.R. 2012. Prognostic studies of canine and feline mammary tumours: the need for standardized procedures. Vet. J. **193**(1): 24-31.

Meinhövel, F., Stange, R., Schnauß, J., Sauer, M., Käs, J.A. and Remmerbach, T.W. 2018. Changing cell mechanics—a precondition for malignant transformation of oral squamous carcinoma cells. Converg. Sci. Phys. Oncol. **4**(3): 034001.

Menck, K., Sönmezer, C., Worst, T.S., Schulz, M., Dihazi, G.H., Streit, F., Erdmann, G., Kling, S., Boutros, M., Binder, C. and Gross, J.C. 2017. Neutral sphingomyelinases control extracellular vesicles budding from the plasma membrane. J Extracell Vesicles. **6**(1).1378056.

Mendt, M., Kamerkar, S., Sugimoto, H., McAndrews, K.M., Wu, C.C., Gagea, M., Yang, S., Blanko, E.V.R., Peng, Q., Ma, X. and Marszalek, J.R. 2018. Generation and testing of clinical-grade exosomes for pancreatic cancer. JCI insight. **3**(8).

Millanta, F., Calandrella, M., Bari, G., Niccolini, M., Vannozzi, I. and Poli, A.L.E.S.S.A.N.D.R.O. 2005. Comparison of steroid receptor expression in normal, dysplastic, and neoplastic canine and feline mammary tissues. Res Vet Sci. **79**(3): 225-30.

Misdorp, W. 1999. Histological classification of the mammary tumors of the dog and the cat. World Health Organization International Histological Classification of Tumors of Domestic Animals second series. **7**: 1-59.

Misdorp, W. 2002. Tumours of mammary gland. In: Tumours in domestic animals, ed. Meuten DJ, 4th ed., Iowa State Press, Ames, IA. 575-606.

Moccia, V., Sammarco, A., Ferro, S., Cavicchioli, L. and Zappulli, V. 2023. Characterization and function of extracellular vesicles in a canine mammary tumour cell line: Ultracentrifugation versus size exclusion chromatography. Vet. Comp. Oncol. **21**(1): 36-44.

Mol, J. A., Van Garderen, E., Rutteman, G. R., and Rijnberk, A. 1996. New insights in the molecular mechanism of progestin-induced proliferation of mammary epithelium: induction of the local biosynthesis of growth hormone (GH) in the mammary gland of dogs, cats and humans. J. Steroid Biochem. Mol. Biol. **57**(1-2): 67-71.

Morris, J.S., Nixon, C., King, O.J., Morgan, I.M. and Philbey, A.W. 2009. Expression of TopBP1 in canine mammary neoplasia in relation to histological type, Ki67, ERα and p53. Vet. J. **179**(3): 422-429.

Moulton, J. E. 1990. Tumours of mammary gland. In:Moulton J E (ed) Tumours in domestic animals. 3rd edn. Univercity of California Press, Berkeley and Los Angeles. **3**: 518-52.

Moulton, J. E., D. O. N. Taylor, C. R. Dorn, and A. C. Andersen. 1970. Canine mammary tumors. Pathol. Vet. **7**(4): 289-320.

Mukhopadhayay, S. and Som, T. L. 1992. Cutaneous neoplasms in dogs in and around Calcutta. Indian J. Vet. Pathol. **16**(2): 122-123.

Mulas, J., Ordás, J., Millán, Y., Fernández-Soria, V., Ramón, Y. and Cajal, S. 2003. Oncogene HER2 in canine mammary gland carcinomas: an immunohistochemical and chromogenic in situ hybridization study. Breast Cancer. Res. Treat. **80**(3): 363-7.

Murua, C., Miyazaki, H., Miyamoto, A., & Shimizu, T. 2012. Luteinizing hormone (LH) regulates production of androstenedione and progesterone via control of histone acetylation of StAR and CYP17 promoters in ovarian theca cells. Mol. Cell. Endocrinol. **350**(1) 1-9.

Mylonas, I., Jeschke, U., Shabani, N., Kuhn, C., Kunze, S., Dian, D. and Friese, K. 2007. Steroid receptors ERalpha, ERss, PR-A and PR-B are differentially expressed in normal and atrophic human endometrium. Histol. Histopathol. **22**(1): 169.

Nadhiya, C., Nair, M.G., Kumar, R., Uma, A.W.L.S. and Alphonse, R.M.D. 2020. Occurrence and pathology of canine mammary neoplasms-A prospective study. J Entomol Zool Stud. **8**(4): 1498-1503.

Nazarenko, I., Rana, S., Baumann, A., McAlear, J., Hellwig, A., Trendelenburg, M., Lochnit, G., Preissner, K.T. and Zöller, M. 2010. Cell surface tetraspanin Tspan8 contributes to molecular pathways of exosome-induced endothelial cell activation. Cancer Res. **70**(4): 1668-1678.

Nieto, A., Pena, L., Pérez-Alenza, M. D., Sanchez, M. A., Flores, J. M. nd Castano, M. 2000. Immunohistologic detection of estrogen receptor alpha in canine mammary tumors: clinical and pathologic associations and prognostic significance. Vet. Pathol. **37**(3): 239-247.

Ohno, S.I., Takanashi, M., Sudo, K., Ueda, S., Ishikawa, A., Matsuyama, N., Fujita, K., Mizutani, T., Ohgi, T., Ochiya, T. and Gotoh, N. 2013. Systemically injected exosomes targeted to EGFR deliver antitumor microRNA to breast cancer cells. Mol. Ther. **21**(1): 185-191.

Owen, L.N. and World Health Organization, 1980. TNM Classification of Tumours in Domestic Animals/edited by LN Owen (No. VPH/CMO/80.20). World Health Organization.

Parker, M. G. 1995. Structure and function of estrogen receptors. Vitam. Horm. **51**(1): 267 287.

Parolini, I., Federici, C., Raggi, C., Lugini, L., Palleschi, S., De Milito, A., Coscia, C., Iessi, E., Logozzi, M., Molinari, A. and Colone, M. 2009. Microenvironmental pH is a key factor for exosome traffic in tumor cells. J. Biol. Chem. **284**(49): 34211-34222.

Patel, H. K., and Bihani, T. 2018. Selective estrogen receptor modulators (SERMs) and selective estrogen receptor degraders (SERDs) in cancer treatment. Pharmacol. Ther. **186**(1) 1-24.

Pawaiya, R. V. S. 2004. Pathology of chemically induced neoplasms and evaluation of molecular markers in diagnosis of animal tumours. Thesis, PhD (Vety. Pathology) submitted to Deemed University, Indian Veterinary Research Institute, Izatnagar.

Peña, L., Gama, A., Goldschmidt, M.H., Abadie, J., Benazzi, C., Castagnaro, M., Díez, L., Gärtner, F., Hellmén, E., Kiupel, M. and Millán, Y. 2014. Canine mammary tumors: a review and consensus of standard guidelines on epithelial and myoepithelial phenotype markers, HER2, and hormone receptor assessment using immunohistochemistry. Vet. Pathol. **51**(1): 127-47.

Petroušková, P., Hudáková, N., Maloveská, M., Humeník, F. and Cizkova, D. 2022. Non-exosomal and Exosome-derived miRNAs as promising biomarkers in canine mammary cancer. Life. **12**(4): 524.

Pierce, J. H., Arnstein, P., DiMarco, E., Artrip, J., Kraus, M. H., Lonardo, F. and Aaronson, S. A. 1991. Oncogenic potential of erbB-2 in human mammary epithelial cells. Oncogene. **6**(7): 1189-1194.

Port Louis, L.R., Varshney, K.C. and Nair, M.G. 2012. An immunohistochemical study on the expression of sex steroid receptors in canine mammary tumors. Int. Sch. Res. Notices. **1**: 78607.

Raffo-Romero, A., Aboulouard, S., Bouchaert, E., Rybicka, A., Tierny, D., Hajjaji, N., Fournier, I., Salzet, M. and Duhamel, M. 2023. Establishment and characterization of canine mammary tumoroids for translational research. BMC Biol. **21**(1): 1-19.

Rahman A.T, 2021. Molecular classification of canine mammary tumours with special reference to triple-negative phenotype: corelation with prognostic factors, Thesis, M.V.Sc. (Veterinary Pathology), Deemed Univeristy, I.V.R.I., Izatnagar.

Ranganath, G. J., Kumar, R., Reddy, A. P., Mayilkumar, K., Pawaiya, R. V. S. and Debroy, B. 2011. Expression pattern of c-erbB2 and estrogen receptor-á in spontaneous canine mammary tumours. Indian J. Vet. Pathol. **35**(2): 136-141.

Raposo, L.R., Roma Rodrigues, C., Faísca, P., Alves, M., Henriques, J., Carvalheiro, M.C., Corvo, M.L., Baptista, P.V., Pombeiro, A.J. and Fernandes, A.R. 2017. Immortalization and characterization of a new canine mammary tumour cell line FR37 CMT. Vet. Comp. Oncol. **15**(3): 952-967.

Reddy, G. B. M. 2007. Pathology and evaluation of tumour markers in spontaneous canine skin and mammary tumours. M.V.Sc. Thesis, Indian Veterinary Research Institute (IVRI), Izatnagar, Bareilly, U.P, India.

Rezia, A., Tavasoli, A., Bahonar, A. and Mehrazma, M., 2009. Grading in canine mammary gland carcinoma. J. Biol. Sci. **9**: 333-338.

Riches, A., Campbell, E., Borger, E. and Powis, S. 2014. Regulation of exosome release from mammary epithelial and breast cancer cells–a new regulatory pathway. Eur. J. Cancer. **50**(5): 1025-1034.

Rivera, P. and Von Euler, H., 2011. Molecular biological aspects on canine and human mammary tumors. Vet. Pathol. **48**(1): 132-146.

Ruivo, C.F., Adem, B., Silva, M. and Melo, S.A. 2017. The biology of cancer exosomes: insights and new perspectives. Cancer Res. **77**(23): 6480-6488.

Rungsipipat, A., Sunyasootcharee, B., Ousawaphlangchai, L., Sailasuta, A., Thanawongnuwech, R. and Teankum, K., 2003. Neoplasms of dogs in Bangkok. Thai. J. Vet. Med. **33**(1): 59-66.

Rutteman, G. R., Misdorp, W., Blankenstein, M. A., and Van den Brom, W. E. 1988. Oestrogen (ER) and progestin receptors (PR) in mammary tissue of the female dog: different receptor profile in non-malignant and malignant states. Br. J. Cancer. **58**(5): 594 599.

Sahabi, K., Selvarajah, G.T., Noordin, M.M., Sharma, R.S.K. and Dhaliwal, G.K. 2015. Retrospective histopathological study of canine mammary gland tumours diagnosed from 2006–2012 in University Putra Malaysia. J. Vet. Malays. **27**: 1-6.

Salas, Y., Márquez, A., Diaz, D. and Romero, L. 2015. Epidemiological study of mammary tumors in female dogs diagnosed during the period 2002-2012: a growing animal health problem. PloS one. **10**(5): 0127381.

Salehi, M. and Sharifi, M. 2018. Exosomal miRNAs as novel cancer biomarkers: Challenges and opportunities. J. Cell. Physiol. **233**(9): 6370-6380.

Sassi, F., Benazzi, C., Castellani, G. and Sarli, G. 2010. Molecular-based tumour subtypes of canine mammary carcinomas assessed by immunohistochemistry. BMC Vet. Res. **6**(1): 5.

Sawyers, C. 2004. Targeted cancer therapy. Nature. **432**(7015): 294-297.

Shafiee, R., Javanbakh, J., Atyabi, N., Kheradmand, P., Kheradmand, D., Bahrami, A., Daraei, H. and Khadivar, F. 2016. Diagnosis, classification and grading of canine mammary tumours as a model to study human breast cancer: an Clinico-Cytohistopathological study with environmental factors influencing public health and medicine. **13**(79).

Shamseddine, A.A., Airola, M.V. and Hannun, Y.A. 2015. Roles and regulation of neutral sphingomyelinase-2 in cellular and pathological processes. Adv. Biol. Regul. **57**: 24-41.

Shekhar, C. S., Vijaysarathi, S. K., Gowda, R. N. S. and Suguuna, R. R. 2001. An epidemiology study on canine mammary tumors. Ind. Vet. J. **78**(2): 107-109.

Simon, D., Schoenrock, D., Baumgärtner, W. and Nolte, I. 2006. Postoperative adjuvant treatment of invasive malignant mammary gland tumors in dogs with doxorubicin and docetaxel. J. Vet. Intern. Med. **20**(5): 1184-1190.

Sinha, D., Roy, S., Saha, P., Chatterjee, N. and Bishayee, A. 2021. Trends in research on exosomes in cancer progression and anticancer therapy. Cancers. **13**(2): 326.

Slamon, D. J. 1990. Studies of the HER-2/neu proto-oncogene in human breast cancer. Cancer Invest. **8**(2): 253-254.

Sleeckx, N., De Rooster, H.E.J.V.K., EJ, V.K., Van Ginneken, C. and Van Brantegem, L. 2011. Canine mammary tumours, an overview. Reprod. Domest. Anim. Zuchthygiene. **46**(6): 1112-1131.

Spugnini, E.P., Sonveaux, P., Stock, C., Perez-Sayans, M., De Milito, A., Avnet, S., Garcìa, A.G., Harguindey, S. and Fais, S., 2015. Proton channels and exchangers in cancer. Biochim. Biophys. Acta - Biomembr. **1848**(10): 2715-2726.

Suchorska, W.M. and Lach, M.S. 2016. The role of exosomes in tumor progression and metastasis. Oncol. Rep. **35**(3): 1237-1244.

Tai, Y.L., Chen, K.C., Hsieh, J.T. and Shen, T.L. 2018. Exosomes in cancer development and clinical applications. Cancer Sci. **109**(8): 2364-2374.

Tan, A.R. and Swain, S.M. 2003, October. Ongoing adjuvant trials with trastuzumab in breast cancer. In Semin. Oncol. **30**: 54-64.

Tanaka, M., Yamaguchi, S., & Iwasa, Y. 2020. Enhanced risk of cancer in companion animals as a response to the longevity. Sci. Rep. **10**(1): 1-10

Tavasoly, A., Golshahi, H., Rezaie, A. and Farhadi, M. 2013. Classification and grading of canine malignant mammary tumors. Vet. Res. Forum. **4**(1): 25.

Taylor, D.D., Lyons, K.S. and Gerçel-Taylor, Ç. 2002. Shed membrane fragment-associated markers for endometrial and ovarian cancers. Gynecol. Oncol. **84**(3): 443-448.

Taylor, S., Spugnini, E.P., Assaraf, Y.G., Azzarito, T., Rauch, C. and Fais, S., 2015. Microenvironment acidity as a major determinant of tumor chemoresistance: Proton pump inhibitors (PPIs) as a novel therapeutic approach. Drug. Resist. Updat. **23**: 69-78.

Tian, Y., Li, S., Song, J., Ji, T., Zhu, M., Anderson, G.J., Wei, J. and Nie, G. 2014. A doxorubicin delivery platform using engineered natural membrane vesicle exosomes for targeted tumor therapy. Biomaterials. **35**(7): 2383-2390

Todorova, I. 2006. Prevalence and etiology of the most common malignant tumours in dogs and cats. Bulg. J. Vet. Med. **9**(2): 85-98.

Tomasetti, M., Lee, W., Santarelli, L. and Neuzil, J. 2017. Exosome-derived microRNAs in cancer metabolism: possible implications in cancer diagnostics and therapy. Exp. Mol. Med. **49**(1): 285-e285.

Trajkovic, K., Hsu, C., Chiantia, S., Rajendran, L., Wenzel, D., Wieland, F., Schwille, P., Brugger, B. and Simons, M. 2008. Ceramide triggers budding of exosome vesicles into multivesicular endosomes. Science. **319**(5867): 1244-1247.

Tremblay, G. B., Tremblay, A., Copeland, N. G., Gilbert, D. J., Jenkins, N. A., Labrie, F. and Giguere, V. 1997. Cloning, chromosomal localization, and functional analysis of the murine estrogen receptor â. Mol. Endocrinol. **11**(3): 353-365.

Uyama, R., Nakagawa, T., Hong, S.H., Mochizuki, M., Nishimura, R. and Sasaki, N. 2006. Establishment of four pairs of canine mammary tumour cell lines derived from primary and metastatic origin and their E cadherin expression. Vet. Comp. Oncol. **4**(2): 104-113.

Van Garderen, E., van der Poel, H. J., Swennenhuis, J. F., Wissink, E. H., Rutteman, G. R., HellmeÞn, E. and Schalken, J. A. 1999. Expression and molecular characterization of the growth hormone receptor in canine mammary tissue and mammary tumors. Endocrinology. **140**(12): 5907-5914.

Vlassov, A.V., Magdaleno, S., Setterquist, R. and Conrad, R. 2012. Exosomes: current knowledge of their composition, biological functions, and diagnostic and therapeutic potentials. Biochim. Biophys. Acta - Gen. Subj. **1820**(7): 940-948.

Wan, X., Fang, Y., Du, J., Cai, S. and Dong, H. 2023. GW4869 Can Inhibit Epithelial-Mesenchymal Transition and Extracellular HSP90α in Gefitinib-Sensitive NSCLC Cells. OncoTargets. Ther. 913-922.

Wang, J., Hendrix, A., Hernot, S., Lemaire, M., De Bruyne, E., Van Valckenborgh, E., Lahoutte, T., De Wever, O., Vanderkerken, K. and Menu, E. 2014. Bone marrow stromal cell–derived exosomes as communicators in drug resistance in multiple myeloma cells. Blood, J. Am. Soc. Hematol. **124**(4): 555-566.

Wang, Q. and Greene, M. I. 2008. Mechanisms of resistance to ErbB-targeted cancer therapeutics. J. Clin. Investig. **118**(7): 2389-2392.

Yager, J. D. 2015. Mechanisms of estrogen carcinogenesis: The role of E2/E1–quinone metabolites suggests new approaches to preventive intervention–A review. Steroids. **99**: 56-60.

Yang, W.Y., Liu, C.H., Chang, C.J., Lee, C.C., Chang, K.J. and Lin, C.T. 2006. Proliferative activity, apoptosis and expression of oestrogen receptor and Bcl-2 oncoprotein in canine mammary gland tumours. J. Comp. Pathol. **134**: 70–9.

Yokota, J., Tsunetsugu-Yokota, Y., Battifora, H., Le Fevre, C. and Cline, M.J. 1986. Alterations of myc, myb, and ras Ha proto-oncogenes in cancers are frequent and show clinical correlation. Science. **231**(4735): 261-265.

Yue, W., Yager, J. D., Wang, J. P., Jupe, E. R., & Santen, R. J. 2013. Estrogen receptor dependent and independent mechanisms of breast cancer carcinogenesis. Steroids. **78**(2): 161-170.

Zatloukal, J., Lorenzova, J., Tichý, F., Nečas, A., Kecova, H. and Kohout, P. 2005. Breed and age as risk factors for canine mammary tumours. Acta vet. Brno. **74**(1): 103-109.

Zeng, L., Li, W. and Chen, C.S. 2020. Breast cancer animal models and applications. Zool. Res. **41**(5): 477.

Zhang, H., Lu, J., Liu, J., Zhang, G. and Lu, A. 2020. Advances in the discovery of exosome inhibitors in cancer. J. Enzyme Inhib. Med. **35**(1): 1322-1330.

APPENDIX

1 X Phosphate buffer saline

Sodium chloride	8 grams
Potassium chloride	0.2 grams
di-Sodium hydrogen phosphate	1.44 grams
Potassium di-hydrogen phosphate	4.8 grams
Distilled water	Made to 1000 ml
Adjust the pH to 7.4 with NaOH	

0.01M sodium citrate buffer (pH 6.0)

Solution A: 0.1 M citric acid solution	
Citric acid (MW = 210.4)	21.01 grams
Distilled water	Made to 1000 ml
Solution B: 0.1 M sodium citrate solution	
Sodium citrate (MW = 294.12)	29.4 grams
Distilled water	Made to 1000 ml
Preparation of 0.01M citrate buffer add	
Solution 'A'	19 ml
Solution 'B'	81 ml
Distilled water	900 ml
Adjust pH to 6.0 if necessary	

Neutral buffered formalin (pH 6.8)

40% formaldehyde	100 ml
Sodium dihydrogen phosphate ($NaH_2 PO_4$)	4 g
Disodium hydrogen phosphate ($Na2 HPO_4$)	6.5 g
Distilled water	Made to 1000 ml

70% ethanol

Absolute ethanol	70 parts
Distilled water	20 parts

MTT working solution

MTT powder	5 mg
1X PBS	1 ml

GW4869 Stock solution (10mM)

GW4869 powder	1 mg
DMSO	170 µl

10% Minimum Essential Medium (MEM) (100 ml)

Minimum essential media	89
Fetal Bovine Serum (FBS)	10
Antibiotic - antimycotic solution (100X)	1